Understanding Cell Fate Decisions in the Embryonic Gonad

by

Samantha Ann Jameson

Department of Cell Biology
Duke University

Date:________________________
Approved:

____
Blanche Capel, Supervisor

____
John Klingensmith

____
Fan Wang

____
Mariano A Garcia-Blanco

Dissertation submitted in partial fulfillment of
the requirements for the degree of Doctor of Philosophy in the Department of
Cell Biology in the Graduate School
of Duke University

2011

ABSTRACT

Understanding Cell Fate Decisions in the Embryonic Gonad

by

Samantha Ann Jameson

Department of Cell Biology
Duke University

Date: ________________________
Approved:

____
Blanche Capel, Supervisor

____
John Klingensmith

____
Fan Wang

____
Mariano A Garcia-Blanco

An abstract of a dissertation submitted in partial
fulfillment of the requirements for the degree
of Doctor of Philosophy in the Department of
Cell Biology in the Graduate School
of Duke University

2011

Copyright by
Samantha Ann Jameson
2011

Abstract

The divergence of distinct cell populations from multipotent progenitors is poorly understood, particularly *in vivo*. The gonad is an ideal place to study this process because it originates as a bipotential primordium where multiple distinct lineages acquire sex-specific fates as the organ differentiates as a testis or an ovary. The early gonad is composed of four lineages: supporting cells, interstitial/stromal cells, germ cells, and endothelial cells. Each lineage in the early gonad consists of bipotential progenitors capable of adopting either a male or female fate, which they do in a coordinated manner to form a functional testis or ovary. The supporting cell lineage is of particular interest because the decision of these cells to adopt the male or female fate dictates the fate of the gonad as a whole.

To gain a more detailed understanding of the process of gonadal differentiation at the level of the individual cell populations, we conducted microarrays on sorted cells of the four lineages from XX and XY mouse gonads at three time points spanning the period when the gonadal cells transition from sexually undifferentiated progenitors to their respective sex-specific fates. Our analysis identified genes specifically depleted and enriched in each lineage as it underwent sex-specific differentiation. We also determined that the sexually undifferentiated germ cell and supporting cell progenitors showed lineage priming. Multipotent progenitors that show lineage priming express markers of the various fates into which they can differentiate and subsequently silence genes associated with the fate not adopted as they differentiate. We found that germ cell progenitors were primed with a bias toward the male fate. In contrast, supporting cell progenitors were primed with a female bias. This yields new insights into the mechanisms by which different cell types in a single organ adopt their respective fates.

We also used a genetic approach to investigate how individual factors contribute to the adoption of the male supporting cell fate. We previously demonstrated that *Fgf9* and *Wnt4* act as mutually antagonistic factors to promote male or female development of the bipotential mammalian gonad. *Fgf9* is necessary to maintain *Sox9* expression, which drives male development. However, whether FGF9 acted directly on *Sox9* or indirectly through repression of *Wnt4*, was unknown. *Wnt4* is a female-primed gene, and is therefore repressed during male development. To determine how *Fgf9* functioned, we generated double *Fgf9*/*Wnt4* and *Fgfr2*/*Wnt4* mutants. While single XY *Fgf9* and *Fgfr2* mutants showed partial or complete male-to-female sex reversal, loss of *Wnt4* in an *Fgf9* or *Fgfr2* mutant background rescued normal testis development. We also found that *Wnt4* and another female-associated gene (*Rspo1*) were derepressed in *Fgf9* mutants prior to the down-regulation of *Sox9*. Thus, the primary function of *Fgf9* is the repression of female genes, including *Wnt4*. We also tested the reciprocal possibility: that de-repression of *Fgf9* was responsible for the aspects of male development observed in XX

Wnt4 mutants. However, we show that loss of *Fgf9* in XX *Wnt4*$^{-/-}$ gonads does not rescue the partial female-to-male sex reversal.

Based on the *Fgf9*/*Wnt4* double mutant studies, we propose a two part model of male sex determination in which both the activation of male genes and repression of female genes is required. Also, this work demonstrates that the repression of the female-primed gene *Wnt4* is required for male development, and *Fgf9* is one factor that leads to the repression of female-primed genes.

Contents

Abstract iv

List of Tables.....xi

List of Figures xii

Acknowledgements xiv

1. Introduction 1

    1.1 Gonad development.....1

    1.2 Models of sex determination.....5

    1.3 The role of Fgf9 and Wnt4 during gonad development 11

2. Materials and Methods.....15

    2.1 Performing microarrays 15

        2.1.1 Mice for the microarray analysis.....15

        2.1.2 Collection of gonadal lineages.....16

        2.1.3 Preparation of samples and microarrays 17

        2.1.4 Immunofluorescence validating microarray data 18

    2.2 Microarray analysis.....19

        2.2.1 Initial microarray processing and analysis.....19

        2.2.2 Pairwise comparisons used to indentify genes of interest 20

        2.2.3 *Sf1-EGFP* microarray analysis 29

    2.3 Determining the mechanism of Fgf action.....32

        2.3.1 Mice 32

2.3.2 Immunofluorescence 33

2.3.3 qRT-PCR 35

3. Transcriptional Profiling of Gonadal Cell Lineages 39

3.1 Summary 39

3.2 Introduction 39

3.3 Results 43

3.3.1 Sorted cell microarrays accurately reflect known gene expression patterns 43

3.3.2 Lineage, sex, and stage all influence gene expression 51

3.3.3 Each lineage has uniquely expressed enriched and depleted genes that provide insight into the biology of the cells. 58

3.3.4 The XX stroma and supporting cells express some of the same genes 65

3.4 Discussion 69

3.4.1 Insights from whole transcriptome characterization of multiple gonadal lineages 69

3.4.2 Lineage- and sex-specific transcriptional depletion in the differentiating gonad 73

4. Lineage priming of Sexual Fate in Gonadal Cells 75

4.1 Summary 75

4.2 Introduction 75

4.3 Results 77

4.3.1 Germ cell progenitors are primed with a bias toward the male fate 77

4.3.2 Supporting cell progenitors are primed with a bias toward the female fate 84

4.4 Discussion 103

4.4.1 A role for priming in the bipotential supporting cell lineage 104

4.4.2 Priming during germ cell development 109

4.4.3 Priming during differentiation 111

5. Testis Development Requires the Repression of *Wnt4* by Fgf Signaling 114

5.1 Summary 114

5.2 Introduction 115

5.3 Results 116

5.3.1 The partial sex reversal observed in XY *Fgfr2* mutants is rescued by deleting *Wnt4*, consistent with the *Wnt4* repression model 116

5.3.2 Male-to-female sex reversal caused by *Fgf9* deletion is completely rescued by deleting *Wnt4* 122

5.3.3 *Fgf9* represses *Wnt4* by E11.75 in XY gonads 131

5.3.4 The partial sex reversal phenotype of XX *Wnt4* mutants is not rescued by deletion of *Fgf9* 135

5.4 Discussion 141

6. Future Directions 152

6.1 Alternative transcript processing during gonad development 152

6.2 The mechanisms of repression of female genes in the XY supporting cells 156

6.3 Exploring the divergence of the supporting cells, interstitial/stromal cells, and the coelomic domain 165

Appendix A: Localization of FGFR2 169

Appendix B: Analysis of *Fgfrl1* mutants 184

References 201

Biography 219

List of Tables

Table 1: Primers used for qRT-PCR..37

List of Figures

Figure 1: Gonadal cell lineages. 2

Figure 2: Models of sex determination 8

Figure 3: Models of Fgf action during gonad development. 13

Figure 4: Lineage-specific fluorescent tags used for FACS. 41

Figure 5: *αSma-EYFP* labeled a heterogeneous population containing supporting cell precursors 46

Figure 6: Microarray validation. 49

Figure 7: Gene expression was affected by lineage, sex, and stage. 53

Figure 8: Alternative methods showed generally similar patterns indicating the importance of lineage, sex, and stage 56

Figure 9: Lineage-specific enriched and depleted genes revealed distinct differentiation programs. 60

Figure 10: Overlap between lineages of genes that are sexually dimorphic. 66

Figure 11: Model of differentiation for the interstitial/stromal lineage 71

Figure 12: Germ cells showed lineage priming with a male bias 79

Figure 13: Supporting cells showed lineage priming with a female bias. 85

Figure 14: Data from sorted *Sf1-EGFP* cells starting at E11.0 also shows female-biased priming for supporting cells 90

Figure 15: E10.5 *Sf1-EGFP* primed genes generally supported female-biased priming, but the E11.0 analysis was more informative. 96

Figure 16: Overlap of primed genes between the *Sf1-EGFP* and *Sry-EGFP/Sox9-ECFP* data sets. 101

Figure 17: Models of differentiation for the gonadal lineages 105

Figure 18: Predictions of the models of Fgf action 117

Figure 19: Deleting *Wnt4* rescued the partial sex reversal induced by loss of *Fgfr2*, supporting the *Wnt4* repression model. 120

Figure 20: Deleting *Wnt4* rescued the full sex reversal induced by loss of *Fgf9*, further supporting the *Wnt4* repression model. 124

Figure 21: XY *Fgf9*/*Wnt4* double mutants express molecular markers typical of testis development consistent with a full rescue of sex reversal. 127

Figure 22: Female pathway components were derepressed in XY *Fgf9* mutants prior to loss of *Sox9*. 133

Figure 23: Deleting *Fgf9* did not rescue the phenotypes of XX *Wnt4* mutants. 137

Figure 24: Deleting *Fgfr2* in endothelial cells does not disrupt coelomic vessel formation. 139

Figure 25: Model of sex determination. 143

Figure 26: Alternative processing candidate genes. 154

Figure 27: Gene expression during gonad development. 160

Figure 28: Data inconsistent with the FGFR2 antibody recognizing SOX9. 171

Figure 29: Localization of FGFR2-EGFP. 175

Figure 30: Gonads electroporated with *Fgfr2-EGFP*. 181

Figure 31: Reproductive system phenotypes in XX *Fgfrl1* mutants. 186

Figure 32: Müllerian duct development in an *Fgfrl1* mutant. 189

Figure 33: *In situ* of *Fgfrl1* in an E12.5 XX gonad and mesonephros. 192

Figure 34: Gene expression in XX *Fgfrl1* mutant gonads. 195

Figure 35: Vascular migration out of the ovary. 198

Acknowledgements

Even though I was a joint J.D./Ph.D. student with no intention of pursuing a career in academic science, Blanche welcomed me into her lab. When the early results of my work were not promising, I am grateful to Blanche for letting me continue to pursue other avenues of investigation to reach this point. Throughout the process, she has always been supportive of my non-traditional career goals. None of this work would have been possible without her support, insights, and mentorship. I would not be where I am today without her.

My committee members (John Klingensmith, Ken Poss, Fan Wang, and Mariano Garcia-Blanco) have also provided a great deal of valuable advice and support, for which I thank them.

Other members of the Capel lab have contributed significantly to this work. Jonah Cool, Tony DeFalco, and Danielle M. Maatouk all helped collect the cells to run the microarrays. Anirudh Natarajan helped to implement the microarray analysis and develop statistical tests for the results. Lindsey Mork and Steven C. Munger provided many helpful insights into the analysis, figures, and techniques used. Jordan Batchvarov's help managing the colony and Allison Navis's exceptional efforts genotyping the mice used in these studies and processing samples have been instrumental in the completion of this work. Other members of the Capel lab, present

and past, have been generous in their friendship and advice (Ximena Bustamante, Jason Garness, Michael Czerwinski, Yi-tzu Lin, Hao Tang, Leo DiNapoli, and Yuna Kim). I also need to give special acknowledgement to Danielle M. Maatouk, who has been a mentor and friend. She helped me get my project started when I joined the lab, taught me how to manage my mouse colony, and helped me develop my project as it evolved.

I also need to thank my family. I would never have been able to complete this work without the love, support, and care of my husband Martin Jameson. He does almost everything necessary for me to survive and thrive. This includes caring for our amazing daughter Keena Jameson, who lights up my days with her enthusiasm. Children are explorers, and the spark I see when she discovers something reminds me why I love science.

The encouragement and support of my parents (Christopher James and Andrea Westerinen), has also been instrumental in my achievements. They helped me become the person I am today, and their successes helped me reach my goals. My wider family (Jeff, Stephanie, Charlene, Jim, Lauren, Rick, Tim, and Jackie) and my grandparents (Tony, Rita, and Dorothy) all supported and influenced me in many ways, and I thank them as well.

1. Introduction

1.1 Gonad development

The bipotential gonad is a unique system for studying cell fate decisions during mammalian organ development. In mice, the gonads arise around embryonic day 10 (E10.0) as thickenings on the surface of the mesonephros (Brennan and Capel 2004). Until E11.25 the gonad primordia harbor the potential to become testes or ovaries irrespective of genetic sex, making them bipotential (Brennan and Capel 2004; Hiramatsu et al. 2009).

The early gonad is composed of four lineages: supporting cells, interstitial/stromal cells, germ cells, and endothelial cells (Figure 1). Supporting cells and interstitial/stromal cells arise within the urogenital ridge from a common mesodermal progenitor, while the primordial germ cells and endothelial cells migrate into the developing gonad (Karl and Capel 1998; Wylie 1999; Coveney et al. 2008a; Martineau et al. 1997). Despite their distinct origins, cells of each lineage in the early gonad are bipotential progenitors capable of adopting either a male or female fate, which they do in a coordinated manner to form a functional testis or ovary (Albrecht and Eicher 2001; Adams and McLaren 2002; Swain and Lovell-Badge 1999).

Figure 1: Gonadal cell lineages.

Illustration of the developing XX and XY gonad with supporting cells (blue), interstitial/stromal cells (purple), germ cells (green), and endothelial cells (red). Testis cords with supporting cells and germ cells form in the XY gonad.

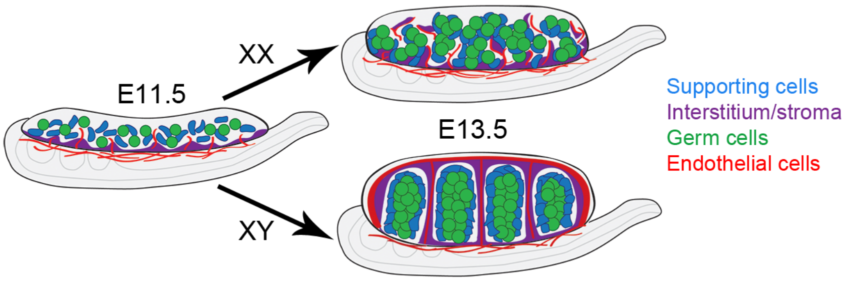
E11.5
XX
XY
E13.5
Supporting cells
Interstitium/stroma
Germ cells
Endothelial cells

The process by which the bipotential gonad adopts the ovarian or testicular fate is known as primary sex determination, and involves a binary fate decision within cells of each gonadal lineage. The fate of the organ is decided by the supporting cells. In the mouse, the adoption of the male fate is determined by the expression of the testis-determining gene from the Y-chromosome, *Sry*, which up-regulates *Sox9* in supporting cells, and initiates testis development (Koopman et al. 1991; Gubbay et al. 1990; Sekido and Lovell-Badge 2008; Sekido et al. 2004). *Sox9* expression is critical for testis development (Huang et al. 1999; Wagner et al. 1994; Chaboissier et al. 2004; Bishop et al. 2000; Vidal et al. 2001). While no "ovary determining gene" (Eicher and Washburn 1986) analogous to *Sry* has been identified, ovarian development is also characterized by unique gene expression (Nef et al. 2005; Bouma et al. 2010; Bouma et al. 2007) and the deletion of female-associated genes results in a disruption of ovarian development (Uhlenhaut et al. 2009; Chassot et al. 2008; Vainio et al. 1999).

There is a complex transcriptional network present in the early gonad that influences sex determination (Munger et al. 2009). Subnetworks of co-expressed male genes and co-expressed female genes are present in the sexually undifferentiated gonad (Munger et al. 2009). Differences in the network state may affect phenotype. For example, the C57BL/6J strain of mice is particularly sensitive to sex reversal and has higher expression of female-associated genes (Eicher et al. 1982; Munger et al. 2009). The work in this dissertation further explores the transcriptional state of the diverse cell types in the gonad over time, and how perturbation of an individual gene disrupts the network and the normal process of development.

1.2 Models of sex determination

Various theories have been proposed to understand gonadal sex determination. It has been suggested that the female fate is the "default" state because expression of *Sry* is required to "divert" the cells to the male fate (Jost 1947; McLaren 1991; Capel 1998). Conversely, others proposed that a female-promoting "Z" gene normally blocks male development and that Z is itself blocked by *Sry* (McElreavey et al. 1993). Still others have proposed that both the female and male programs require an active switch to initiate differentiation from their initially "bipotential" state (i.e., that there is an "ovary-determining gene" as well as a "testis-determining gene") (Eicher and Washburn 1986). More recently, it has been suggested that the gonad is balanced between the male and female fates by antagonistic signaling pathways (Kim et al. 2006; Chassot et al. 2008; Swain et al. 1998; Munger et al. 2009).

The concept of lineage priming provides a novel way to view these theories. Studies suggest that multipotent cells are not a "blank slate", but rather are "lineage primed" by expressing markers of all potential fates they can adopt (Delorme et al. 2009; Hu et al. 1997; Ng et al. 2009; Zipori 2004; Miyamoto et al. 2002; Enver and Greaves 1998; Hipp et al. 2010; Golan-Mashiach et al. 2005). During their differentiation, multipotent cells repress markers of specific fates that were not adopted while maintaining gene expression associated with the fate that was adopted (Delorme et al. 2009; Hu et al. 1997; Ng et al. 2009; Zipori 2004; Miyamoto et al. 2002; Enver and Greaves 1998; Hipp et al. 2010; Golan-Mashiach et al. 2005). A similar phenomenon has also been observed in the early embryo, where individual blastomeres express transcripts that later become restricted to the specific lineages of the blastocyst (Guo et al. 2010; Dietrich and Hiiragi 2007; Plusa et al. 2008). It is possible for progenitor cells to be equally "balanced" between their multiple fates, expressing similar numbers of genes associated with each alternative differentiated fate. However, the progenitors need not have all differentiation programs equally represented (Delorme et al. 2009). Instead a progenitor may show "biased priming" if markers characteristic of one of its possible fates predominate, indicating the closer relationship of the progenitor to that fate.

The previously proposed models can be formulated in the context of linage priming (Figure 2). The "female" model predicts that the transcriptome shared by XY and XX progenitors should be predominately associated with the differentiated female fate (i.e., "female-primed"). Conversely, the "male" model predicts that the transcriptome shared by XY and XX progenitors should be predominately associated with the differentiated male fate (i.e. "male-primed"). If both the male and female programs are activated *de novo* as progenitors differentiate, those progenitors should be a "blank slate" in that they would not express transcripts associated with either the differentiated male or female cells. Alternatively, the progenitors could fit the “balanced priming” model and express a similar number of both male- and female-associated transcripts at the time when they are poised to adopt either fate. Finally, the progenitors could be primed to adopt either fate, but there could be more genes associated with the female (“female-biased priming”) or the male (“male-biased priming”) fate.

Figure 2: Models of sex determination.

Illustrations of the various models of sex determination in the context of lineage priming. The left portion of each "Y" shaped graph is the gene expression of sexually undifferentiated progenitor cells in the gonad, and the right is the level of expression characteristic of the differentiated male ("♂") and female ("♀") cells.

Models	**Name**	Blank slate	Female	Female-biased priming	Balanced priming	Male-biased priming	Male
	Illustration	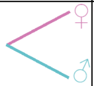	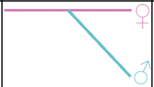	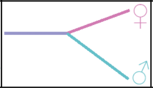	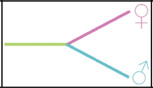	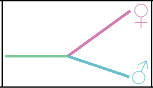	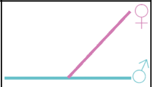

To determine which model best describes the cells of the gonad, temporal transcriptional profiling is required. Some gonadal lineages have been studied at the transcriptome level in independent experiments (Bouma et al. 2010; Nef et al. 2005; Mise et al. 2008; Beverdam and Koopman 2006; Rolland et al. 2011; Bouma et al. 2007), resulting in the identification of genes that are up-regulated in a sex- or (in some cases) lineage-specific manner. However, previous studies did not fully characterize the undifferentiated progenitors or the temporal sequence for the divergence of the multiple progenitors to their sexual fates.

Other aspects of transcription have also not been addressed by these previous transcriptome studies. For example, the molecular relationship between the somatic lineages (i.e., supporting cells versus interstitial/stromal cells) has never been examined, as these lineages were not separated in previous studies. Also, transcriptional patterns potentially important to differentiation and fate commitment were not analyzed, such as the specific transcript depletion previously noted in the *Arabidopsis* root and in early primordial germ cells (Brady et al. 2007; Saitou et al. 2002).

In this dissertation, we use temporal transcriptional profiling both to better characterize unappreciated transcriptional patterns and to determine which model of sex determination best describes the process of sex determination in multiple cell types.

1.3 The role of Fgf9 and Wnt4 during gonad development

To understand how the gene expression network functions during sex determination, we need to understand how the individual genes in that network function. In addition to *Sox9* and *Sry*, other genes are also required for male development, such as *Fgf9* and its receptor *Fgfr2*. Deletion of *Fgf9* (Colvin et al. 2001), or *Fgfr2* (Kim et al. 2007) results in male-to-female sex reversal. In XY *Fgf9* mutants (*Fgf9*$^{-/-}$), SOX9 was initially expressed in supporting cell precursors, but was lost between E12.0 and E12.5, and the ovary-promoting gene *Wnt4* was up-regulated by E12.5 (Kim et al. 2006). These experiments suggested that FGF9 is needed to maintain SOX9 expression and commitment to the male pathway (Kim et al. 2006).

In a somewhat reciprocal manner, XX animals mutant for the Wnt signaling components, *Wnt4*, *Rspo1* or *β-catenin*, show partial female-to-male sex reversal. In these mutants, endothelial cells migrate into the XX gonad and form a coelomic vessel and XX cells express steroidogenic enzymes (Vainio et al. 1999; Jeays-Ward et al. 2003; Liu et al. 2009; Chassot et al. 2008). Studies suggested that *Fgf9* is expressed in XX *Wnt4* mutants (Kim et al. 2006), and exogenous FGF9 can induce migration of mesonephric endothelial cells into the XX gonad (Colvin et al. 2001). Thus, it remained an open question whether derepression of *Fgf9* was responsible for any of the XX *Wnt4* mutant phenotypes.

Previously, we provided evidence that an antagonistic relationship exists between *Fgf9* and *Wnt4* during gonad development (Kim et al. 2006). *Wnt4* is initially expressed in XX and XY bipotential gonads, and is down-regulated during male development and maintained during female development (Vainio et al. 1999; Nef et al. 2005). *Fgf9* shows the reciprocal pattern: *Fgf9* is up-regulated during male development, and is absent during female development. We proposed that *Fgf9* and *Sox9* act in a feed-forward loop to reinforce SOX9 expression, and repress *Wnt4* (Kim et al. 2006). However, the existing data could not distinguish a direct activating effect of FGF9 on *Sox9* (Fgf activation model, Figure 3), from an alternative model where *Fgf9* acts indirectly to promote SOX9 expression by repressing *Wnt4*, which could otherwise repress SOX9 (*Wnt4* repression model, Figure 3). This dissertation also addresses which model of Fgf action is correct, with broad implications for the process of sex determination.

Figure 3: Models of Fgf action during gonad development.

The existing data was consistent with multiple models of Fgf action. Fgf could positively promote SOX9 expression (Fgf activation model), as was previously proposed (Kim et al. 2006). Alternatively, Fgf could repress *Wnt4*, which would otherwise repress SOX9 (*Wnt4* repression model).

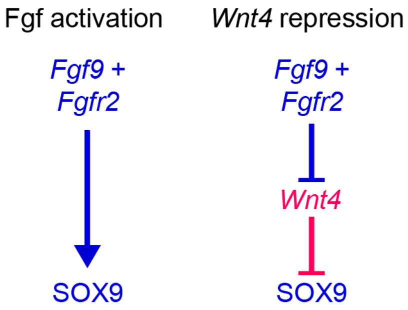

Models of Fgf action:

Fgf activation
Wnt4 repression
Fgf9 +
Fgfr2
SOX9
Fgf9 +
Fgfr2
Wnt4
SOX9

2. Materials and Methods

2.1 Performing microarrays

2.1.1 Mice for the microarray analysis

All animals were maintained and experiments were conducted according to DUMC-IACUC and NIH guidelines, based on existing protocols. We used six different transgenic mouse lines with fluorescent reporters: *Sry-EGFP* [Tg(Sry-EGFP)92Ei] (Albrecht and Eicher 2001), *Sox9-ECFP* (Kim et al. 2007), *Mafb-EGFP* [Mafb$^{\mathrm{tm1Jeng}}$] (a gift from S. Takahashi) (Moriguchi et al. 2006), *αSma-EYFP* (a gift from J. Lessard) (Cool et al. 2008), *Flk1-mCherry* [Tg(Kdr-mCherry)1Medi] (a gift from M. Dickinson) (Larina et al. 2009; Poche et al. 2009), and *Oct4-EGFP* [Tg(Pou5f1-EGFP)2Mnn] (Szabo et al. 2002). In most cases, males from these lines were crossed to CD-1 females (Charles River) or females from other mixed genetic backgrounds, and gonads were pooled to reduce the impact of strain variation. All of the males were homozygous for the marker, with the exception of *Mafb-EGFP* males. This line is a targeted insertion of GFP into the *Mafb* locus, which results in a *Mafb* mutant when homozygous. *Mafb-EGFP* embryos collected in this study were therefore heterozygous for *Mafb*; however, we know of no defects in gonad development in *Mafb* heterozygotes (data not shown). To increase the fluorescence intensity for both the *αSma-EYFP* and *Flk1-mCherry* reporters, homozygous males were crossed to homozygous females.

2.1.2 Collection of gonadal lineages

Timed matings were performed, with the day the vaginal plug was detected considered E0.5. Embryos were collected at E11.5, E12.5, and E13.5. For the *Mafb-EGFP* line, only GFP-positive embryos were used for sorting. The sex of the gonad is obvious by eye at E12.5 and E13.5. The E11.5 embryos were genotyped to determine the sex as previously described using primers to detect *Kdm5c* (X chromosome) and *Kdm5d* (Y chromosome) (Mroz et al. 1999; Munger et al. 2009).

To collect gonadal cells, the urogenital ridge and dorsal aorta were removed, and the gonad/mesonephric complex was isolated. In most cases, the gonad was separated from the mesonephros. However, for the *Oct4-EGFP* sorts, the gonad was left attached because *Oct4* expression is highly specific to germ cells (data not shown). For the E11.5 *Flk1-mCherry* sorts, only the anterior and posterior portions of the mesonephros were removed by cutting at a 45º angle from the end of the gonad. The gonad vasculature arises from a plexus in the mesonephros (Coveney et al. 2008a); thus, the gonadal and a portion of the mesonephric endothelial cells represent one population. This procedure retained the mesonephric plexus while removing most of the vasculature associated with the mesonephric ducts. At E12.5 and E13.5, the mesonephros was removed completely for the *Flk1-mCherry* sorts.

XY and XX gonads were separately pooled from one or more litters and incubated in 250 µl 0.25% Trypsin EDTA (Gibco #25200) at 37ºC for 5-10 minutes. The trypsin was removed and replaced with 400 µl PBS with or without 4 µl RNase-free DNase (Promega #M6101). The tissue was dissociated, and the cells were passed through a strainer (BD Falcon #352235). FACS was performed by the Duke Comprehensive Cancer Center Flow Cytometry Shared Resource. The positive fraction was pelleted, the liquid supernatant was removed, and the cells were immediately frozen at -80ºC.

2.1.3 Preparation of samples and microarrays

For many lineages, cells from multiple litters were pooled. RNA was extracted from over 100,000 cells to as few as 10,000 cells using the RNeasy Micro kit (Qiagen #74004) following the manufacturer's instructions for "Cells." However, the protocol was started at step 2 (disruption with RLT), and β-ME was not added. The cells from multiple sorts were pooled during disruption with RLT, step 3 (homogenization) was skipped, and in step 10, three RPE washes were performed.

Samples were prepared for the Affymetrix Genechip Mouse Gene 1.0 ST Arrays (#901168) using the Nugen WT-Ovation Pico RNA Amplification System (#3300), WT-Ovation Exon Module (#2000), and the Encore Biotin Module (#4200), following the manufacturer's instructions. For purification following the Pico and Exon kits, the

Qiagen QIAquick PCR Purification Kit (#28104) was used following the instructions provided by Nugen. Fragmented and labeled product was submitted to the Duke Institute for Genome Sciences and Policy Microarray Facility for hybridization and reading.

We ran a total of 91 arrays. This included the arrays on our five sorted cell types at the three time points with separate XX and XY samples in biological triplicate as well as one array on a whole P1 mouse RNA (a gift from S. Potter) sample for normalization across GUDMAP.

2.1.4 Immunofluorescence validating microarray data

Samples were fixed, stained, and imaged as whole gonads with the mesonephros attached as previously described (Cook et al. 2009). Some samples were first processed through a methanol series and stored at -80ºC prior to rehydration and staining (Barske and Capel 2010). Primary antibodies used were: anti-3β-HSD (Santa Cruz sc-30820, 1:100 in samples processed through methanol; TransGenic Inc. KO607, 1:500; a gift from K. Morohashi), anti-FLK1 (BD Pharmingen #550549, 1:250), anti-PECAM (BD Pharmingen 553370, 1:250), anti-SRY (a gift from P. Koopman and D. Wilhelm), and anti-SOX9 (a gift from P. Koopman and D. Wilhelm). Secondary antibodies used included Alexa 647- and 488- conjugated secondary antibodies (Molecular Probes, 1:500) and Cy3- and Cy5-

conjugated secondary antibodies (Jackson ImmunoResearch, 1:500). DAPI (Sigma-Aldrich) was used to label nuclei.

2.2 Microarray analysis

2.2.1 Initial microarray processing and analysis

The .cel files were processed with Partek® Genomics Suite version 6.5 (6.11.0207) (Copyright 1993-2010, Partek Inc. Partek and all other Partek Inc. product or service names are registered trademarks or trademarks of Partek Inc., St. Louis, MO, USA) by RMA with quantile normalization and median polish summarization at the transcript cluster (gene) level. Probes were adjusted for GC content and probe sequence. The data were transformed into log base 2. We removed all transcript clusters that did not have a cross hybridization category of 1 (perfect match) in the Affymetrix annotation, that did not have a gene symbol, or that did not have a log base 2 normalized expression value > 6 in at least two out of three replicates of at least one sample. The genes that passed this filtering step, and only these genes, were used in subsequent analyses.

In the case of the analysis of the *αSma-EYFP* cells Figure 5, this initial processing of the arrays included all 91. However, for all other analyses, we used data generated by processing only 72 of our arrays because the *αSma-EYFP* and P1 whole mouse data were not included. The processed data on the 72 arrays were used in all portions of the analysis and are provided as a resource for the community (Supplemental File 1). The P1 whole mouse array was performed for normalization across the GUDMAP consortium (GenitoUrinary Molecular Anatomy Project, http://www.gudmap.org/), of which this study was a part, and was not intended to be used for our analysis of the data. The data from the *αSma-EYFP* cells indicated that this marker labeled a heterogenous populations of cells, and so was excluded from the analysis (see Figure 5).

Partek® Genomics Suite was used to generate the hierarchical clustering dendrograms and perform the ANOVA sources of variation analysis (Figures 7-8). The clustering methods used are described in the figure legends. One of the E11.5 XY endothelial samples was somewhat of an outlier in the clustering. This may be due in part to its processing, which resulted in unusually low (but still adequate) yield after the amplification with the Pico kit. However, we do not believe this compromised the sample as it still clustered with endothelial cells.

2.2.2 Pairwise comparisons used to indentify genes of interest

This analysis was performed at the level of the transcript cluster (gene), but some genes have multiple transcript clusters. Thus, the lists of transcript clusters may include multiple entries for the same gene. For graphical display of the numbers of genes identified (Figures 9-10 and 12-16), each gene was counted only once (i.e., duplicates were removed). However, in tables, all transcript clusters are shown (i.e., duplicates are not removed) (Supplemental Files 2-5).

To identify genes of interest, we adopted a simple and flexible method using multiple or single pairwise comparisons between samples (analogous to (Beckervordersandforth et al. 2010)). The same p-value and fold change cutoffs were used throughout. In all cases where we identified a difference between samples, we used a p-value cutoff of 0.05, and a fold change cutoff of 1.5 for each comparison. A gene was deemed to be identically expressed in two samples if the p-value was > 0.05 and the fold change was between -1.5 and 1.5. When multiple pairwise comparisons were done, the intersection of the multiple lists generated was taken as the genes of interest.

To identify sex-specifically and lineage-specifically enriched genes (using E12.5 XY supporting cells as an example), we used the following pairwise comparisons with the above cutoffs:

1. The gene was more highly expressed in XY supporting cells than XX supporting cells at E12.5 (i.e., sex-specific expression).
2. The gene was more highly expressed in XY supporting cells than the XY interstitium, germ cells, and endothelial cells at E12.5 (XY supporting cells versus XY interstitium, XY supporting cells versus XY germ cells, etc.) (i.e., lineage-specific expression).

The intersection of these multiple lists were the genes considered enriched in XY supporting cells at E12.5 (Figure 9A). Similar comparisons were also used to identify the sex- and lineage-specifically depleted genes, but a gene was deemed “depleted” when its expression was higher in all other cell lineages than the E12.5 XY supporting cells in the example. Because of the nature of these comparisons, it is possible for a gene to be considered "lineage-specific" for one XY lineage and a different XX lineage since all of the opposite sex lineages were not used in the comparisons (i.e., the XY supporting cells were not compared to the XX germ cells in the example).

To identify sex-independent and lineage-specifically enriched genes indicative of sexually undifferentiated progenitor expression (Figure 9A), we used the following pairwise comparisons (using the E11.5 supporting cells as an example):

1. The gene was more highly expressed in XY supporting cells than the XY interstitium, germ cells, and endothelial cells at E11.5 (i.e., lineage-specific expression among XY cells).
2. The gene was more highly expressed in XX supporting cells than the XX stroma, germ cells, and endothelial cells at E11.5 (i.e., lineage-specific expression among XX cells).
3. The gene was identically expressed in XX and XY supporting cells at E11.5 (i.e., identically expressed in progenitors).

Again, similar comparisons were used to identify the lineage-specifically depleted genes, but a gene was deemed "depleted" when its expression was higher in all other cell lineages than the E11.5 XY and XX supporting cells in the example. Occasionally, multiple transcript clusters for a gene may behave differently. In this case that gene may be identified in multiple lists. For example, different *Myo9a* transcript clusters were identified as sex-specifically enriched in E11.5 XX supporting cells and sex-independently enriched in E11.5 XX and XY supporting cells (Supplemental File 2A). The different behavior of the different transcript clusters in the gene could be caused by off-target probe binding or alterative splicing.

Leydig cell genes were a special case because both our sorted interstitial and "endothelial" cells contained Leydig cells (Figure 6B-E). To identify Leydig cell genes (Figure 9A), using E13.5 an example, we used the following pairwise comparisons:

1. The gene was more highly expressed in the XY interstitium than XY supporting cells and germ cells at E13.5 (i.e., lineage-specific expression).
2. The gene was more highly expressed in XY endothelial cells than XY supporting and germ cells at E13.5.
3. The gene was more highly expressed in the XY interstitium than the XX stroma at E13.5 (i.e., sex-specific expression).
4. The gene was more highly expressed in XY endothelial cells than XX endothelial cells at E13.5.

Depleted genes were identified similarly, but a gene was deemed "depleted" when its expression was higher in all other cell lineages than the E13.5 XY interstitium and endothelial cells in the example. The genes identified as E13.5 Leydig cell genes were removed from the E12.5 and E13.5 XY endothelial cell gene lists (Supplemental File

2A). In all cases, we used the E13.5 Leydig cell lists to remove the maximum number of genes associated with Leydig cells. Some of these genes were also identified in the XY interstitial lists, and they appear in both lists of genes (Supplemental File 2A), but the overlapping genes were removed from the Leydig cell bar for the graphical depiction (Figure 9A).

Permutation testing was done to estimate the false discovery rate in the gene lists. The array data from the samples being used in the generation of a gene list (in the first example above: XY supporting cells, XX supporting cells, XY interstitium, XY germ cells and XY endothelial cells; all at E12.5) were permuted. The series of operations was run on the permuted columns, and the number of genes generated from each permutation was stored. The permutations were performed 200 times, and the mean number of genes was used to compute the false discovery rate. In all cases, we considered a false discovery rate of 20% or less as acceptable (Supplemental File 2B). Most lists actually had a much lower false discovery rate. In any case where some of the genes were removed from the list, such as the removal of Leydig genes from endothelial cell lists, this operation was ignored in the permutation tests.

The lists of transcript clusters for the lists considered significant were inputted into DAVID (http://david.abcc.ncifcrf.gov/) (Huang da et al. 2009b, 2009a) to identify pathway and GO term enrichment. The full list of transcript clusters used in the analysis (Supplemental File 1A) was inputted as the background. We included all KEGG and

BioCarta pathways as well as GO_FAT molecular function (MF) and Biological Process (BP) terms with a p-value > 0.05 (Supplemental File 2C-D).

Primed genes were identified by multiple methods (Figures 12-13). In general, we defined a gene as primed when it was expressed in the progenitor, then repressed by one sex and maintained or activated by the other sex. To identify all male-primed genes, using germ cells as an example, we used the following pairwise comparisons:

1. The gene was identically expressed in XX and XY germ cells at E11.5 (i.e., identically expressed in progenitors).
2. The gene was more highly expressed in XY than XX germ cells at E13.5 (i.e., specific to XY cells).
3. The gene was more highly expressed in XX germ cells at E11.5 than at E13.5 (i.e., this gene is repressed in XX cells).
4. If the gene was also more highly expressed in XY germ cells at E11.5 than at E13.5, it was removed (i.e., genes showing differential repression were eliminated).

In the second analysis, we used more stringent criteria to define genes characteristic of the progenitor cells at E11.5 and differentiated cells at E13.5 by incorporating information on lineage-specific expression. To identify the enriched and primed genes, we used the above comparisons in addition to requiring that:

5. The gene was more highly expressed in XY germ cells at E11.5 than XY supporting cells, interstitium, and endothelial cells at E11.5.
6. The gene was more highly expressed in XX germ cells at E11.5 than XX supporting cells, stroma, and endothelial cells at E11.5.
7. The gene was more highly expressed in XY germ cells at E13.5 than XY supporting cells, interstitium, and endothelial cells at E13.5.

Finally, we also wanted to explore the possibility of depleted gene priming. Continuing with the example of XY germ cells, we used the following pairwise comparisons to identify depleted and primed genes:

1. The gene was identically expressed in XX and XY germ cells at E11.5 (i.e., identically expressed in progenitors).
2. The gene was more highly expressed in XY supporting cells, interstitium, and endothelial cells at E11.5 than XY germ cells at E11.5 (i.e., lineage specific repression).
3. The gene was more highly expressed in XX supporting cells, stroma, and endothelial cells at E11.5 than XX germ cells at E11.5.
4. The gene was more highly expressed in XX than XY germ cells at E13.5 (i.e., remains repressed in XY cells).

5. The gene was more highly expressed in XY supporting cells, interstitium, and endothelial cells at E13.5 than XY germ cells at E13.5 (i.e., lineage-specific repression).
6. The gene was more highly expressed in XX germ cells at E13.5 than at E11.5 (i.e., this gene is activated in XX cells).
7. If the gene was also more highly expressed in XY germ cells at E13.5 than at E11.5, it was removed (i.e., genes showing differential activation were eliminated).

The same methods were used to analyze priming in the supporting cells, but E12.5 was used as the end point of the analysis. Permutation tests were run on all of these lists of primed genes.

We then examined these primed genes in two ways. First, we compiled all genes identified as male or female-primed and determined the percentage associated with each sex (Figures 12B, D, and F; 13B, D, and F). We used a binomial test for the different extreme models to determine whether priming showed a sex-specific bias. A one-tailed test was used for the "female" and "male" models, which were defined as predicting that 90% of the genes were female-primed or male-primed, respectively. A two-tailed binomial test was used for the balanced model, which predicts 50% male and 50% female genes. Any model resulting in a p-value < 0.05 was excluded. If all models were excluded, an intermediate ("biased") model was selected.

To ensure that this result was not a statistical artifact of the size of the underlying lists of male and female markers, we also displayed primed genes as a percentage of the total "male" or "female" genes (Figures 12C, E, and G; 13C, E, and G). These male and female genes were determined in different ways to account for differences in the method of defining primed genes. When identifying all primed genes, the list of all male genes included everything identified in step 2 alone of the process for generating the primed genes. For the enriched and primed genes, male genes were required to meet the requirements of step 2 and 7. For the depleted and primed genes, male genes were required to meet steps 4 and 5. A 2x2 contingency table (with the actual numbers of genes, not percentages) and a two-tailed hypergeometric test were used to determine if there was a significant difference in the percentage of primed genes in the male and female programs. A p-value < 0.05 was considered significant. A significant p-value meant that sex and priming were not independent variables and that there was a bias in the representation of the two programs in the progenitor cells.

We further characterized the primed genes identified by each method based on their expression level. We divided these into two categories: similar and intermediate expression relative to the expression in the differentiated cells (Figures 12I-K and 13I-K). For similarly expressed genes, using XY germ cells as an example, the gene was required to be primed and identically expressed in XY germ cells at E11.5 and E13.5. For intermediate expression genes, the gene was required to be primed and more highly expressed in XY germ cells at E13.5 than E11.5 (or more highly expressed at E11.5 for depleted and primed genes). Any gene that did not fall into one of these categories, or had transcript clusters that fell into both similar and intermediate categories, was counted as "other." If a gene had transcript clusters that fell into the defined similar or intermediate categories and others that did not fall into either, the gene was still counted as similar or intermediate. GO term enrichment for all of the primed genes with similar expression for both supporting and germ cells was determined using DAVID as described above.

2.2.3 *Sf1-EGFP* microarray analysis

To examine earlier expression in supporting cells, we reanalyzed previously generated microarray data from *Sf1-EGFP* sorted cells (Nef et al. 2005) (raw data available at http://www.ebi.ac.uk/arrayexpress/browse.html?keywords=Nef&expandefo=on). Because these data used a different array format (Affymetrix Mouse Genome 430 2.0 arrays), they were analyzed separately. The .cel files were processed with Partek® Genomics Suite in the same manner as our own, and the same criteria were used to remove probe sets. The only difference was that rather than using the cross-hybridization category, the annotation grade was obtained from NetAffx (http://www.affymetrix.com) (Liu et al. 2003), and only probes with unambiguous A and B grade annotation were retained. Control probes were also removed.

We used the same method to identify and analyze primed genes as described above. This analysis used the *Sf1-EGFP* data at E11.0 (or E10.5) and E12.5 (Figures 14-15, Supplemental File 5). The priming analysis was limited to probes associated with the supporting cells by two methods, although the list of all primed genes is provided (Supplemental File 5A-B). First, we examined only genes that were lineage-specifically enriched in our XX or XY E12.5 *Sry-EGFP*/*Sox9-ECFP* data (Figure 9A, Supplemental File 2A) and *Sf1-EGFP* primed (Figures 14A, C-D, and G; 15A-B and E). Because different arrays were used, we compared between the data sets using the gene symbol. If the gene symbol for an *Sf1-EGFP* primed gene was also found in the lineage-specific *Sry-EGFP*/*Sox9-ECFP* lists, the gene was retained in the analysis. Second, we removed the genes associated with the interstitial/stromal cells at E12.5 from the *Sf1-EGFP* primed genes (Figures 14B, E-F, and H; 15C-D and F). Using XY cells as an example, we identified the genes to remove using the following pairwise comparisons and removal steps (illustrated in Figure 14B):

1. We identified genes more highly expressed in XY interstitial cells than XY supporting cells at E12.5.

2. We identified genes more highly expressed in XY supporting cells than XX supporting cells and also XY interstitial cells than XX stromal cells, then removed the genes identified in step 1.
3. We identified all genes more highly expressed in XY interstitial cells than the XX stromal cells, and removed all of the genes remaining in step 2. This list contains genes sexually dimorphic in the interstitial cells and not the supporting cells, and genes sexually dimorphic in both the interstitial/stromal cells and the supporting cells if expression was higher in the interstitial/stromal cells.

The lists of the genes identified for removal is provided in Supplemental File 5C. Again, the comparison between the two data sets was based on the gene symbol: gene symbols found in the interstitial/stromal-associated lists were removed from the *Sf1-EGFP* primed list.

To calculate the percentage of male and female genes showing priming (Figures 14D and F, and 15B and D), we used the same method used in analyzing all primed genes in our own data. However, in addition to being more highly expressed in one sex at E12.5, the total number of male or female genes was also required to pass the appropriate filter used for identifying supporting cell-associated genes.

2.3 Determining the mechanism of Fgf action

2.3.1 Mice

All animals were maintained and experiments were conducted according to DUMC-IACUC and NIH guidelines, based on existing protocols. A mixed background *Fgfr2*^{flox} line (Yu et al. 2003) was backcrossed multiple generations to C57BL/6, partly in the processes of crossing on the *Wnt4* null allele (Stark et al. 1994) and the *Sf1-Cre* allele (Bingham et al. 2006) that are maintained on C57BL/6. These mice were intercrossed to generate *Fgfr2*$^{flox/flox}$; *Wnt4*$^{+/-}$ mice, some of whom also had *Sf1-Cre*, and the line was maintained by intercrossing to preserve homozygosity at the *Fgfr2* locus. Timed matings were established between fertile *Sf1-Cre*; *Fgfr2*$^{flox/flox}$; *Wnt4*$^{+/-}$ males (see Figure 19 for explanation) and *Fgfr2*$^{flox/flox}$; *Wnt4*$^{+/-}$ females. Similar methods were also used to generate mice that had *Flk1-Cre* (Motoike et al. 2003) and *Fgfr2*$^{flox/+}$ to cross to *Fgfr2*$^{flox/flox}$ females. E0.5 was defined as noon on the day a mating plug was detected. Embryos were collected from pregnant females on the morning of day E13.5. The genotypes (Yu et al. 2003; Stark et al. 1994) and chromosomal sex (Munger et al. 2009) of the embryos were determined as previously described. We determined whether Cre was present using the primers 5′-CTGCCACGACCAAGTGACAGC-3′ (Dietrich et al. 2000) and 5′-CCAGGGCGCGAGTTGATAGC-3′. "Control" mice were all *Fgfr2*$^{flox/flox}$, negative for *Sf1-Cre*, and either *Wnt4*$^{+/-}$ or *Wnt4*$^{+/+}$.

Fgf9$^{+/-}$ (Colvin et al. 2001) and *Wnt4*$^{+/-}$ (Stark et al. 1994) were separately maintained as heterozygotes on the C57BL/6 strain. These mice were intercrossed to generate *Fgf9*$^{+/-}$; *Wnt4*$^{+/-}$ offspring, which were intercrossed to generate double mutant embryos. The genotypes and chromosomal sex of the embryos were determined as previously described (Munger et al. 2009; Colvin et al. 2001; Stark et al. 1994). Embryos were collected around E16.5-E17.5. Brightfield images of the gonads were collected on a Leica MZ12 following the dissection. "Control" mice were heterozygous or homozygous wild type at the *Fgf9* and *Wnt4* loci.

For qRT-PCR experiments, *Fgf9*$^{-/-}$ embryos and their wild type littermates were generated by intercrossing *Fgf9*$^{+/-}$ mice. For more precise staging, tail somites distal to the hindlimb were counted (Hacker et al. 1995). Embryos with 20-21 tail somites were considered E11.75 and used in the analysis. Gonads were dissected away from the mesonephros prior to RNA extraction.

2.3.2 Immunofluorescence

Gonads were immunostained as previously described (Cook et al. 2009). All E13.5 gonads were stained as whole mounts with the mesonephros attached. At/after E16.5, phenotypically female samples (including XY *Fgf9*$^{-/-}$ samples) were stained as whole mounts after removing mesonephric structures. The whole mount samples were either immunostained immediately, or processed through a methanol series and stored at -80ºC prior to rehydration and immunostaining (Barske and Capel 2010). Phenotypically male samples from E16.5 and after were cryosectioned after removing the mesonephric structures. Since the male and female samples were processed separately at E16.5-E17.5, we included CD-1 (Charles River) positive/negative controls in each batch of immunostained samples (e.g., E13.5 CD-1 male gonads were stained as whole mounts with the E16.5 female samples, and E16.5 CD-1 female gonads were cryosectioned and stained with the E16.5-E17.5 males).

Primary antibodies used were: anti-3β-HSD (Santa Cruz, sc-30820, 1:75 in samples processed through methanol; TransGenic Inc., KO607, 1:250), anti-AMH (MIS, Santa Cruz, sc-6886, 1:500), anti-CDH1 (Invitrogen, 13-1900, initially reconstituted in 400 µl, used at 1:250), anti-FOXL2 (Novus Biologicals, NB100-1277; 1:250), anti-NRP1 (R&D Biosystems, AF566, 1:350), anti-PECAM1 (CD31, BD Pharmingen, 553370, 1:250), anti-SCP3 (Abcam, ab15093, 1:500-1:1000), and anti-SOX9 (Millipore, AB5535, 1:3000-1:5000). Secondary antibodies used included Alexa 647- and 488- conjugated secondary antibodies (Molecular Probes, 1:500) and Cy3-conjugated secondary antibodies (Jackson ImmunoResearch, 1:500). DAPI (Sigma-Aldrich) was used to label nuclei. Samples were mounted in 2.5% DABCO (Sigma-Aldrich) in 90% glycerol.

Samples were immunostained at the same time as opposite sex controls to ensure that all antibodies were working properly. Samples stained at the same time were also imaged on a Leica SP2 confocal microscope at the same time. Leica confocal software, copyright 1997-2004, by Leica Microsystems Heidelberg GmbH was used to generate maximum intensity projections of multiple images along the Z axis (Figures 21 and 23). In some cases, multiple overlapping images were taken along the Y axis in a single Z plane, and these were assembled by eye to show the entire gonad and placed on a black background (Figures 19 and 24).

2.3.3 qRT-PCR

Isolated gonads were frozen at -80°C with or without RNA later (Ambion, AM7024). RNA was extracted as previously described (Munger et al. 2009), treated with DNaseI, and converted to cDNA using the iScript cDNA synthesis kit (Bio-Rad, 170-8891). cDNA samples were run in technical triplicate on a StepOnePlus Real-time PCR system (Applied Biosystems). The threshold and baseline were set manually. *Canx* was used as the normalizing gene (van den Bergen et al. 2009). Samples with variable technical replicates were excluded from the analysis. Generally, the average CT value of the technical replicates was inputted into the Rest 2009 software (Pfaffl 2001) available from Qiagen (www.qiagen.com) for analysis. If the difference in C_T values of technical triplicates exceeded 0.5, the outlier sample was excluded from the average. If no sample was an outlier, all replicates were retained so long as the difference in C_T values was less than 0.6. The reaction efficiency was determined by averaging the efficiency calculated from two or three independent dilution series with 4-5 points, and these are provided

(Table 1). The Rest 2009 software was used to calculate the expression level, standard error, and p-value. The list of primers is provided (Table 1), several of which have been previously published (Munger et al. 2009).

Table 1: Primers used for qRT-PCR

Gene	Forward primer	Reverse primer	Efficiency
Canx	5'-gacatgactcctcctgtaaaccct-3'	5'-cgtccatatcctcatcccaatcct-3'	1.00
Rspo1	5'-acggattcaggtccttcaagag-3'	5'-agggactccatctacgctactg-3'	0.98
Sox9	5'-tccagcaagaacaagccacac-3'	5'-tctcgttcagcagcctccag-3'	1.00
Wnt4	5'-ctgtctttgggaaggtggtg-3'	5'-cataggcgatgttgtccgag-3'	1.00

3. Transcriptional Profiling of Gonadal Cell Lineages

3.1 Summary

As part of the GenitoUrinary Molecular Anatomy Project (GUDMAP, http://www.gudmap.org/), we undertook a comprehensive transcriptome analysis of the four principle gonadal lineages (Figure 1) in XX and XY gonads at three time points, spanning the period from the undifferentiated bipotential stage until the cells adopt sex-specific fates. Our validated array data revealed similarities between lineages, and our analysis identified genes specifically depleted and enriched in each lineage as it underwent sex-specific differentiation.

3.2 Introduction

While some gonadal lineages have been studied at the transcriptome level in independent experiments (Bouma et al. 2010; Nef et al. 2005; Mise et al. 2008; Beverdam and Koopman 2006; Rolland et al. 2011; Bouma et al. 2007), these previous studies did not characterize the relationship of the lineages to each other, gene expression patterns beyond dimorphic expression (such as depletion), or the timing of differentiation. We used the markers available for the major cell types of the gonad (Figure 4) to isolate the different populations of gonadal cells and address specific questions related to their differentiation through a microarray analysis. Is there a sexually undifferentiated progenitor for each lineage with a common transcriptional program in XX and XY cells?

Are the lineages distinct by E11.5? Do all lineages adopt sex-specific fates at the same time? Is gene repression part of cell fate specification? The following section will answer these questions.

Figure 4: Lineage-specific fluorescent tags used for FACS.

Images of E13.5 XY and XX gonads with DAPI (blue) and each fluorescent marker used: *Sox9-ECFP* and *Sry-EGFP* (cyan) labeling supporting cells, *Mafb-EGFP* (purple) labeling the interstitial/stromal cells, *Oct4-EGFP* (green) labeling germ cells, and *Flk1-mCherry* (red) labeling endothelial cells. Scale bar = 100 μm.

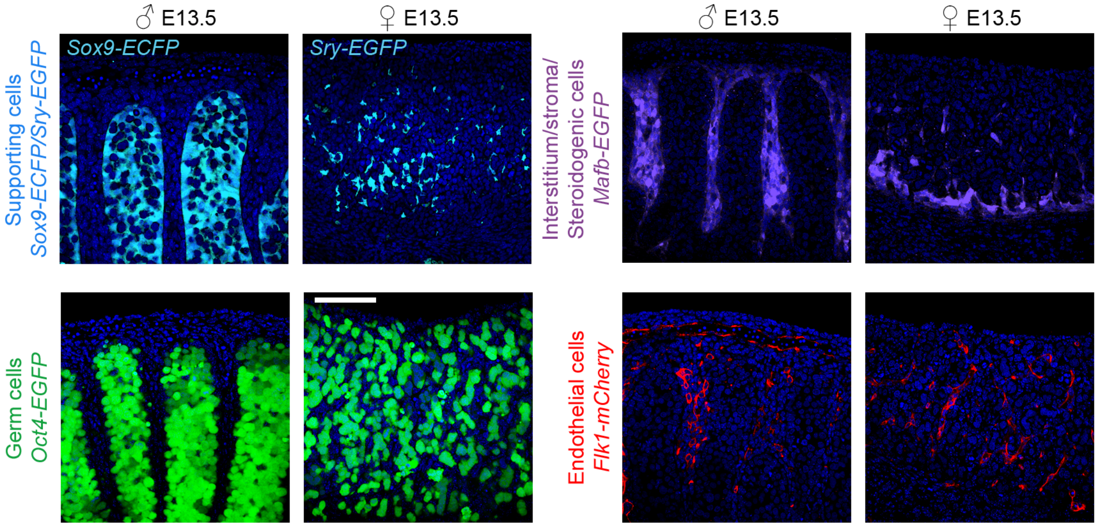
♂ E13.5
♀ E13.5
♂ E13.5
♀ E13.5
Supporting cells
Sox9-ECFP/Sry-EGFP
Sox9-ECFP
Sry-EGFP
Interstitium/stroma/
Steroidogenic cells
Mafb-EGFP
Germ cells
Oct4-EGFP
Endothelial cells
Flk1-mCherry

3.3 Results

3.3.1 Sorted cell microarrays accurately reflect known gene expression patterns

We quantified global gene expression in four lineages of the XX and XY developing mouse gonad at E11.5, E12.5, and E13.5. To isolate individual lineages, we utilized mouse lines expressing fluorescent cell-specific markers (Figures 1 and 4). The cells from separately pooled XX and XY gonads were isolated by fluorescence-activated cell sorting (FACS). *Sry-EGFP* (Albrecht and Eicher 2001) and *Sox9-ECFP* (Kim et al. 2007) were used as markers for supporting cells. In the *Sry-EGFP* line, the *Sry* promoter drives expression of GFP in cells competent to activate the *Sry* promoter in both XX and XY gonads. This labels the supporting cell lineage in both sexes, but because the transgene lacks the SRY open reading frame, transgenic XX gonads express no SRY protein and develop as normal ovaries (Albrecht and Eicher 2001). While *Sry-EGFP* expression persists in XX supporting cell precursors through E13.5, in our hands, expression of the transgene is reduced in XY supporting cell precursors after E11.5 (data not shown), similar to endogenous *Sry* expression (Bullejos and Koopman 2001). Therefore, we used *Sox9-ECFP*, an immediate downstream target of SRY (Sekido and Lovell-Badge 2008), to sort XY supporting cells at E12.5 and E13.5. XY interstitial cells and XX stromal cells were isolated using *Mafb-EGFP* (Moriguchi et al. 2006; DeFalco et al. 2011). The XY interstitial cells are excluded from testis cords and give rise to steroidogenic Leydig cells (DeFalco et al. 2011). The XX stroma is not defined morphologically, but for the purposes of this analysis, is defined as the population labeled with *Mafb-EGFP*. Germ cells were isolated using *Oct4-EGFP* (Szabo et al. 2002), and endothelial cells were isolated using *Flk1-mCherry* (Larina et al. 2009; Poche et al. 2009). After FACS, RNA purified from each XX and XY cell population was used to measure transcript abundance with Affymetrix Mouse Genechip Gene 1.0 ST Arrays. We produced 3 biological replicates for each population. The data are available in GEO (accession number GSM686202) and at http://www.gudmap.org/. RMA normalized values used in our analysis are provided with the capability to generate an expression graph for any gene, as a user-friendly resource for the community (Supplemental File 1).

We also isolated cells from the *αSma-EYFP* transgenic mouse (Cool et al. 2008) with the expectation that this reporter would label a larger population of the interstitium and stroma (Figure 5A). While this population resembled the interstitial/stromal population isolated with the *Mafb-EGFP* line (data not shown), unlike the *Mafb-EGFP* positive cells, the *αSma-EYFP* cells also expressed high levels of *Sry* at E11.5, a gene predicted to be specific to XY supporting cells (Sekido et al. 2004) (Figure 5B). Indeed, E11.5 *αSma-EYFP* cells stained positive for both SRY and SOX9 protein (Figure 5C). Consequently, at least early in development, it appears that *αSma-EYFP* labels a heterogeneous population of cells containing supporting cells as well as interstitial/stromal cells. While this finding may have biological significance, it could also result from leaky expression of the *αSma-EYFP* transgene. Thus, we excluded the *αSma-EYFP* data from this analysis but have made the data available with the rest of the microarrays.

Figure 5: *αSma-EYFP* labeled a heterogeneous population containing supporting cell precursors.

(A) Images of E13.5 XY and XX gonads with DAPI (blue) and *αSma-EYFP* (pink) labeling the interstitial/stromal cells. (B) Graphs of the log-transformed, normalized intensity values. The error bars are standard error. The *Sry* transcript is expressed at similarly high levels in both XY supporting cells and *αSma-EYFP* cells at E11.5, and declines rapidly in both cell types. Expression of *Sry* is lower in the *Mafb-EGFP* cells. However, the pattern seen with *Sry* did not hold true for most supporting cell markers: *Sox9* is expressed at a lower level in both *αSma-EYFP* and *Mafb-EGFP* cells than in supporting cells. (C) SRY and SOX9 proteins are also present in *αSma-EYFP* cells. Antibodies against SRY (red) and SOX9 (blue) co-label *αSma-EYFP* (green) cells. Cells with *αSma-EYFP* and SRY alone are indicated with arrows, whereas cells with *αSma-EYFP*, SRY, and SOX9 are indicated with arrowheads. Scale bar = 25 μm. This suggests that *αSma-EYFP* is expressed in a heterogeneous population of early gonadal cells containing supporting cell progenitors.

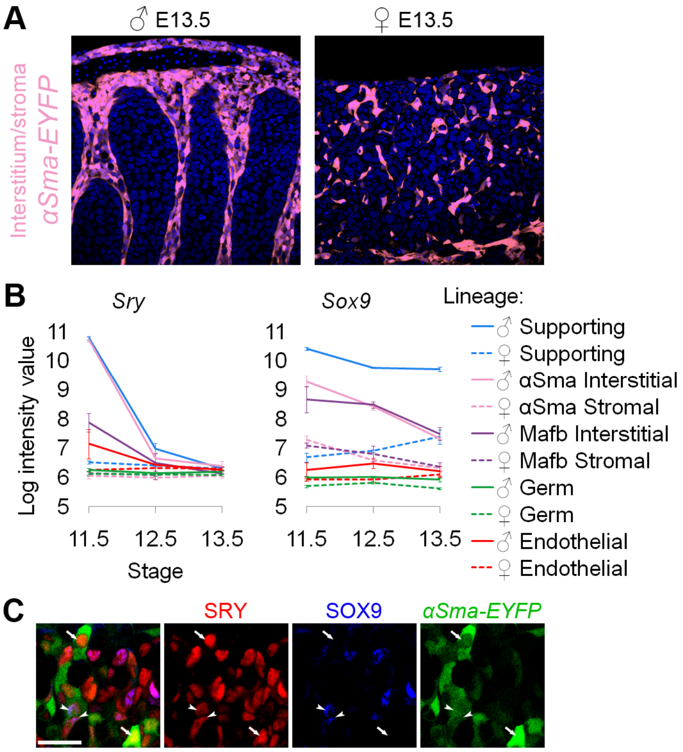
A
♂ E13.5
♀ E13.5
Interstitium/stroma
αSma-EYFP
B
Sry
Sox9
Log intensity value
11
10
9
8
7
6
5
11.5
12.5
13.5
Stage
Lineage:
♂ Supporting
♀ Supporting
♂ αSma Interstitial
♀ αSma Stromal
♂ Mafb Interstitial
♀ Mafb Stromal
♂ Germ
♀ Germ
♂ Endothelial
♀ Endothelial
C
SRY
SOX9
αSma-EYFP

To validate the cell sorting and microarray data, we examined the expression of genes known to be specific to each of the cell populations (Figure 6A). The expression of each control gene was consistent with previous reports: *Dhh* (desert hedgehog) was enriched in XY supporting cells (Bouma et al. 2010), *Wnt4* (wingless-related MMTV integration site 4) was enriched in XX supporting cells (Bouma et al. 2010), *Inhba* (inhibin beta-A) was enriched in the XY interstitium (Yao et al. 2006; Jeanes et al. 2005), *Nanos2* (nanos homolog 2) was enriched in XY germ cells (Tsuda et al. 2003), *Stra8* (stimulated by retinoic acid gene 8) was enriched in XX germ cells (Menke et al. 2003), and *Flt1* (FMS-like tyrosine kinase 1, VEGFR1) was enriched in endothelial cells (Fong et al. 1995). Therefore, the microarrays on the sorted cell populations accurately reflected gene expression patterns that were previously characterized for each of the cell lineages.

Figure 6: Microarray validation.

(A-B and E) Graphs of the log-transformed, normalized intensity values from the microarrays for control genes known to be specific to each lineage. The color for each lineage is conserved in all figures and matches the illustration in Figure 1, with XX values shown as dashed lines, and XY values shown as solid lines. The error bars are standard error of the mean ("standard error") of the log transformed value. The Y-axis scale differs for each graph because each transcript cluster has its own intensity range. (A) The control genes were found in the expected lineage, except for (B) genes characteristic of Leydig cells. Leydig cell genes were highly expressed in both the interstitium (as expected) and the endothelial cell fraction. (C-D) Immunofluorescence of E13.5 XY gonads with *Flk1-mCherry* (red), (C) PECAM1 (germ and endothelial cells, blue) or (D) FLK1 (blue), and 3β-HSD (green). Arrowheads indicate *Flk1-mCherry* and (C) PECAM1 or (D) FLK1 double positive endothelial cells. Arrows indicate *Flk1-mCherry* positive, (C) PECAM1 or (D) FLK1 negative cells that were positive for 3β-HSD, confirming aberrant reporter expression in Leydig cells, and indicating that the contamination of the endothelial population was due to leaky expression of the *Flk1-mCherry* transgene in Leydig cells rather than genuine *Flk1* expression in Leydig cells (interstitium). Scale bar = 25 μm. (E) This was also confirmed by the low level expression of *Flk1* (*Kdr*) transcript in the XY interstitium.

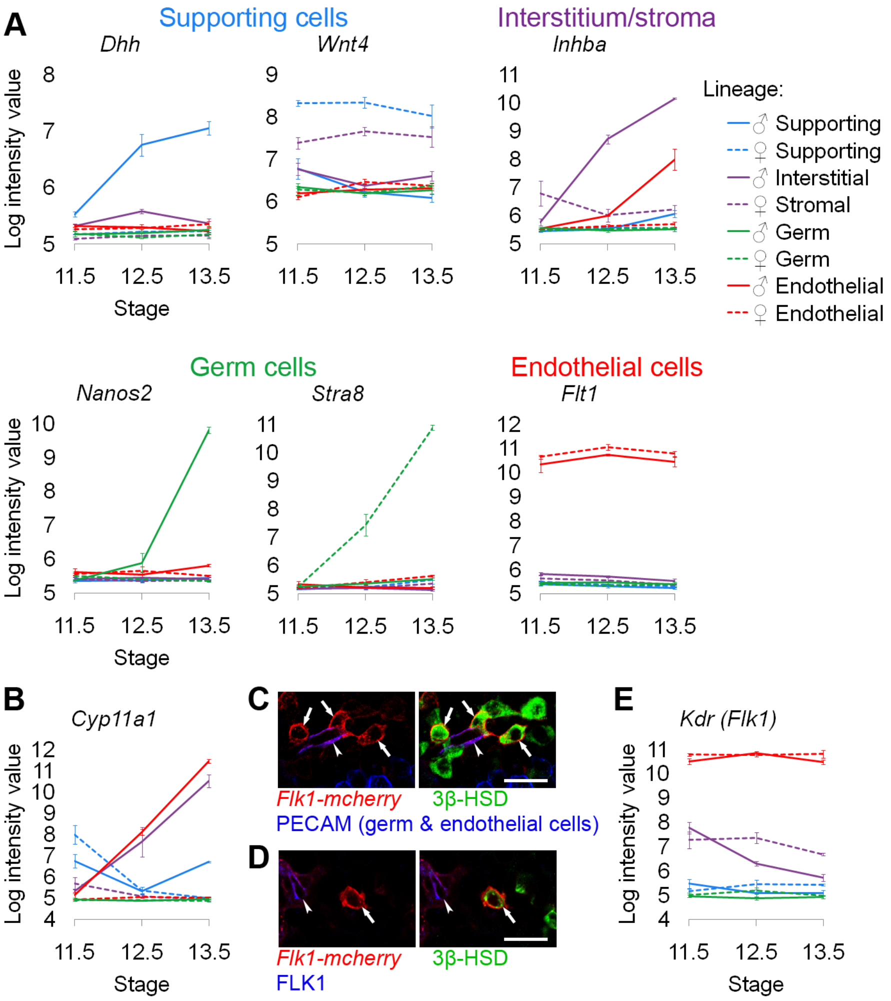
A
Supporting cells
Dhh
Wnt4
Interstitium/stroma
Inhba
Log intensity value
Stage
11.5
12.5
13.5
Lineage:
♂ Supporting
♀ Supporting
♂ Interstitial
♀ Stromal
♂ Germ
♀ Germ
♂ Endothelial
♀ Endothelial
Germ cells
Nanos2
Stra8
Endothelial cells
Flt1
B
Cyp11a1
C
Flk1-mcherry
3β-HSD
PECAM (germ & endothelial cells)
D
Flk1-mcherry
3β-HSD
FLK1
E
Kdr (Flk1)

An unexpected expression pattern was observed in XY *Flk1-mCherry*-positive cells (Figure 6B). We found that genes expressed in Leydig cells, such as *Cyp11a1* (SCC) (Ikeda et al. 1994), were enriched in both XY interstitial (containing steroidogenic Leydig cells) and *Flk1-mCherry*-positive "endothelial" populations. This was surprising given that steroidogenic enzymes have not previously been reported in endothelial cells (DeFalco et al. 2011). To investigate the basis for this finding, we stained E13.5 *Flk1-mCherry* gonads with the vascular marker PECAM1 and an antibody against the Leydig cell marker 3β-HSD. We found *Flk1-mCherry*-positive cells that were negative for the vascular marker, but positive for the Leydig marker (Figure 6C). This suggests that the *Flk1-mCherry* transgene was ectopically expressed in Leydig cells. Consistent with this idea, we did not detect expression of either the FLK1 protein (Figure 6D) or high levels of the corresponding transcript (*Kdr*) (Figure 6E) in the interstitial cells. We concluded that the source of the Leydig cell contamination was leaky expression of the *Flk1-mCherry* transgene in Leydig cells. While this result complicated our analysis of the endothelial population, it provided strong evidence that the microarray data accurately reflected gene expression in the sorted populations.

3.3.2 Lineage, sex, and stage all influence gene expression

To investigate the effects of cell lineage, sex, and stage on global gene expression and to validate the consistency of expression measurements in biological replicates, we clustered all 72 individual microarrays based on the expression of transcript clusters that met our inclusion criteria outlined in the Materials and Methods (Figure 7A). With the exception of one E11.5 XY endothelial array (see Materials and Methods), biological replicates, and even samples of different sexes (early XX and XY germ cells) or stages (late XX supporting cells) that were expected to be similar, showed consistent expression patterns as indicated by the tight clustering of those samples (Figure 7A). This again validates the quality of the microarray data.

Figure 7: Gene expression was affected by lineage, sex, and stage.

(A) Clustering dendrogram of individual microarray samples. The E11.5, E12.5, and E13.5 samples are represented by short, intermediate, and long bars, respectively. The dashed bars indicate XX (♀) samples, and the solid bars indicate XY (♂) samples. Ward's method with squared Euclidean distance as the distance metric was used. The arrays cluster primarily by lineage, and secondarily by sex and stage. (B) Analysis of the sources of variation confirmed that the primary source of variation is lineage, and secondarily sex and stage.

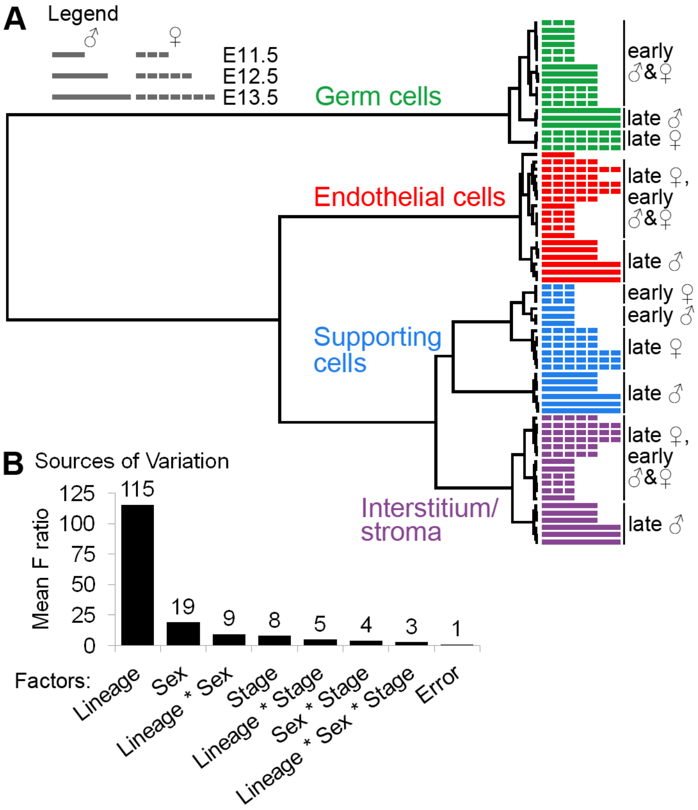
A
Legend
♂
♀
E11.5
E12.5
E13.5
Germ cells
Endothelial cells
Supporting cells
Interstitium/ stroma
early ♂&♀
late ♂
late ♀
late ♀, early ♂&♀
late ♂
early ♀
early ♂
late ♀
late ♂
late ♀, early ♂&♀
late ♂
B
Sources of Variation
Mean F ratio
125
100
75
50
25
0
115
19
9
8
5
4
3
1
Factors:
Lineage
Sex
Lineage * Sex
Stage
Lineage * Stage
Sex * Stage
Lineage * Sex * Stage
Error

The dendrogram indicates that cell lineage is the most significant factor affecting gene expression. The same general patterns were observed using other clustering methods (Figure 8A-B). This result was confirmed by an analysis of the sources of variation (ANOVA), in which lineage was identified as the most significant factor influencing gene expression variation (Figures 7B and 8C). Interstitial/stromal cells were distinct from supporting cells at all stages, indicating that, despite their shared origin (Karl and Capel 1998), these are separate lineages by E11.5.

Figure 8: Alternative methods showed generally similar patterns indicating the importance of lineage, sex, and stage.

Clustering dendrograms of the individual arrays generated using (A) Average linkage with Euclidean distance as a distance metric and (B) Complete linkage with Pearson's dissimilarity as a distance metric. Consistent with Figure 7A, the arrays cluster primarily by lineage, and secondarily by sex and stage. The largest differences were in the relationship of the somatic populations to each other, although the same clusters could always be identified. (C) Examining the sources of variation with the median F ratio shows a similar pattern to the mean F ratio (Figure 7B) with the primary source of variation being lineage.

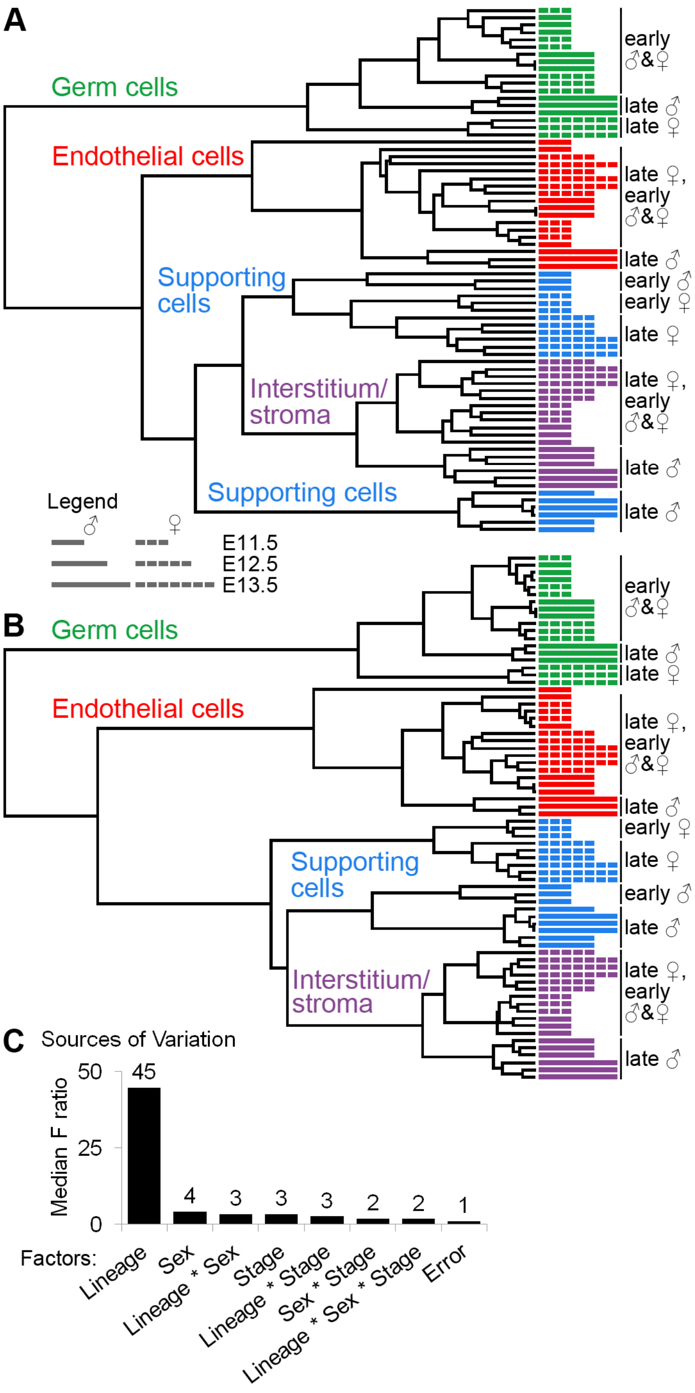
A
Germ cells
Endothelial cells
Supporting cells
Interstitium/ stroma
Supporting cells
early ♂&♀
late ♂
late ♀
late ♀, early ♂&♀
late ♂
early ♂
early ♀
late ♀
late ♀, early ♂&♀
late ♂
late ♂
Legend
♂
♀
E11.5
E12.5
E13.5
B
Germ cells
Endothelial cells
Supporting cells
Interstitium/ stroma
early ♂&♀
late ♂
late ♀
late ♀, early ♂&♀
late ♂
early ♀
late ♀
early ♂
late ♂
late ♀, early ♂&♀
late ♂
C
Sources of Variation
Median F ratio
50
25
0
45
4
3
3
3
2
2
1
Factors:
Lineage
Sex
Lineage * Sex
Stage
Lineage * Stage
Sex * Stage
Lineage * Sex * Stage
Error

Sex and stage were also sources of expression variation in the gonadal cell populations, albeit to a lesser extent than lineage (Figure 7A-B). XY and XX supporting cells clustered in distinct groups at E11.5, confirming that these cells embark on their sex-specific differentiation by E11.5 (Nef et al. 2005; Bouma et al. 2010). There was no distinction between the sexes in the other cell types until E12.5 or E13.5. While the late stage XY endothelial cells clustered away from the early XX and XY endothelial cells, this could be due to the sex-specific contamination by Leydig cells. In summary, this analysis confirms the high quality of the data and shows that each lineage is distinct from E11.5 onwards.

3.3.3 Each lineage has uniquely expressed enriched and depleted genes that provide insight into the biology of the cells.

To explore the differences between the cell types apparent in the dendrogram, we identified "lineage-specific" genes that were specifically enriched and depleted in each lineage relative to the other lineages at each stage. We then determined whether these genes were expressed in a "sex-specific" (expression was different between XY and XX samples) or a "sex-independent" (expression was similar in XY and XX samples) manner. We identified these genes by performing multiple pairwise comparisons on the normalized array values (similar to (Beckervordersandforth et al. 2010)) with a p-value cutoff of 0.05 and a fold change cutoff of 1.5. "Enriched" genes were more highly expressed than in other lineages, and "depleted" genes were less highly expressed than in other lineages. Examples of genes showing these different patterns include the sex-specific enrichment of *Dhh* in XY supporting cells (Figures 6A and 9A), the sex-independent enrichment of *Flt1* in XX and XY endothelial cells (Figures 6A and 9A), the sex-specific depletion of *Ccna2* (cyclin A2) in XX supporting cells (Figure 9A-B), and the sex-independent depletion of *Gata6* (GATA binding protein 6) in germ cells (Figure 9A-B). A full description of our statistical methods is provided in Materials and Methods and a list of all genes identified appears in Supplemental File 2A.

Due to the sex-specific Leydig cell contamination of the endothelial population after E11.5 (Figure 6B-E), we present the gene lists (Supplemental File 2A) but not the graphs (Figure 9A) because we could not determine whether sex-specific gene expression was due to an artifact of the contamination or genuine differences in endothelial cells. We deduced a list of Leydig cell genes (Figure 9A, Supplemental File 2A) by identifying genes specifically up-regulated in both XY endothelial cells and interstitial cells at E12.5 and E13.5. These genes were removed from XY endothelial gene lists at E12.5 and E13.5 (Supplemental File 2A).

Figure 9: Lineage-specific enriched and depleted genes revealed distinct differentiation programs.

(A) Graphs of the number of genes specific to each lineage. The gene lists and permutation tests are provided in Supplemental File 2. The "♂" and "♀" symbols indicate lineage-specific and sex-specific genes, while the "♂+♀" symbol indicates genes that are lineage-specific and sex-independent. Pale bars below the axis indicate genes that are depleted. The E11.5 graphs are on the top row, E12.5 graphs are in the middle, and the E13.5 graphs are on the bottom row. The germ cell Y-axis is scaled to accommodate the larger number of genes specific to this lineage. Leydig cell genes (burgundy) were separately identified by cross-referencing the endothelial and interstitial data and added to the bars for the XY interstitium. Lists with > 20% false positives are indicated by "ns". Lists with no genes are marked with "0". Some bars also have a colored gene name exemplifying the pattern within that category (the graphs for *Dhh* and *Flt1* appear in Figure 6A). (B) Graphs of the log-transformed, normalized intensity values for genes that are sex-specifically (*Ccna2*) and sex-independently (*Gata6*) depleted. The error bars are standard error. Three lineages showed specific gene depletion in addition to enrichment. Each lineage had transcriptionally distinct progenitors as indicated by "♂+♀" genes at E11.5. Supporting cells were already in the midst of their sex-specific differentiation by E11.5 as indicated by genes in the "♂" or "♀" columns at E11.5, but the other cell types were sexually undifferentiated at E11.5.

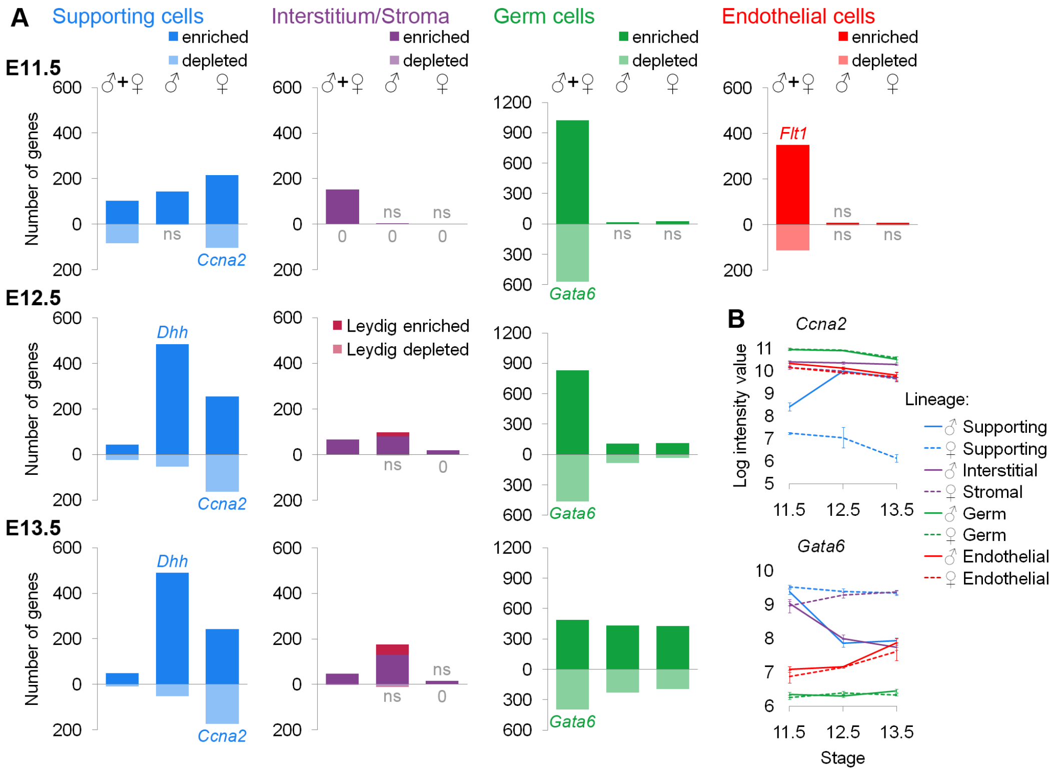
A
Supporting cells
enriched
depleted
Interstitium/Stroma
enriched
depleted
Germ cells
enriched
depleted
Endothelial cells
enriched
depleted
E11.5
♂+♀
♂
♀
Number of genes
600
400
200
0
200
ns
Ccna2
0
Flt1
Gata6
1200
900
600
300
E12.5
Dhh
Leydig enriched
Leydig depleted
E13.5
B
Ccna2
Log intensity value
11
10
9
8
7
6
5
11.5
12.5
13.5
Lineage:
♂ Supporting
♀ Supporting
♂ Interstitial
♀ Stromal
♂ Germ
♀ Germ
♂ Endothelial
♀ Endothelial
Gata6
Stage

To evaluate these lists, we first performed permutation testing (Supplemental File 2B), and considered those with a false positive rate < 20% as acceptable (lists that did not pass this test are marked "ns") (Figure 9A). Second, we determined whether positive control genes with known expression patterns, such as the expression of *Sox9* in XY supporting cells, were found in the expected lists (Supplemental File 2B). Third, we interrogated all significant lists in Figure 3 (not "ns" or "0") for enrichment of Biocarta and KEGG pathways (Supplemental File 2C) as well as GO terms (Supplemental File 2D). As evidence of the high quality of the sorted cell microarray data, functional annotation of the enriched/depleted lists identified expected terms for each cell type: germ cell development in the germ cell lists, steroid production in interstitial and Leydig lists, vascular development in the endothelial list, and sex determination in supporting cell lists (Supplemental File 2C-D).

This analysis identified several novel expression features of these cells. For example, all of the lineages had sex-specific and sex-independent cohorts of depleted genes, with the exception of interstitial/stromal cells (Figure 9A). The genes identified as depleted appear biologically relevant based on individual genes and enriched categories of genes. Both XY and XX germ cells repressed *Gata6* (Figure 9B, Supplemental File 2A), which can drive embryonic stem cells to adopt the extraembryonic endoderm fate (Fujikura et al. 2002). Thus, the repression of *Gata6* may be important for maintaining a totipotent transcriptional state in germ cells. Similarly, *Lef1* became sex-specifically depleted in XY supporting cells (Supplemental File 2A). *Lef1* can interact with β-catenin in a transcriptional complex downstream of Wnt signaling (Huber et al. 1996), and this pathway antagonizes aspects of testis development (Kim et al. 2006; Maatouk et al. 2008; Vainio et al. 1999). Thus, the depletion of *Lef1* may be important for maintaining the male supporting cell fate. The sex-specifically depleted genes in XX supporting cells were enriched for multiple cell cycle-related pathways and GO terms (Supplemental File 2C-D). Interestingly, both XX and XY supporting cells are arrested at E11.5 and only XY supporting cells re-enter the cell cycle; XX supporting cells remain non-proliferative (Schmahl et al. 2000; Mork et al. 2011). It was previously shown that XX cells express higher levels of cell cycle inhibitors (Nef et al. 2005) and that cell cycle genes are over-represented in XY supporting cells (Bouma et al. 2007). However, our data suggest a mechanism of cell cycle arrest involving the active repression of multiple genes important for cell cycle progression in XX supporting cells.

Additionally, we identified transcripts associated with a sexually undifferentiated progenitor cell for each lineage. All cell types had a large number of genes that were lineage-specific and sex-independent at E11.5 (Figure 9A, "♂+♀" category). The identification of shared expression in XX and XY cells demonstrates that there is a sexually undifferentiated progenitor for each lineage with a distinct transcriptional state. This was consistent with previous data showing that XX and XY supporting cells have a common origin (Albrecht and Eicher 2001) as well as the clustering results showing that supporting cells and interstitial/stromal cells are distinct lineages by E11.5 (Figure 7A).

Supporting cells exhibited the largest number of sexually dimorphic genes at E11.5 (Figure 9A, "♂" or "♀" categories). This is consistent with previous evidence that the supporting cell lineage adopts a sex-specific fate early in gonad development and instructs the other lineages as to which fate they should adopt (Bouma et al. 2010; Burgoyne et al. 1988; Sekido et al. 2004; Adams and McLaren 2002). Although it was clear that supporting cells began sex-specific differentiation by E11.5, XX and XY supporting cells still expressed sex-independent genes. Since the supporting cells are in the midst of their sex-specific differentiation at E11.5, the sex-independent genes likely represent remnants of the sexually-undifferentiated progenitor state. The XX and XY supporting cells appear to adopt their distinct sex-specific states by E12.5, as there was little change in expression between E12.5 and E13.5.

The other three cell types exhibited few sex-specific genes at E11.5 (Figure 9A, categories "♂" and "♀"), showing that the differentiation of these lineages is delayed relative to that of the supporting cells. Germ cells and interstitial/stromal cells began to adopt lineage-specific, sex-specific transcriptional states by E12.5, a process that was further advanced by E13.5. This was again consistent with the dendrogram (Figure 7A). We identified few lineage-specific genes in the XX stroma at these stages.

3.3.4 The XX stroma and supporting cells express some of the same genes

To explore why the XX stroma had little lineage-specific expression, we examined a broader category of genes over-expressed (“sexually dimorphic”) in XY or XX cells of each lineage at each stage compared to the opposite sex. Genes were identified by a single pairwise comparison between XX and XY cells for each lineage at each stage (Supplemental File 3A). Many more genes were identified by this analysis (Figure 10) than in the lineage-specific analysis (Figure 9) because of the additional pairwise comparisons to restrict the analysis to lineage-specific genes (Figure 9). While genes were over-expressed in XX stromal cells when compared only to XY interstitial cells, most were also dimorphic in another lineage (Figure 10A).

Figure 10: Overlap between lineages of genes that are sexually dimorphic.

The number of genes over-expressed ("sexually dimorphic") in XY or XX cells of each lineage at each stage. The area proportional Venn diagrams were generated using Venn Diagram Plotter v1.4.3740 from PNNL and OMICS.PNL.GOV (http://omics.pnl.gov/software/VennDiagramPlotter.php). The sizing of the Venn diagrams relative to each other is approximate. Endothelial cells were not analyzed. The numbers shown indicate the number of genes exclusively in each portion of the diagram (except for E11.5 for which the total number of genes dimorphic in the supporting cells is shown). Lists marked "ns" had a false positive rate > 20% (Supplemental File 3B). The overlapping areas on the Venn diagrams indicate genes sexually dimorphic in multiple lineages. (B-D) Graphs of the log-transformed, normalized intensity values. The error bars are standard error. Endothelial cell values are not shown. (B) Many genes sexually dimorphic in multiple lineages were over-expressed in one of the lineages, as was the case for *Sox9*. However, some genes were highly expressed in multiple lineages, such as *Axin2* (C) in all three XX lineages and *Irx3* (D) in the XX stroma and supporting cells. (E) The number of genes in the in the overlap between the interstitium/stroma and supporting cells of each sex that were identically and highly expressed in both of those lineages.

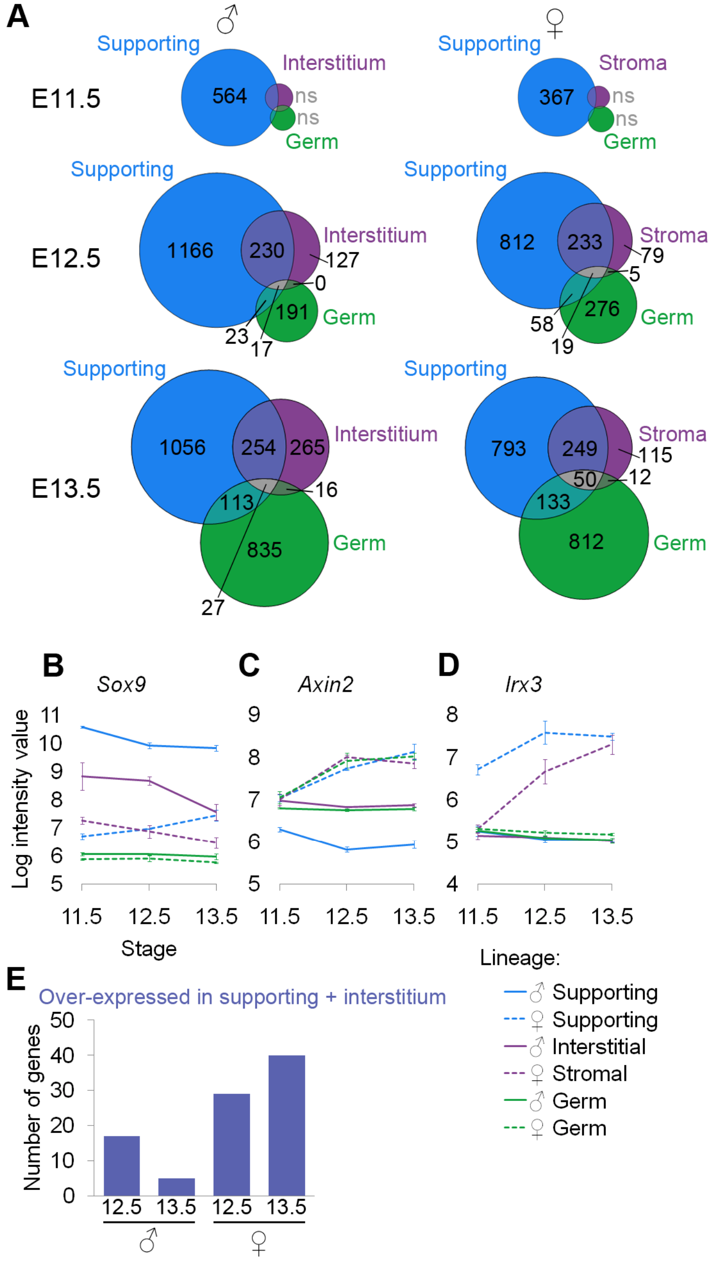
A
♂
♀
E11.5
Supporting
564
Interstitium
ns
ns
Germ
Supporting
367
Stroma
ns
ns
Germ
E12.5
Supporting
1166
230
Interstitium
127
0
191
Germ
23
17
Supporting
812
233
Stroma
79
5
276
Germ
58
19
E13.5
Supporting
1056
254
265
Interstitium
16
113
835
Germ
27
Supporting
793
249
Stroma
115
50
12
133
812
Germ
B
Sox9
C
Axin2
D
Irx3
Log intensity value
11
10
9
8
7
6
5
9
8
7
6
5
8
7
6
5
4
11.5
12.5
13.5
11.5
12.5
13.5
11.5
12.5
13.5
Stage
Lineage:
♂ Supporting
♀ Supporting
♂ Interstitial
♀ Stromal
♂ Germ
♀ Germ
E
Over-expressed in supporting + interstitium
Number of genes
50
40
30
20
10
0
12.5
13.5
12.5
13.5
♂
♀

In many cases of overlapping expression, the genes sexually dimorphic in multiple lineages were over-expressed in one of those lineages when compared to the other, as was the case for *Sox9* (Figure 10B). This could be explained by the low and variable contamination expected after FACS. To address this issue, we used antibody stains of sorted cells to estimate that the XY E13.5 germ cells had < 1% contamination with supporting cells, but the XY E13.5 interstitium was more variable and had between 1% and 15% supporting cell contamination (data not shown). Thus, these expression patterns were not further characterized.

However, not all genes sexually dimorphic in multiple lineages had a pattern consistent with low level contamination. While intermediate levels of expression are consistent with contamination, equally high levels of expression in multiple lineages are not. For example, *Axin2*, a Wnt/β-catenin transcriptional target gene (Jho et al. 2002), was highly expressed in the three XX cell types examined, indicative of widespread Wnt signaling in the ovary (Figure 10C). Similarly, *Irx3* (Iroquois related homeobox 3), a gene known to be ovary-specific (Jorgensen and Gao 2005), showed convergent expression in the XX stroma and supporting cells (Figure 10D).

We identified genes with a pattern similar to *Irx3* as sexually dimorphic in only two lineages, expressed identically in both lineages, and enriched in these two lineages compared to the remaining two (Supplemental File 3C). Genes sexually dimorphic in all three lineages, like *Axin2*, were not analyzed. There were few genes like *Irx3* that met the required criteria in the overlap between the germ cells and other lineages (Supplemental File 3C), but more genes met these criteria in the overlap between interstitial/stromal cells and supporting cells (Figure 10E, Supplemental File 3C).

The XX stroma in particular expressed several transcripts at similar levels to the XX supporting cells (Figure 10E), although the populations are not identical as the XX supporting cells have many more lineage-specific transcripts (Figure 9). Some of these shared transcripts are downstream of *Wnt4* signaling in the ovary (*Calb1*, *Fgfr2*, *Irx3*, *Sema3a*, and *Tkt*) (Supplemental File 3C) (Coveney et al. 2008b), and *Wnt4* itself showed this pattern. Thus, at least some of these similarities may be attributable to widespread Wnt signaling in the ovary, as reported by *Axin2* expression in all 3 lineages (Figure 10C). Regardless of the cause, the XX supporting cells and stroma share the expression of some female-associated genes (Supplemental File 3C).

3.4 Discussion

3.4.1 Insights from whole transcriptome characterization of multiple gonadal lineages

We characterized the transcriptomes of undifferentiated progenitors and analyzed their transition to sexually differentiated cells. All four lineages analyzed (including interstitial/stromal cells) have a sexually undifferentiated progenitor cell with a distinct transcriptome. Although we detected some overlapping sexually dimorphic expression patterns that may have biological significance between the supporting cells and interstitial/stromal cells (Figure 10), these lineages have transcriptionally distinct progenitors at E11.5 (Figure 9). However, the differentiation of the interstitial and stromal cells is sexually asymmetric over this time period (Figure 11). Whereas the XY interstitium expressed lineage-specific transcripts, there were few lineage-specific transcripts in XX stromal cells even at E13.5 (Figure 9). Thus, the XX stroma may not fully differentiate until after E13.5. However, the XX stroma also showed overlapping sexually dimorphic expression with XX supporting cells, possibly due to pathways downstream of widespread Wnt signaling in the ovary (Figure 10).

Figure 11: Model of differentiation for the interstitial/stromal lineage.

The interstitial/stromal cells differentiate asymmetrically over the time period examined, as we detected few genes specific to the XX stroma by E13.5, whereas, the XY interstitial population acquired a larger set of lineage-specific genes.

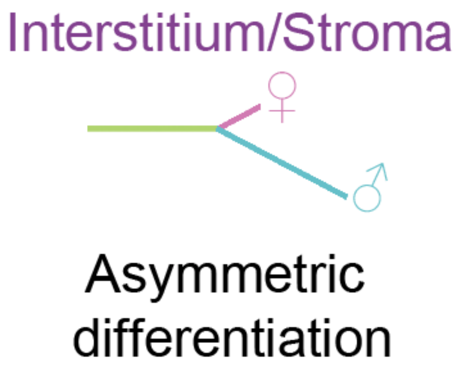
Interstitium/Stroma
♀
♂
Asymmetric differentiation

We also provided global transcriptional evidence that the supporting cells are the first cell type in the gonad to adopt a sex-specific fate (Figure 9) as predicted by previous experiments (Bouma et al. 2010; Nef et al. 2005; Burgoyne et al. 1988; Sekido et al. 2004). While there are some gene expression differences between E12.5 and E13.5, the supporting cells appear to have adopted their sex-specific fates by E12.5 (Figure 9). The sex-specific differentiation of interstitial/stromal cells and germ cells began at E12.5, when the supporting cells had essentially completed their differentiation process (Figure 9). This is consistent with the previous evidence that the supporting cell lineage instructs the other lineages as to which fate they should adopt (Bouma et al. 2010; Burgoyne et al. 1988; Sekido et al. 2004; Adams and McLaren 2002).

3.4.2 Lineage- and sex-specific transcriptional depletion in the differentiating gonad

For supporting cells, germ cells, and endothelial cells, our methods were sensitive enough to detect lineage-specific transcript depletion that could be sex-specific or sex-independent (Figure 9). Given that other studies have also reported specific gene depletion (Brady et al. 2007; Saitou et al. 2002), this likely represents a common regulatory logic in the transcription network of differentiating cells. For example, unique cell fate specification in the sea urchin involves the repression of widely-expressed genes to "lock-down" the selected fate (Davidson et al. 2002). We detected the lineage-specific repression of transcription factors likely involved in specifying alternative fates in both germ and supporting cells (i.e., *Gata6* and *Lef1*, Figure 9, Supplemental File 2A). We also found evidence for lineage-specific repression of genes that regulate cell behavior. The transcriptome of XX supporting cells is characterized by the sex- and lineage-specific repression of cell cycle genes (Figure 9, Supplemental File 2), which is correlated with the failure of XX supporting cells to reenter the cell cycle (Schmahl et al. 2000; Mork et al. 2011). A similar phenomenon was reported in senescence and DNA damage arrest (Larsson et al. 2004; Badie et al. 2000), indicating this may be a widely-used mechanism of cell cycle arrest.

Contrary to our findings in the other lineages, we did not detect lineage-specifically depleted genes in the XY interstitial or XX stromal cells. However, there may be heterogeneity within this population that masks repression characteristic of any one subfraction. Since the purity of the germ and supporting cell populations were likely important for detecting depletion, the ability to isolate distinct populations within the interstitium/stroma may be necessary to do the same for this population. Alternatively, repression may be a characteristic of fate commitment, and its absence in this population may reflect a more undifferentiated state.

4. Lineage priming of Sexual Fate in Gonadal Cells

4.1 Summary

The analysis in chapter 3 defined the transcriptome shared between XX and XY progenitors for each lineage, and traced the timing of differentiation and acquisition of sex specific fate for each cell type. Informed by this analysis, we investigated whether the transcriptome shared by XX and XY progenitors in the germ cell and supporting cell lineages showed evidence of lineage priming toward the female or male fate. We identified different variations of biased lineage priming in these gonadal lineages. The germ cells showed male-biased priming and the supporting cells showed female-biased priming. To reach this conclusion, we analyzed the data in multiple ways, and in the case of the supporting cells used multiple data sets. In addition to identifying lineage priming, we also found that these primed genes were expressed at a high level in the sexually undifferentiated progenitor cells. This provides a molecular explanation reconciling the female default and balanced models of sex determination. In addition, it affords insight into the mechanisms by which different cell types in a single organ adopt their respective fates.

4.2 Introduction

While this type of comprehensive transcriptome analysis has been performed in other developing systems (Brady et al. 2007; Brunskill et al. 2008), the relative simplicity of the gonad and the theoretical framework for sex determination allowed us to extend our analysis to test distinct models for the process of cell fate determination, and to evaluate the fit of these models to the theories of sex determination that have been proposed in the past 50 years.

Four predominant models have been proposed to account for gonad differentiation. It has been proposed that (1) the female state is a default pathway (McLaren 1991; Jost 1947), (2) a female "Z" gene actively represses the male program (McElreavey et al. 1993), (3) both the female and male programs are actively initialized (Eicher and Washburn 1986), and (4) the gonad is balanced between the male and female fates (Kim et al. 2006; Chassot et al. 2008; Swain et al. 1998; Munger et al. 2009). We reframed these models in the context of lineage priming (Figure 2). Progenitors that show lineage priming express markers of the various fates into which they can differentiate and subsequently silence genes associated with the fate not adopted as they differentiate (Delorme et al. 2009; Hu et al. 1997; Ng et al. 2009; Zipori 2004; Miyamoto et al. 2002; Enver and Greaves 1998; Hipp et al. 2010; Golan-Mashiach et al. 2005).

The "female" model predicts that the transcriptome shared by XY and XX progenitors should be predominately associated with the differentiated female fate (i.e., for statistical analysis, 90% of the "primed" genes were female). Conversely, the "male" model predicts that the transcriptome shared by XY and XX progenitors should be predominately associated with the differentiated male fate (i.e., 90% of the primed genes were male). If both the male and female programs are activated *de novo* as progenitors differentiate, those progenitors should be a "blank slate" in that they would not express transcripts associated with either the differentiated male or female cells. Alternatively, the progenitors could fit the "balanced priming" model and express a similar number of both male- and female-associated transcripts at the time when they are poised to adopt either fate (i.e., 50% of primed genes were associated with each sex). Finally, the progenitors could be primed to adopt both fates, but there could be more genes associated with the female fate ("female-biased priming", 50-90% of the primed genes were female) or the male fate ("male-biased priming", 50-90% of the primed genes were male) (Figure 2).

4.3 Results

4.3.1 Germ cell progenitors are primed with a bias toward the male fate

We analyzed the relationship between XX and XY germ cell progenitors and their final sexually differentiated fates in multiple ways to ensure that our methods did not skew the results. We defined a gene as "primed" if it showed identical levels of expression in XY and XX germ cells at E11.5, and those levels were retained or elevated in one sex and not in the other at E13.5 (Figure 12A, *Esrp1* and *Pcgf5*). This was an unbiased method of identifying genes characteristic of the female and male fates (Mansson et al. 2007). Similarly, we determined "expression" in the E11.5 sexually undifferentiated progenitors in an unbiased way. We inferred “expression” from the fact that these genes showed down-regulation in one of the sexes. In the first approach, all primed genes were analyzed, regardless of whether they were specific to germ cells (Figure 12B-C).

Figure 12: Germ cells showed lineage priming with a male bias.

(A and H) Graphs of the log-transformed, normalized intensity values. The error bars are standard error. Only the values for germ cells are shown, except in the depleted and primed example where all lineages are shown for comparison (A). (A) *Esrp1* and *Pcgf5* are examples of male- and female-primed genes and *Mosc2* is an example of a male-primed depleted gene. We used three different methods to identify primed genes: (B-C and I) all primed genes were considered, (D-E and J) only primed and lineage-specifically enriched genes were considered, and (F-G and K) lineage-specifically depleted primed genes were analyzed. (B, D, and F) The percentages of primed genes that were male-primed and female-primed: all methods showed male-biased priming. The boxes contain the p-values from the binomial tests with the expected percentages of the extreme models: 90% male genes ("Male"), 50% male and female genes ("Balanced"), and 90% female genes ("Female"). All of the extreme models were excluded because p-values were < 0.05. (C, E, and G) The percentages of male or female genes that were primed. Significance (*) was determined with the hypergeometric test ($p\text{-value} < 0.05$). (H) Graphs illustrating two primed genes whose expression in progenitors is "similar" to the differentiated cell of one sex or "intermediate" between the two sexes. (I-K) In all cases, for both sexes, the majority of primed genes were similarly expressed in germ cell progenitors and differentiated cells of one sex. Gene lists and permutation tests are provided in Supplemental File 4.

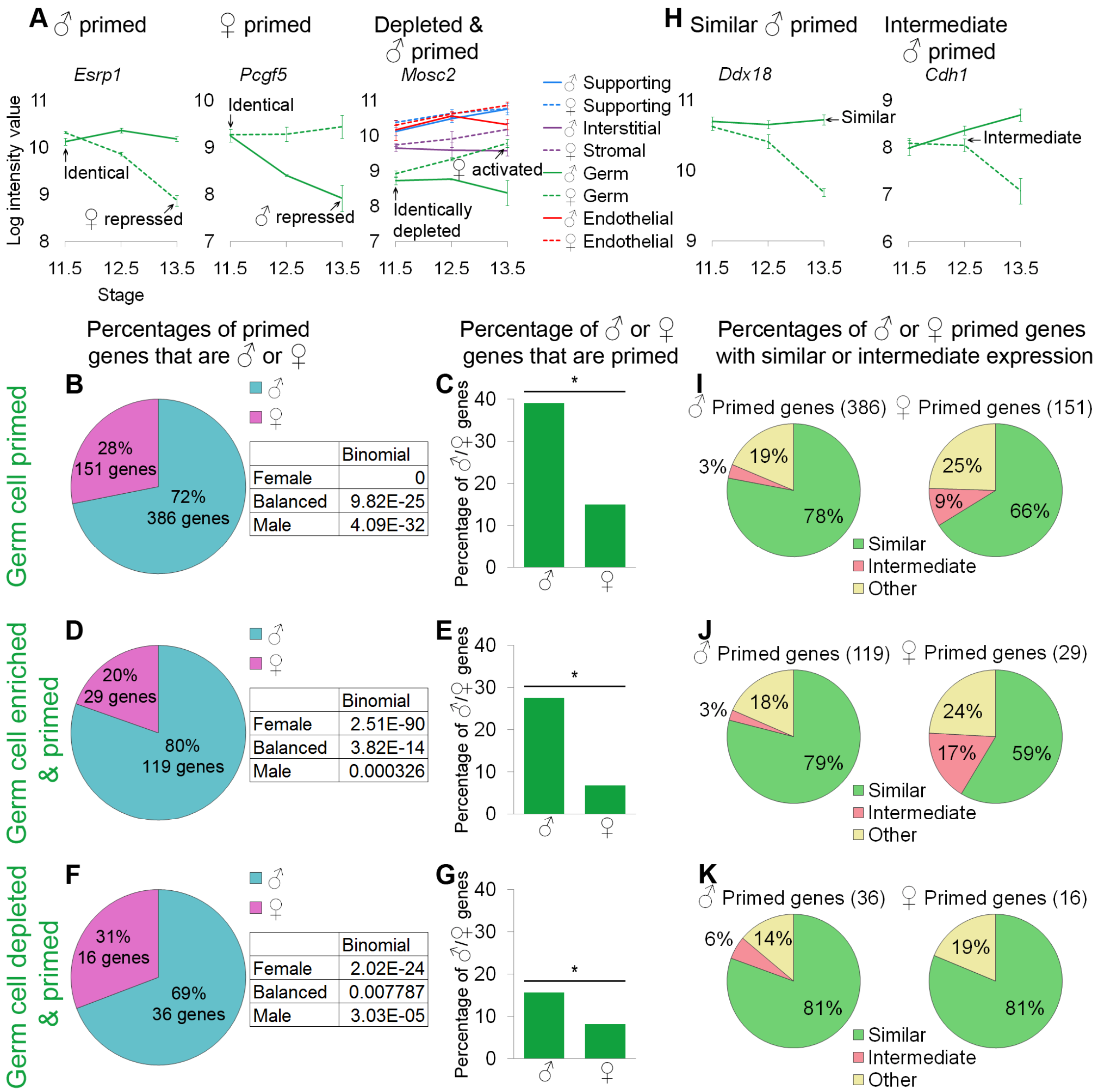

	Binomial
Female	0
Balanced	9.82E-25
Male	4.09E-32

	Binomial
Female	2.51E-90
Balanced	3.82E-14
Male	0.000326

	Binomial
Female	2.02E-24
Balanced	0.007787
Male	3.03E-05

In a second approach, we adopted more stringent, but still unbiased, definitions for the set of genes analyzed (Figure 12D-E). In this approach, we restricted our analysis to primed genes that were lineage-specifically enriched in E11.5 germ cells and in differentiated E13.5 germ cells of one sex (Figure 9). Using an analogous method, we also explored depleted and primed genes that were specifically depleted in XY and XX E11.5 progenitors, were activated by one sex, and remained sex-specifically and lineage-specifically depleted in the other (Figure 12A, *Mosc2*, Figure 12F-G). Gene lists and associated permutation tests are provided (Supplemental File 4A and C).

With all methods tested, germ cells showed male-biased priming. When comparing the percentage of primed genes that were male or female-primed, we observed a clear bias toward male genes (Figure 12B, D, and F). We performed a binomial test using the expected percentages predicted by each model to determine if we could exclude the extreme models. In all cases, the pattern of genes observed was significantly different from the extreme female and male models as well as the completely balanced priming model (Figure 12B, D, and F). Thus, a male-biased priming model best described the transcriptome in undifferentiated XX and XY germ cell progenitors. This finding was consistent with the clustering dendrogram showing a closer relationship between the undifferentiated early germ cells and the late XY germ cells than the late XX germ cells (Figure 7A).

We also wanted to ensure that this result was not a statistical artifact of the size of the underlying lists of male and female markers. For example, if the male program contained a larger number of genes than the female program, seeing a male bias in the number of primed genes could reflect the higher relative percentage of male pathway genes, rather than a real priming bias in the progenitor. Thus, we examined the percentage of male and female genes that showed priming (Figure 12C, E, and G). Again, in all cases, we saw that the same male bias was preserved. Given the large number and percentage (nearly 40%) of genes that showed priming (Figure 12C), the blank slate model could be discarded. Thus, germ cell progenitors showed male-biased priming, including the priming of some depleted genes (Figure 12G).

Lastly, we were interested in determining whether genes that showed priming were expressed at high or low levels. The expression levels of differentiation markers in the progenitor cells are low in the hematopoietic system (Hu et al. 1997), but high levels of expression of differentiation markers were observed in progenitors in the early embryo (Guo et al. 2010). For our analysis, expression level was defined relative to the differentiated cell. A gene with "similar" expression was expressed in progenitors at a level similar to that in sexually differentiated cells maintaining expression (Figure 12H, *Ddx18*), analogous to the high expression observed in the early embryo. A gene with "intermediate" expression was expressed in progenitors at a level between the levels observed in the two sexes (Figure 12H, *Cdh1*), analogous to the low expression observed in hematopoietic cells (Hu et al. 1997).

We analyzed the expression level for genes identified as primed by each method (Figure 12I-K). A majority of both male and female-primed genes were similarly expressed in the undifferentiated germ cell progenitors and the sexually differentiated cells, regardless of how the set of primed genes was defined or whether enriched or depleted genes were considered (Figure 12I-K). Thus, not only did germ cells show male-biased priming, but the progenitors frequently expressed these primed genes at the same level as the sexually differentiated cells.

We analyzed the lists of genes that exhibited a primed expression pattern (including all primed genes), and were regulated in the same way (similar expression in the progenitor and sexually differentiated cells, Figure 12I) for enrichment of GO terms (Supplemental File 4D). The genes primed toward the male germ cell fate showed a strong enrichment for categories related to RNA biology, such as RNA binding (Supplemental File 4D). This is consistent with the previously reported importance of gene control at the RNA level during germ cell development, especially in the male (Raz 2000; Cook et al. 2011; Tsuda et al. 2003).

All the data indicate that the germ cells are primed with a male-bias, and that these primed genes are expressed at a similar level in the progenitor and differentiated cell.

4.3.2 Supporting cell progenitors are primed with a bias toward the female fate

We also examined the relationship between supporting cell progenitors and their sexually differentiated states. We used the same method and tested the same models as with germ cells, but the end point of the analysis for supporting cells was E12.5 because their transcriptome changes little between E12.5 and E13.5 (Figures 9-10, Supplemental Files 2A and 3A). As in the germ cell analysis, we defined a gene as “primed” if it showed identical levels of expression in both XY and XX germ cells at E11.5, which were retained or elevated in one sex and not in the other by E12.5 (Figure 13A). The same variations of the analytical methods used for germ cells were also used to identify supporting cell-specifically enriched and depleted primed genes (Figure 13A). The gene lists, permutation test results, and GO terms are provided (Supplemental File 4B-D).

Figure 13: Supporting cells showed lineage priming with a female bias.

(A and H) Graphs of the log-transformed, normalized intensity values of genes. The error bars are standard error. Only the values for supporting cells are shown, except in the depleted and primed example where all cell types are shown. (A) *Mdk* and *Rasgrp1* are examples of male- and female-primed genes and *Cenpa* is an example of a female-primed depleted gene. As in the germ cell analysis, we examined all primed genes (B, C, and I), primed and lineage-specifically enriched genes (D, E, and J), and primed and lineage-specifically depleted genes (F, G, and K). (B, D, and F) The percentages of primed genes that were male-primed and female-primed. The boxes contain the p-values from the binomial tests with the expected percentages of the extreme models. (B) Using the first method, all of the extreme models could be excluded because they had a p-value < 0.05. (D and F) However, using the second and third methods, the balanced and female models could not be excluded, respectively. (C, E, and G) Nevertheless, examining the percentage of male or female genes that were primed, all methods showed a significant (*) bias toward the female pathway, as determined by the hypergeometric test (p-value < 0.05). Taken together, the data supported female-biased priming. (H) Graphs illustrating two primed genes, whose expression in the progenitor is "similar" to the differentiated cell of one sex, or "intermediate" between the two sexes. (I-K) The female-primed genes were predominantly similarly expressed, but the male-primed genes showed more variability. Gene lists and permutation tests are provided in Supplemental File 4.

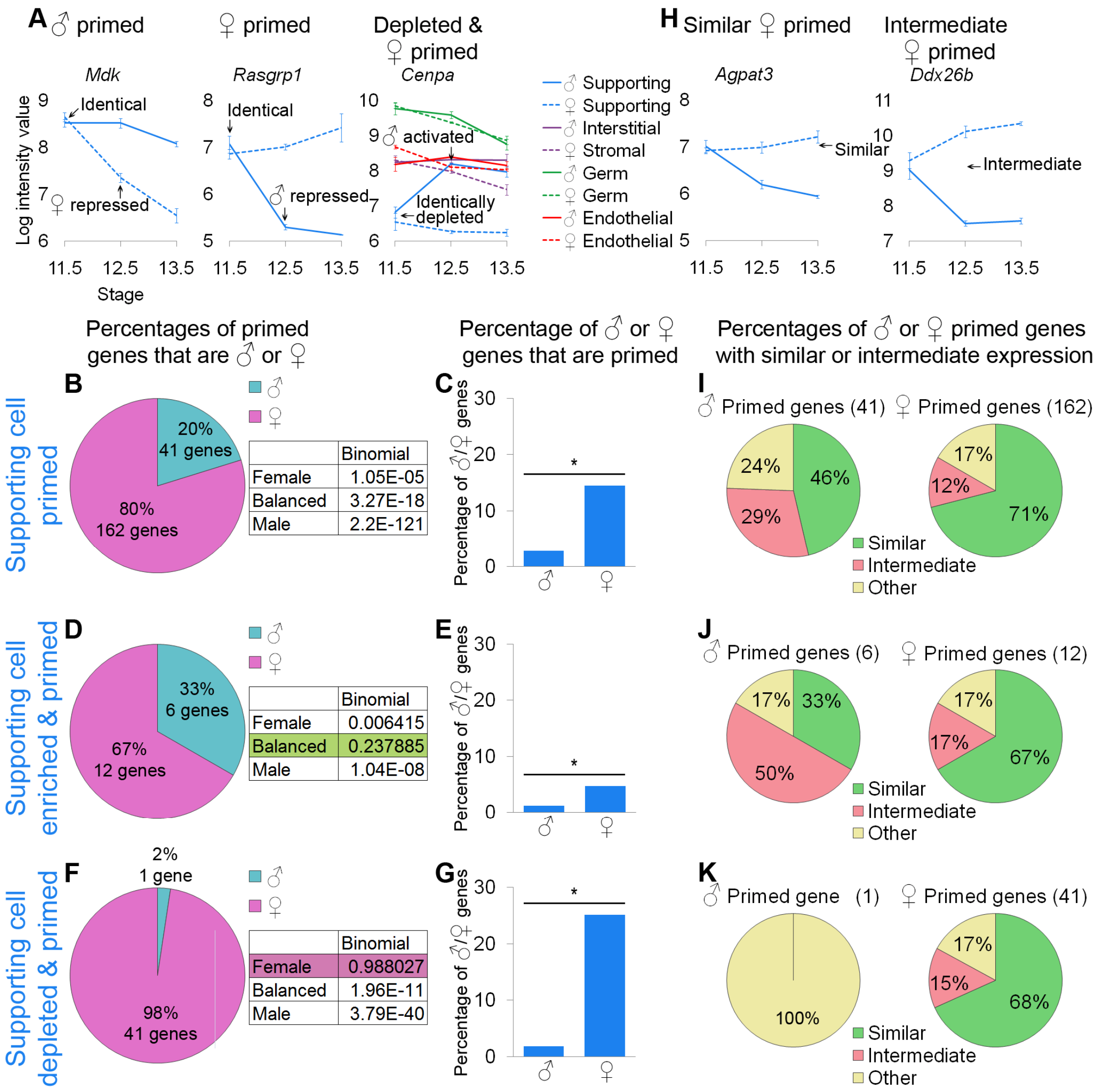

	Binomial
Female	1.05E-05
Balanced	3.27E-18
Male	2.2E-121

	Binomial
Female	0.006415
Balanced	0.237885
Male	1.04E-08

	Binomial
Female	0.988027
Balanced	1.96E-11
Male	3.79E-40

The pattern in supporting cells was less consistent than the pattern observed for germ cells, but was indicative of female-biased priming. Examining all of the primed genes, there was a clear female bias both for the primed genes as a percentage of the priming program (Figure 13B) and the primed genes as a percentage of the XY and XX sexually dimorphic genes (Figure 13C). When restricting our analysis to the genes specifically enriched in supporting cells (Figure 13D-E), we observed a similar female bias in the percentage of XX and XY genes that were primed (Figure 13E), but the bias in the percentage of primed genes associated with the male and female pathways was not sufficient to exclude the balanced priming model (Figure 13D). This is likely a statistical artifact due to the small number of primed genes and the difference in size between the E12.5 XX and XY enriched supporting cell gene lists (Figure 9). The genes specifically depleted in supporting cells showed a strong female bias (Figure 13F-G), such that the female model could not be excluded (Figure 13F). All of these analyses suggested female-biased priming, consistent with the clustering showing the closer relationship between the less differentiated early supporting cells and the late XX supporting cells compared to the late XY supporting cells (Figure 7A).

We also determined if the genes primed in supporting cell progenitors showed similar or intermediate expression in undifferentiated supporting cell progenitors (Figure 13H). For the female-primed genes, we consistently observed that most genes were similarly expressed (Figure 13I-K). Expression levels of male-primed genes were more variable (Figure 13I-K), which again could be due to the small number of genes analyzed. Nevertheless, supporting cell progenitors expressed at least some of the primed genes at levels similar to the sexually differentiated supporting cells.

However, the XX and XY supporting cells were already expressing sexually dimorphic genes by E11.5 (Figure 9A) and therefore were not fully undifferentiated at the start of our analysis. With the reporters available to us, collection of a pure population of progenitors from an earlier stage was not feasible. To determine whether our results were affected by the differentiation process already in progress, we reanalyzed a publically available microarray time course on sorted *Sf1-EGFP* cells from the urogenital ridge that included earlier time points than were collected here (Nef et al. 2005) (Figure 14, Supplemental File 5). While the *Sf1-EGFP* reporter allows for the collection of earlier time points, it also labels a mixed population that includes at least supporting cells and interstitial/stromal cells (Nef et al. 2005; Ikeda et al. 1994). This is concerning because different cell types can have different priming patterns (Figures 12-13). Therefore, we identified genes from the *Sf1-EGFP* data set that showed priming, and then restricted our analysis to only those genes whose expression patterns were associated with the supporting cell lineage as defined by our data set.

Figure 14: Data from sorted *Sf1-EGFP* cells starting at E11.0 also shows female-biased priming for supporting cells.

(A-B) Graphical illustrations of the genes included in our analysis of priming in the *Sf1-EGFP* data. Because the *Sf1*-positive population is a mixture of lineages, we used two methods to identify the primed genes associated with supporting cells. XY cells are illustrated in this example, but the same operations were also performed for XX cells. (A) "*Sf1* primed and supporting cell enriched" genes were both male-primed in the *Sf1-EGFP* data (E11.0 to E12.5) and lineage-specifically enriched in our XY *Sry-EGFP*/*Sox9-ECFP* purified supporting cells at E12.5. Red indicates genes being removed from the analysis, and green indicates genes being retained. (B) For the "*Sf1* primed, removing interstitial/stromal genes", we removed genes associated with the interstitial/stromal cells at E12.5 (i.e., sexually dimorphic in the interstitium/stroma) from the *Sf1-EGFP* primed genes. Genes that were expressed sexually dimorphically in both the interstitial/stromal cells and the supporting cells were removed only if expression was higher in the interstitial/stromal cells than in the *Sry-EGFP*/*Sox9-ECFP* supporting cells. The *Sf1-EGFP* primed genes that were enriched in the *Sry-EGFP*/*Sox9-ECFP* supporting cells (C-D and G) and those that were identified by removing interstitial/stromal genes (E-F and H) were analyzed separately. (C and E) The percentages of primed genes that were male-primed and female-primed. Both methods showed a female bias. The boxes contain the p-values from the binomial tests with the expected percentages of the extreme models, and all extreme models could be rejected as having a p-value < 0.05. (D and F) The percentage of male or female genes that were primed showed a significant (*) bias toward the female pathway, as determined by the hypergeometric test (p-value < 0.05). (G and H) Many primed genes in both sexes were expressed at similar levels in progenitors and E12.5 supporting cells of one sex. While supporting cell progenitors have a female bias, they also expressed some markers of the male pathway at levels similar to male supporting cells at E12.5. Gene lists and permutation tests are provided in Supplemental File 5.

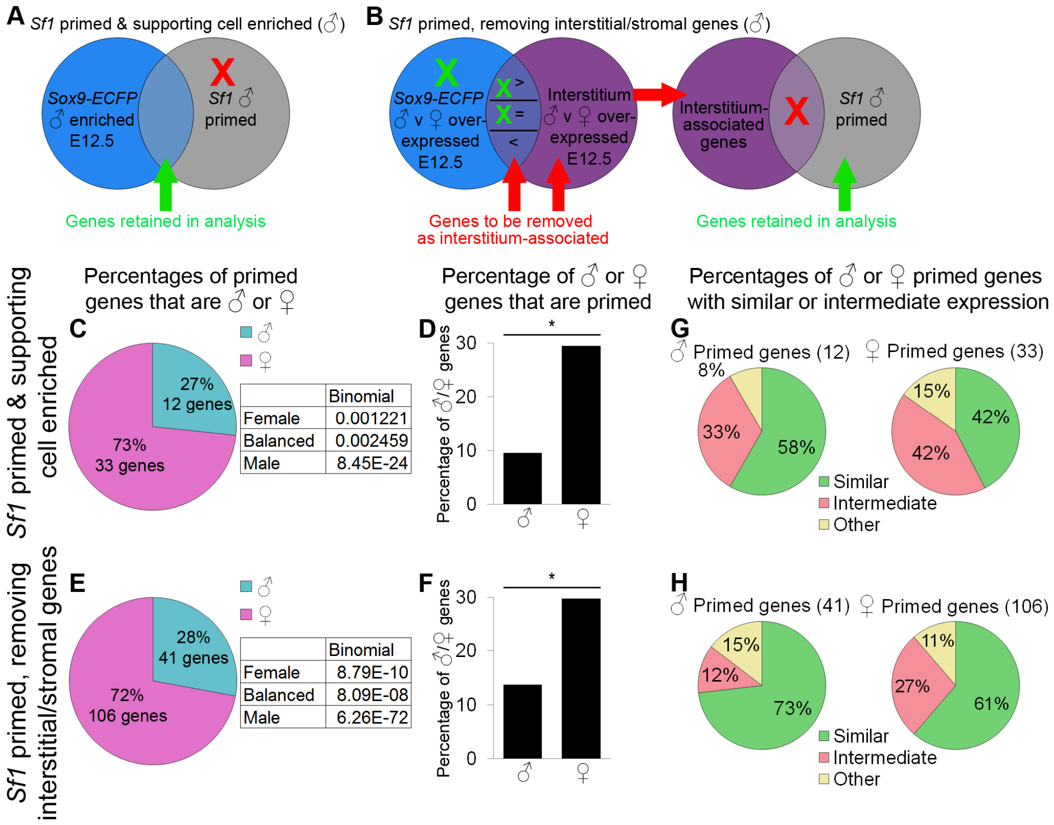

C

	Binomial
Female	0.001221
Balanced	0.002459
Male	8.45E-24

E

	Binomial
Female	8.79E-10
Balanced	8.09E-08
Male	6.26E-72

Using the same approach as in the analysis of the *Sry-EGFP/Sox9-ECFP* sorted supporting cell progenitors, we identified primed genes within the *Sf1-EGFP* undifferentiated progenitor population. To limit the contribution of genes from interstitial/stromal cells and for consistency, we set the end point of the analysis at E12.5. E11.0 *Sf1-EGFP* cells were selected as the starting point for the analysis presented in Figure 14 because it was closest to the sexual divergence point of the primed genes.

While lists of all primed genes identified in the *Sf1-EGFP* cells are provided (Supplemental File 5A), we limited our analysis to only those genes associated with supporting cells. To define this gene set, we used two different methods utilizing our purified supporting cell (*Sry-EGFP/Sox9-ECFP*) and interstitial/stromal cell data as a reference. First, we used a rigorous threshold for inclusion and retained only those genes that were also found to be lineage-specifically and sex-specifically enriched in our E12.5 XX or XY *Sry-EGFP/Sox9-ECFP* supporting cells (Figure 14A, C-D, and G; Supplemental Files 2A and 5A). In a second approach, we used less rigorous criteria and removed genes sexually dimorphic in the interstitial/stromal cells (Figure 14B, E-F, and H; Supplemental File 5A and C). Genes that were sexually dimorphic in both the *Sry-EGFP/Sox9-ECFP* supporting cells and the interstitial/stromal population were only removed if they were expressed at higher levels in interstitial/stromal cells than in supporting cells.

Regardless of the method used, these data also supported female-biased priming of the supporting cells. Most of the primed genes were female, although the progenitors expressed some male genes as well (Figure 14C-F). Many of these genes were also similarly expressed (Figure 14G-H).

While similar conclusions were also reached starting the analysis of the *Sf1-EGFP* data at E10.5 (Figure 15A-F, Supplemental File 5B), E10.5 was a problematic starting point. For the E10.5 analysis, the data was processed similarly, but the analysis was performed using the E10.5 *Sf1-EGFP* data rather than the E11.0 data. However, the different methods of processing the E10.5 data did not produce consistent results (Figure 15A-D). One method suggested female-biased priming (Figure 15A-B), and the other suggested balanced priming (Figure 15C-D). This was likely because E10.5 was not the appropriate starting point for the priming analysis. No primed genes identified by starting the analysis at E10.5 became different between XX and XY cells by E11.0, and so no advantage was gained by starting the analysis at E10.5 (Figure 15G). Primed genes at E11.0 did become dimorphic by E11.5, indicating that E11.0 was the closest time point preceding the divergence of gene expression of the primed genes (Figure 15G). Between E10.5 and E11.0, significantly more genes were changing expression level identically in both XX and XY cells than between E11.0 and E11.5 (Figure 15H). Genes with this type of expression pattern are illustrated in Figure 15I. This may be caused by changes in the number of supporting cell progenitors, or alternatively, the continued transcriptional development of the progenitors between E10.5 and E11.0 to establish the priming program. This type of change in expression confounds the analysis because we compared expression at E10.5 and E12.5. This is illustrated by the fact that the genes shown in Figure 15I were called as primed starting at E10.5 and not at E11.0. Since there was repression by both sexes and then up-regulation in XY cells, rather than XX repression, we did not want to these genes to be considered primed. Thus, it appeared important to begin the analysis as close to the divergence point as possible to eliminate these other expression patterns. For these reasons, we chose to start the analysis at E11.0. The gene lists for these analyses are also provided in Supplemental File 5D-E.

Figure 15: E10.5 *Sf1-EGFP* primed genes generally supported female-biased priming, but the E11.0 analysis was more informative.

The analysis of the *Sf1-EGFP* primed genes (beginning the analysis at E10.5 and comparing to *Sf1-EGFP* cells at E12.5) was also limited to genes enriched in the *Sry-EGFP*/*Sox9-ECFP* supporting cells at E12.5 (A, B, and E) or to those genes identified by removing interstitial/stromal genes (C, D, and F). (A and C) The percentages of primed genes that were male-primed and female-primed. The first, but not the second, method showed a female bias. The boxes contain the p-values from the binomial tests with the expected percentages of the extreme models. The balanced model can be rejected with the first (A), but not the second (C), method. (B and D) Examining the percentage of male or female genes that were primed similarly showed a significant (*) bias toward the female pathway, as determined by the hypergeometric test ($p\text{-value} < 0.05$), for the first (B), but not the second (D, "ns"), method. (E and F) The primed genes for both sexes are predominantly similarly expressed in progenitors and E12.5 differentiated cells. (G) No primed genes (identified by removing interstitial/stromal genes) became dimorphic between E10.5 and E11.0 (gray "0"). Thus starting the analysis at E11.0 did not result in the loss of any information. (H) Between E10.5 and E11.0, 98% of the primed genes were identically expressed in XX and XY samples at both E10.5 and E11.0. Between E11.0 and E11.5, 76% of the primed genes were identically expressed in XX and XY samples at both E11.0 and E11.5 (data not shown). Of these genes, 16% were changing expression level in the same way (see I) in both XX and XY cells between E10.5 and E11.0, whereas only 4%

fell in this category between E11.0 and E11.5. This difference was significant (*), as determined by the hypergeometric test with a p-value < 0.05, and affects how primed genes are called. This problem is illustrated in I by the graphs of the log-transformed, normalized intensity values from *Sf1-EGFP* cells (black) of two genes identified as primed at E10.5, but not at E11.0. *Tpx2* showed significant identical changes in expression in XX and XY cells between E10.5 and E11.0. A similar pattern was observed in many other genes that did not reach significance, such as *Ppil5*, and so this pattern may be more pervasive than indicated by the number meeting the significance thresholds shown in H.

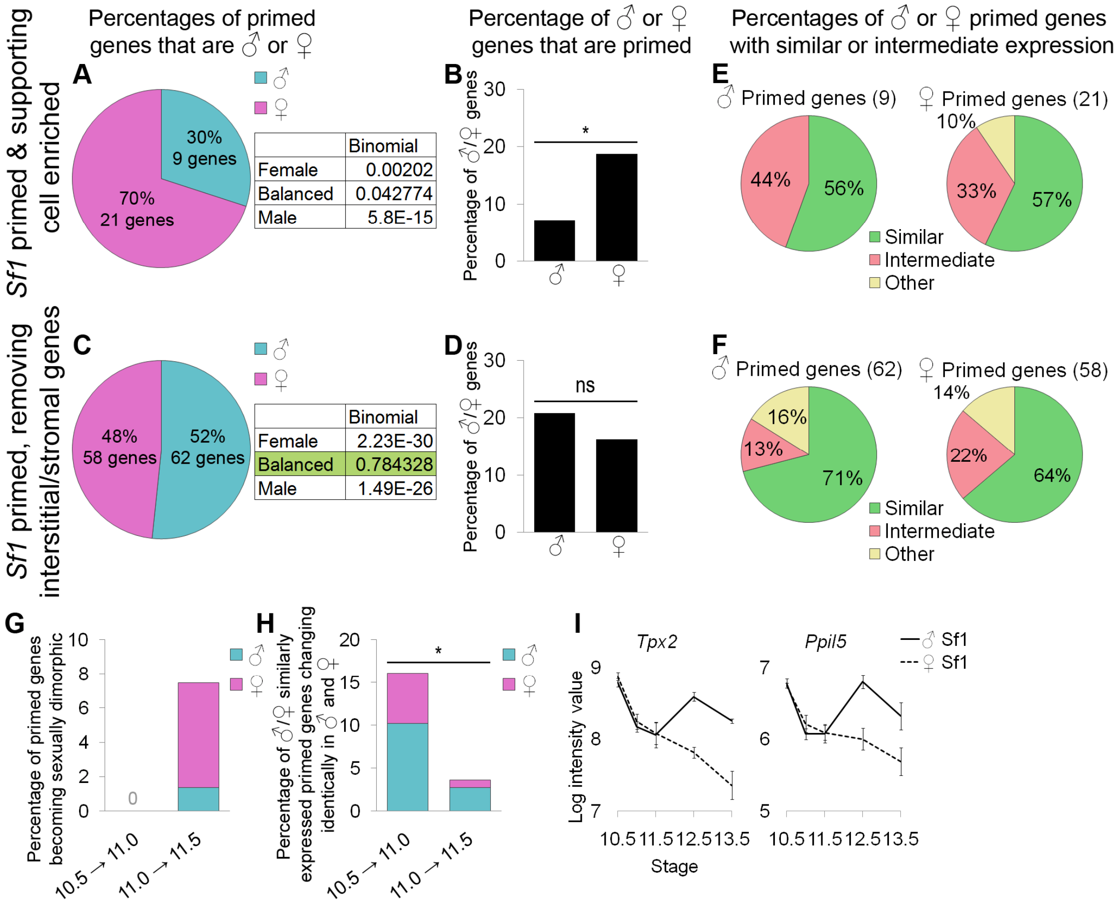

	Binomial
Female	0.00202
Balanced	0.042774
Male	5.8E-15

	Binomial
Female	2.23E-30
Balanced	0.784328
Male	1.49E-26

Returning to the analysis starting at E11.0, because nearly 30% of female genes showed priming in the *Sf1-EGFP* data (Figure 14D and F), the blank slate model can be rejected. The E11.5 *Sry-EGFP/Sox9-ECFP* progenitors showed a lower percentage of primed transcripts (Figure 13C) than the E11.0 *Sf1-EGFP* progenitors (Figure 14D and F), which may be explained by the fact that the *Sry-EGFP/Sox9-ECFP* supporting cell progenitors were already partially sexually differentiated by E11.5 (Figure 9A).

Nevertheless, the results from the *Sf1-EGFP* cells were consistent with the findings from the *Sry-EGFP/Sox9-ECFP* data. To investigate the overlap in these data sets, we determined whether similar transcripts were identified as primed in both the *Sf1-EGFP* and *Sry-EGFP/Sox9-ECFP* data sets (Figure 16). While a small percentage of the genes primed in the *Sf1-EGFP* cells were also identified as primed in the *Sry-EGFP/Sox9-ECFP* data, a larger proportion were already sexually dimorphic by E11.5, although indications of priming could be observed in some of the expression patterns (Figure 16A-B). This is not surprising since primed genes were already becoming dimorphic at E11.5 based on the *Sf1-EGFP* data (Figure 15G). These genes with indications of previous priming in the *Sry-EGFP/Sox9-ECFP* data met the same requirements for defining a primed pattern outlined in the Materials and Methods, but rather than being identical at E11.5, the sex for which the gene was primed had higher expression at E11.5. Together, these primed or E11.5 dimorphic categories account for over half of the *Sf1-EGFP* primed genes, indicating both arrays showed consistent results for many genes. 48% of the genes primed in the *Sf1-EGFP* data were not identified as primed or sexually dimorphic in *Sry-EGFP/Sox9-ECFP* cells at E11.5 (Figure 16A). This was expected as probe sets for the two arrays, as well as the cell types collected, were different. The identification of similar patterns for the same genes in these two different data sets, despite their differences, gives us confidence in the results.

Figure 16: Overlap of primed genes between the *Sf1-EGFP* and *Sry-EGFP/Sox9-ECFP* data sets.

(A) To cross-validate the analysis, we determined whether genes primed in the *Sf1-EGFP* data (removing interstitial/stromal genes, Figure 14E) were also identified as primed in the *Sry-EGFP/Sox9-ECFP* data (all genes with a priming pattern, Figure 13B). Some of the same primed genes were identified in both data sets (blue). Many more of the *Sf1* primed genes were already sexually dimorphic in the *Sry-EGFP/Sox9-ECFP* cells by E11.5 (light and dark green). Some of the genes that were already sexually dimorphic in the E11.5 *Sry-EGFP/Sox9-ECFP* cells showed some indication of previous priming in the *Sry-EGFP/Sox9-ECFP* data (light green). This pattern is illustrated in (B) by the graphs of the log-transformed, normalized intensity values for the *Sf1-EGFP* (black) and *Sry-EGFP/Sox9-ECFP* (blue) cells for the gene *Dock4*. The error bars are standard error. (A) A number of *Sf1-EGFP* primed genes (48%) were not identified as primed or sexually dimorphic in *Sry-EGFP/Sox9-ECFP* cells at E11.5 (yellow). The gene lists for these analyses are provided in Supplemental File 5F.

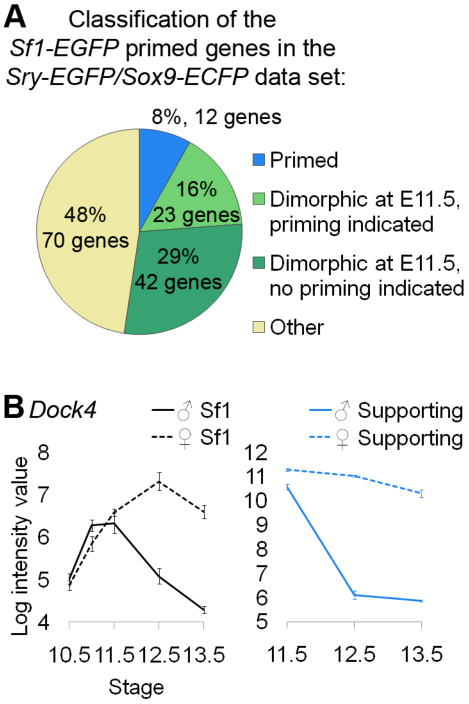
A
Classification of the
Sf1-EGFP primed genes in the
Sry-EGFP/Sox9-ECFP data set:
8%, 12 genes
16%
23 genes
48%
70 genes
29%
42 genes
Primed
Dimorphic at E11.5, priming indicated
Dimorphic at E11.5, no priming indicated
Other
B Dock4
♂ Sf1
♀ Sf1
♂ Supporting
♀ Supporting
Log intensity value
8
7
6
5
4
10.5
11.5
12.5
13.5
Stage
12
11
10
9
8
7
6
5
11.5
12.5
13.5

This analysis was also consistent with previous findings showing that individual genes we identified as primed were expressed in the sexually undifferentiated XX and XY supporting cell progenitors and then became sex-specific: *Dax1/Nr0b1*, *Wnt4*, *Sox9*, and *Cbln4* (Kent et al. 1996; Morais da Silva et al. 1996; Bradford et al. 2009; Swain et al. 1998; Vainio et al. 1999) (Supplemental Files 4B and 5A). Thus, the analysis of these two independent data sets produced results consistent with each other and previous data, and they reached the same overall conclusion that the supporting cells are primed with a female-bias.

4.4 Discussion

A comprehensive understanding of organogenesis requires systems-level knowledge of transcriptional network dynamics underlying cell differentiation. By performing a microarray analysis on sorted cell populations in the fetal mouse gonad over the course of sex-specific differentiation, we quantified the transcription dynamics of diverse cell types as they build one of two different organs from similar pools of progenitors. This study provided an expression resource for the field of gonad development, but more importantly, it yielded new insights into patterns of cell fate determination and lineage commitment.

4.4.1 A role for priming in the bipotential supporting cell lineage

We determined that the supporting cell progenitors are primed with a female bias, indicating that both male and female genes are expressed in the progenitor, but that the female program is over-represented (Figure 17). This female-biased priming model bridges the more recent evidence for a balance in the gonad between the male and female fates (Kim et al. 2006; Chassot et al. 2008; Swain et al. 1998; Munger et al. 2009) and the classic theory of the female "default" state (McLaren 1991; Jost 1947; Capel 1998). Although we found genes characteristic of both the male and female programs in supporting cell progenitors, the over-representation of the female program in progenitors explains why the female fate is the "default" state in the absence of *Sry*.

Figure 17: Models of differentiation for the gonadal lineages.

Supporting cells are primed with a female bias. The natural progression of the primed state may be to adopt the female differentiated state, but in the presence of *Sry* the cells repress the female program and adopt the male fate. Conversely, germ cells are primed with a male bias. An extrinsic signal may be required from the mesonephros to induce the adoption of the female fate; otherwise, germ cells adopt the male fate.

Cell type	Supporting cells	Germ cells
Model	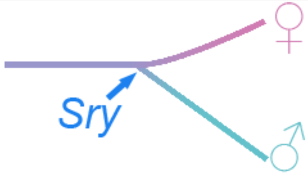	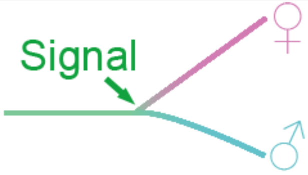
	Female-biased priming	Male-biased priming

The female fate may be the "default" state because the over-represented female program of supporting cell progenitors is self-sustaining without additional inputs and leads to silencing of the alternative testis pathway. The high level expression of primed genes may make the primed state in the progenitors unstable. Whereas, low-level expression of fate determinates has been associated with a stable primed state, the expression of determinates at high levels has been associated with instability of the primed state (Laslo et al. 2006). As priming with high level expression has also been noted in the early embryo (Guo et al. 2010), this may be a common developmental mechanism to ensure that development progresses and does not become stalled. Thus, this unstable primed state would naturally lead to female differentiation in the absence of intervention from *Sry*. Under these circumstances, an ovary-determining gene, as proposed by Eicher and Washburn (Eicher and Washburn 1986), would not be necessary.

Bipotential supporting cells show priming toward the male and female fates (Figures 13-14). A previous study identified a female subnetwork in E11.5 XY gonads (Munger et al. 2009). We identified many of these genes as female-primed (*Wnt4*, *Fst*, *Rspo1*, *Dapk1*, *Pld1*, *Actr6*, and *Dock4*, Supplemental File 5A). The expression of female genes in XX and XY supporting cell progenitors could be consistent with a female transcriptional state in the progenitors that is repressed by the activation of *Sry* in XY cells rather than by the concept of male and female priming.

However, the coexpression of male genes in both XX and XY supporting cell progenitors strongly supports the idea that these cells are primed to adopt either of their potential fates. These genes likely represent a male subnetwork operating in the early XX and XY cells independent of *Sry*, as *Sry* is not present in the XX cells. This work provides a molecular explanation for the concept of bipotentiality due to the coexpression of both male and female transcripts in the XX and XY supporting cell progenitors.

The mechanism of priming remains to be determined. It has been speculated that priming is a byproduct of open chromatin (Enver and Greaves 1998; Laslo et al. 2006; Hu et al. 1997). Bivalent chromatin has been reported in embryonic stem cells at loci expressed at low levels (Bernstein et al. 2006). However, this is inconsistent with our findings in the gonad, where primed genes in bipotential supporting cell precursors tended to be expressed at high levels. Other studies in the laboratory are aimed at investigating the state of chromatin at primed loci.

While priming may be important to establish a bipotential state, mounting evidence suggests that the repression of the primed genes associated with the alternative sex is important for supporting or maintaining cell fate commitment. Genes important for testis (*Sox9* and *Dmrt1*) (Matson et al. 2011; Raymond et al. 2000; Chaboissier et al. 2004) and ovary (*Wnt4*, *Fst*, and *Rspo1*) (Vainio et al. 1999; Yao et al. 2004; Chassot et al. 2008) development were identified as expressed in XX and XY supporting cell precursors and repressed in the opposite sex (Supplemental File 4B and 5A). Over-expression of *Sox9* is known to result in female-to-male sex reversal (Vidal et al. 2001). Ectopic activation of the downstream target of WNT4, β-catenin, can reverse differentiation of XY supporting cells and trigger their differentiation as female cells (Maatouk et al. 2008). Thus, the repression of genes associated with the opposite sex (which we identified in these experiments) may be as essential to the cell fate decision as the genes that are expressed.

4.4.2 Priming during germ cell development

The testicular-biased primed state of germ cell progenitors was surprising because germ cell fate is determined by the somatic environment (Adams and McLaren 2002). Germ cells that enter an ovarian environment initiate meiosis (the female fate), while germ cells that enter a testis environment undergo mitotic arrest (the male fate) (Ewen and Koopman 2010). Historically, entry into meiosis was thought to be the default state for germ cell differentiation (McLaren and Southee 1997; Adams and McLaren 2002; Upadhyay and Zamboni 1982; Chuma and Nakatsuji 2001; Farini et al. 2005). However, the weight of current evidence indicates that meiosis (the female fate) is the result of an external inducing signal produced in the mesonephros and specifically degraded in the testis by *Cyp26b1* (Bowles et al. 2006; Kumar et al. 2011; Koubova et al. 2006; Byskov 1974; O and Baker 1976). While there is some evidence for a signal promoting the male fate (DiNapoli et al. 2006; Bowles et al. 2010; Barrios et al. 2010;

Francavilla and Zamboni 1985; Best et al. 2008), this signal may act by antagonizing the female-promoting signal (Bowles et al. 2010; Bowles et al. 2006) and/or providing a permissive environment for male germ cell development (DiNapoli et al. 2006).

The male-biased transcriptome of germ cell progenitors is consistent with a male developmental "default" state in the absence of the female-promoting signal (Figure 17). Interestingly, in both supporting and germ cells, the dominant fate-determining signal is associated with the fate under-represented in the progenitor's transcriptome (Figure 17). *Sry* expression in XY supporting cells is required to stabilize the male program and repress the female program in supporting cells. Similarly, the external female signal initiates the meiotic program in germ cells and represses the alternative male program. XY germ cells adopt the female fate if *Cyp26b1* activity is eliminated (resulting in the presence of the meiosis-inducing signal), even in an otherwise male environment (Bowles et al. 2006; Kumar et al. 2011). Our priming model suggests that the over-represented male program may need only subtle reinforcement from the somatic environment. On the other hand, the under-represented female program cannot be stabilized without its instructive cue, but once that input is received, it is able to suppress the male program.

Another reason why E13.5 XY germ cells share more transcriptional features with the progenitor than XX germ cells may be due to their maintenance in a more stem cell-like state (Supplemental File 4A) (Phillips et al. 2010). However, XY germ cells at

E13.5 are not identical to the sexually undifferentiated germ cell progenitors at E11.5. Specifically, by E13.5 XY germ cells have repressed genes associated with the female germ cell program (Figure 12), which may explain why, even when put into a female environment after E11.5, XY germ cells can no longer adopt the female fate (McLaren and Southee 1997; Adams and McLaren 2002).

4.4.3 Priming during differentiation

This study revealed previously unknown systems-level aspects of the differentiation of two critical cell types during gonad development, with implications for other developing cells. Supporting and germ cells arise from different embryonic origins and respond to different cues during their terminal differentiation, and yet both show priming. Priming may be a common feature of differentiation from multipotent progenitors at all levels, as it has now been identified in the early embryo (Guo et al. 2010), multipotent hematopoietic cells (Hu et al. 1997), bone marrow mesenchymal stem cells (Delorme et al. 2009), germ cells, and somatic gonadal cells.

However, each priming program appears surprisingly lineage specific. Even the cells within the gonad do not share a common bias in their priming programs (Figure 17). Priming may limit the developmental potential of cells by preparing them to respond in a unique manner to the same signals used throughout development. Only certain avenues of differentiation are available while others are closed (Ng et al. 2009;

Mansson et al. 2007; Delorme et al. 2009). For example, male supporting cells and male germ cells exposed to similar *Fgf9* signals adopt different fates (Barrios et al. 2010; Bowles et al. 2010; Colvin et al. 2001; Kim et al. 2006) because they have different underlying transcriptional networks that prepare the cell to respond differently. *In vivo*, a supporting cell progenitor cannot become a germ cell because the required transcriptional avenues are not available. The ability to induce pluripotent cells from differentiated cells *in vitro* may be related to the ability to return the cell to a primitive primed state, where many avenues of differentiation are open.

We identified priming patterns using simple, yet flexible, statistical methods that can be applied to any microarray time course on a single purified cell population isolated immediately preceding and following differentiation. While we were able to analyze the priming of lineage-specific enriched and depleted transcripts to validate our results (Figure 12-13), the results were similar regardless of the method used. Because having other cell types for comparison is not required, this method can be broadly applied to other systems exploring differentiation.

Systems biology entails the use of both whole genome analysis and molecular genetic approaches to inform each other (Ideker et al. 2001). While studies disrupting the function of individual genes have clearly identified critical components of the system, they are unlikely to be sufficient on their own to fully elucidate the combinatorial interactions within the complex transcriptional network governing organ development.

Recent studies show that developmental transcriptional networks are highly buffered and contain redundant factors, suggesting that many important network players may not have a developmental phenotype when disrupted (Munger et al. 2009; Brady et al. 2011). In conjunction with the traditional functional studies examining individual genes, our understanding of gonad organogenesis (and development in general) is facilitated by a whole system view of the process as it reveals novel phenomena that cannot be identified by studying single genes. This analysis leads to many new and exciting hypotheses related to the role of priming in the differentiation of gonadal cells and provides new insight into the processes of cellular differentiation and lineage commitment.

A manuscript containing the work in Chapters 3 and 4 was provisionally accepted (the manuscript will be considered for formal acceptance after minor revisions) by PLoS Genetics.

5. Testis Development Requires the Repression of *Wnt4* by Fgf Signaling

5.1 Summary

The work in chapters 3-4 gave us a better understanding of the gonad as a whole transcriptional system, but that system is ultimately composed of individual genes. In this chapter, we further characterized the genetic relationship of individual genes important for gonad development: *Fgf9*, *Fgfr2*, and *Wnt4*. Whether Fgf signaling acted by directly up-regulating the key testis promoting gene *Sox9* or repressing the ovary-promoting, female-primed gene *Wnt4* was unknown. To test these models, we generated XY double mutant mice for both *Wnt4* and *Fgf9* or its receptor *Fgfr2*. In both cases, the additional deletion of *Wnt4* rescued the XY *Fgf9*/*Fgfr2* sex reversal phenotype. This evidence indicated that the primary function of *Fgf9* during male sex determination is the repression of *Wnt4* in XY gonads prior to E11.75. On the other hand, we found that the partial male sex reversal in the XX *Wnt4* mutants was not rescued by deleting *Fgf9*, indicating that this partial sex reversal in XX gonads does not occur through the up-regulation of *Fgf9*. Thus, Fgf signaling is not required to directly up-regulate male genes, but it is required to repress the female-primed gene *Wnt4* during testis development.

5.2 Introduction

In chapter 4, we found that the supporting cells showed female-biased lineage priming because the sexually undifferentiated progenitors expressed many genes that later become associated with the female fate, and some genes that later became associated with the male fate. The defining characteristic of the primed gene expression pattern is the repression by the opposite sex, which means that XY supporting cells repress the many female-primed genes expressed in the progenitors. However, we did not know what factors mediated this repression of the female program, or if this repression was functionally required for testis development.

Our lab previously proposed that *Fgf9* created a feedforward loop with SOX9 to maintain SOX9 expression and male development (Kim et al. 2006). However, there was also evidence suggesting that *Fgf9* and *Wnt4* acted in a mutually antagonistic manner with *Fgf9* promoting male fate and *Wnt4* promoting female fate (Kim et al. 2006). Thus, we wanted to clarify how Fgf signaling promoted SOX9 expression, and whether it was direct or indirect through *Wnt4* repression (Figure 3).

XX *Wnt4* mutants develop an ectopic coelomic vessel and ectopic steroidogenic cells (Jeays-Ward et al. 2003; Vainio et al. 1999), and there was some data showing that *Fgf9* was expressed in XX *Wnt4* mutants (Kim et al. 2006). Also, exogenous FGF9 could induce migration of mesonephric endothelial cells into the XX gonad (Colvin et al. 2001).

Thus, it remained an open question whether derepression of *Fgf9* was responsible for any of the XX *Wnt4* mutant phenotypes.

5.3 Results

5.3.1 The partial sex reversal observed in XY *Fgfr2* mutants is rescued by deleting *Wnt4*, consistent with the *Wnt4* repression model

We tested two models for the mechanism of Fgf action (Figure 3). As was previously proposed, Fgf signaling could act by positively promoting SOX9 expression (Fgf activation model) (Kim et al. 2006). Alternatively, Fgf signaling could act by repressing *Wnt4*, which would otherwise repress SOX9 (*Wnt4* repression model). Consistent with previous data (Kim et al. 2006; Kim et al. 2007), both models predict that the genetic deletion of *Fgf9* or *Fgfr2* should result in loss of SOX9 (Figure 18A). However, the models make different predictions when an Fgf component and *Wnt4* are both deleted. The Fgf activation model predicts that SOX9 will still be lost, while the *Wnt4* repression model predicts that deleting *Wnt4* will rescue SOX9 expression (Figure 18B).

Figure 18: Predictions of the models of Fgf action

(A) Both models are consistent with previous data showing that loss of Fgf signaling results in loss of SOX9. SOX9 loss when *Fgf9* or *Fgfr2* are deleted could result from either the loss of the positive activation of SOX9 or the derepression of *Wnt4* causing repression of SOX9. Genetic deletion of a factor is shown by a red strikethrough, loss of a genetic interaction is shown by a red "X", expression is shown by a green arrow, and the absence of expression is shown by a red arrow. (B) The models make different predictions for the effect of the losing both Fgf signaling and *Wnt4*. Under the Fgf activation model, the genetic elimination of *Wnt4* should have no effect on the loss of SOX9 because the positive activation from Fgf signaling is still lost. However, under the *Wnt4* repression model, the genetic elimination of *Wnt4* should rescue SOX9 expression.

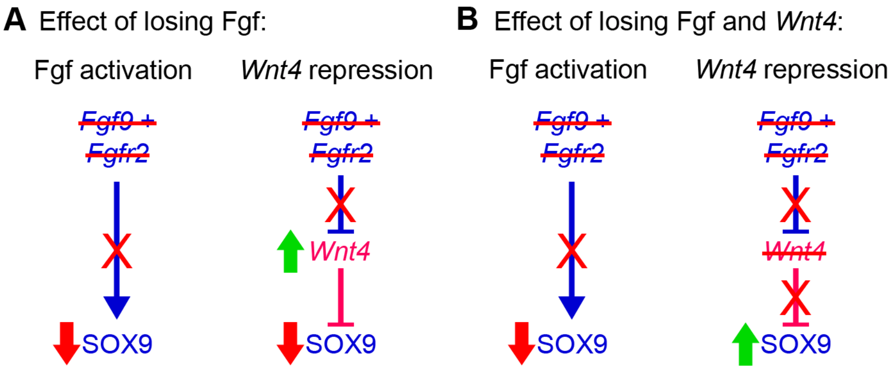
A
Effect of losing Fgf:
Fgf activation
Wnt4 repression
~~Fgf9 + Fgfr2~~
SOX9
~~Fgf9 + Fgfr2~~
Wnt4
SOX9
B
Effect of losing Fgf and Wnt4:
Fgf activation
Wnt4 repression
~~Fgf9 + Fgfr2~~
SOX9
~~Fgf9 + Fgfr2~~
~~Wnt4~~
SOX9

We first tested the models by deleting both *Fgfr2* and *Wnt4*. We used a null allele of *Wnt4* (Stark et al. 1994), and a floxed allele of *Fgfr2* (Yu et al. 2003) conditionally deleted using the *Sf1-Cre* transgene (Bingham et al. 2006). We used a mixed strain with a large C57BL/6 contribution, since this phenotype is sensitive to strain background (Bagheri-Fam et al. 2008). Gonads were collected at E13.5. FOXL2 was used as a marker of the female supporting cell fate, and SOX9 was used as a marker of the male supporting cell fate (Figure 19A-B). PECAM1 labels the germ cells and the vasculature. Deleting *Wnt4* alone did not disrupt general male development (Figure 19C), although subtle effects on male development have been previously observed (Jeays-Ward et al. 2004).

Figure 19: Deleting *Wnt4* rescued the partial sex reversal induced by loss of *Fgfr2*, supporting the *Wnt4* repression model.

Immunofluorescence of E13.5 gonads stained with PECAM1 (labeling germ cells and vasculature, blue), SOX9 (red), and FOXL2 (green). XX controls (A) had no testis cords and expressed FOXL2. In contrast, XY controls (B) and XY *Wnt4* mutants (C) had SOX9-positive Sertoli cells surrounding the germ cells to make testis cords with rare FOXL2-positive cells (arrowheads). (D) XY mice with *Fgfr2* deleted in the supporting cells were partially sex reversed. Cells at the poles of the gonad (arrows) expressed FOXL2 and cords were absent, as in the female control. The center of the gonad was more testicular with SOX9-positive cells and testis cord structure. (E-F) Loss of one or two alleles of *Wnt4* substantially rescued the *Fgfr2* phenotype. Particularly in the XY *Sf1-Cre*; *Fgfr2*$^{flox/flox}$; *Wnt4*$^{-/-}$ samples (F), there were testis cords throughout the gonad with SOX9 and few FOXL2-positive cells (arrowheads). Images were captured using a 40X objective, assembled to span the entire gonad, and placed on a black background. Scale bar = 100 μm.

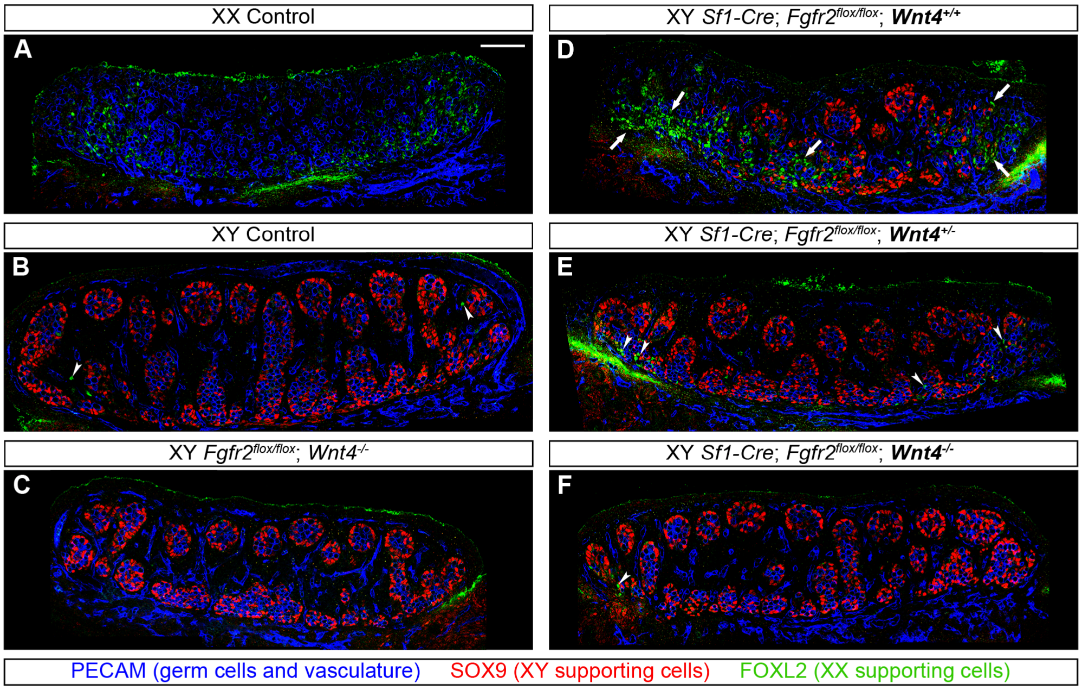
XX Control
A
XY *Sf1-Cre*; *Fgfr2*$^{flox/flox}$; ***Wnt4***$^{+/+}$
D
XY Control
B
XY *Sf1-Cre*; *Fgfr2*$^{flox/flox}$; ***Wnt4***$^{+/-}$
E
XY *Fgfr2*$^{flox/flox}$; *Wnt4*$^{-/-}$
C
XY *Sf1-Cre*; *Fgfr2*$^{flox/flox}$; ***Wnt4***$^{-/-}$
F
PECAM (germ cells and vasculature)
SOX9 (XY supporting cells)
FOXL2 (XX supporting cells)

XY *Sf1-Cre*; *Fgfr2*$^{flox/flox}$ gonads exhibited partial male-to-female sex reversal, consistent with previous observations (Kim et al. 2007; Bagheri-Fam et al. 2008) (Figure 19D). They expressed substantially more FOXL2 and less SOX9 than XY controls, and testis cord structures were disrupted at the poles of the gonad. In XY *Sf1-Cre; Fgfr2*$^{flox/flox}$ gonads that were heterozygous or homozygous null for *Wnt4*, there was substantial rescue of the *Fgfr2* mutant phenotype (Figure 19E-F). The rescue phenotype of XY *Sf1-Cre; Fgfr2*$^{flox/flox}$*; Wnt4*$^{+/-}$ mice was robust and resulted in fertile males that were used in breeding (Figure 19E). In the *Wnt4* null samples, SOX9 positive testis cords clearly extended to the poles of the gonad, and few cells were positive for FOXL2 (Figure 19F). These data support the *Wnt4* repression model of Fgf action.

5.3.2 Male-to-female sex reversal caused by *Fgf9* deletion is completely rescued by deleting *Wnt4*

While the data from *Sf1-Cre; Fgfr2*$^{flox/flox}$*; Wnt4*$^{-/-}$ gonads supported the *Wnt4* repression model, the *Fgfr2* phenotype was relatively mild. This, coupled with the variability associated with the mixed background, complicated interpretation of the rescue. To solve these problems, we collected gonads from embryos on the C57BL/6 strain around E16.5-E17.5 null for both *Fgf9* and *Wnt4*. XX and XY gonads were visibly distinct, and the XY *Wnt4* mutant gonads had testicular morphology (Figure 20A-C). On this background, XY *Fgf9* mutants showed full male-to-female sex reversal (Schmahl et al. 2004) (Figure 20D). Unlike the case for *Fgfr2* mutants, *Fgf9*$^{-/-}$ XY gonads heterozygous for *Wnt4* (*Wnt4*$^{+/-}$) resembled the *Fgf9* mutants alone and did not show rescue of the ovarian morphology (Figure 20D). However, in XY *Fgf9*$^{-/-}$; *Wnt4*$^{-/-}$ homozygous mutant gonads, we observed a complete rescue of the *Fgf9*$^{-/-}$ sex reversal, with only a slight reduction in gonad size. All seven XY *Fgf9*/*Wnt4* double mutant gonads collected were phenotypically male with visible testis cords (Figure 20E).

Figure 20: Deleting *Wnt4* rescued the full sex reversal induced by loss of *Fgf9*, further supporting the *Wnt4* repression model.

Brightfield images of E16.5-E17.5 gonads with mesonephric-derived structures. Control XX ovaries (A) and XY testes (B) had distinct morphologies. Dotted lines surround the ovaries. (C) XY gonads carrying a deletion of *Wnt4* developed as testes, but (D) the deletion of *Fgf9* (homozygous wild type or heterozygous for *Wnt4*) resulted in sex reversal and development of an ovary. (E) Deleting both *Wnt4* and *Fgf9* rescued testis development. Scale bar = 1 mm.

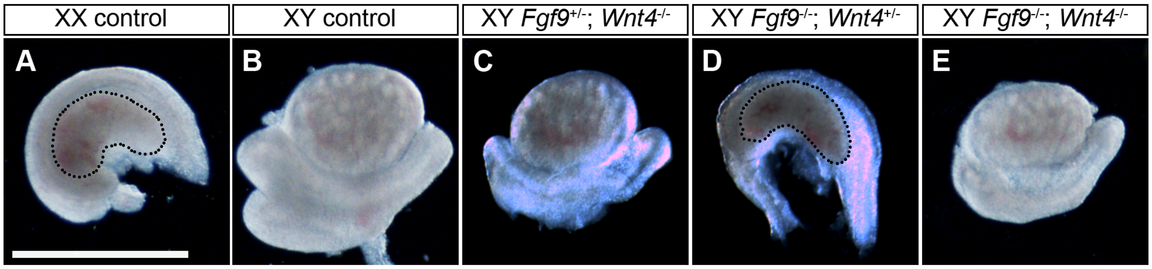
XX control
XY control
XY Fgf9+/-; Wnt4-/-
XY Fgf9-/-; Wnt4+/-
XY Fgf9-/-; Wnt4-/-
A
B
C
D
E

Male cell types were properly specified in XY *Fgf9*$^{-/-}$; *Wnt4*$^{-/-}$ gonads (Figure 21). We examined multiple aspects of male development. First, we checked for the presence of Sertoli cells in testis cords, which are co-labeled with SOX9 and AMH. The XX controls lacked Sertoli cells labeled with SOX9 and AMH (Figure 21A). Sertoli cells were present in XY controls and *Wnt4* mutants (Figure 21B-C). XY *Fgf9* mutants resembled ovaries and did not have Sertoli cells co-labeled with SOX9 and AMH (Figure 21D). A variable number of SOX9-positive cells were observed in the XY *Fgf9* mutant gonads, but they were not AMH positive as Sertoli cells normally are at this stage. In contrast, the XY *Fgf9*$^{-/-}$; *Wnt4*$^{-/-}$ gonads had testis cords with SOX9- and AMH-positive Sertoli cells similar to control XY gonads (Figure 21E).

Figure 21: XY *Fgf9/Wnt4* double mutants express molecular markers typical of testis development consistent with a full rescue of sex reversal.

(A-E) E16.5-E17.5 gonads labeled with the Sertoli-cell markers SOX9 (red) and AMH (green). Sertoli cells labeled with SOX9 and AMH were absent in XX controls (A), but present in XY controls (B) and XY *Wnt4* mutants (C). For XY *Wnt4* (C, H, and M) and *Fgf9* (D, I, and N) single mutants, the other locus could be homozygous wild type or heterozygous (designated "*Fgf9*$^{+}$" and "*Wnt4*$^{+}$"). Similar to XX controls, sex reversed XY *Fgf9* mutants (D) lacked differentiating Sertoli cells, although a variable number of SOX9 positive cells were observed that did not express AMH (arrows). Sertoli cells were rescued by deleting *Wnt4* in XY *Fgf9* mutants (E). (F-J) E16.5-E17.5 gonads labeled with the germ cell marker CDH1 (red) and the Leydig cell marker 3β-HSD (green). In the XX control (F), germ cells were present but not clustered into testis cords and Leydig cells were absent. In the XY control (G) and XY *Wnt4* mutant (H), germ cells were clustered into testis cords with Leydig cells positive for 3β-HSD outside of testis cords. Sex reversed XY *Fgf9* mutants (I) resembled the XX controls, but deleting *Wnt4* in an XY *Fgf9* mutant (J) rescued Leydig cells and the presence of germ cells in testis cords. (K-O) E16.5-E17.5 gonads labeled with the meiosis marker SCP3 (red) that is nuclear in meiotic germ cells. Meiotic germ cells are present in XX controls (K), absent in XY controls (L) and XY *Wnt4* mutants (M), and present in sex reversed XY *Fgf9* mutants (N). The germ cells in the *Fgf9/Wnt4* double mutants are not in meiosis (O). Thus, deleting *Wnt4* rescued the *Fgf9* phenotype in the XY samples based on the presence or absence of molecular markers characteristic of the prominent testicular and ovarian cell types. All images shown are maximum intensity projections of 12 images over approximately 12 μm using a 40X objective. Scale bar = 100 μm.

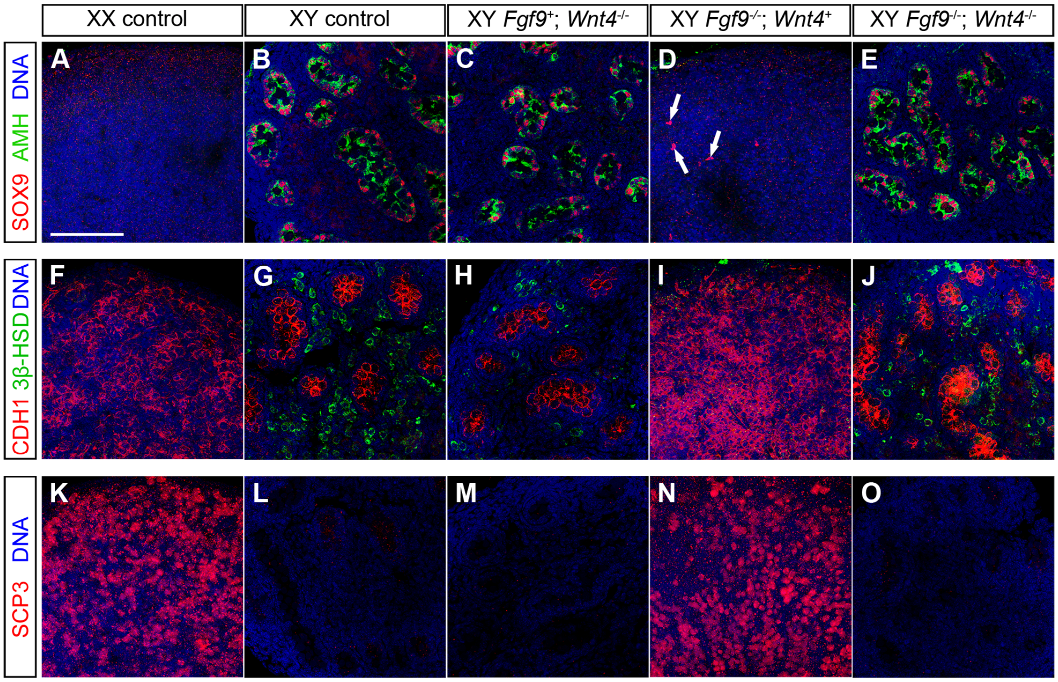
XX control
XY control
XY Fgf9+; Wnt4-/-
XY Fgf9-/-; Wnt4+
XY Fgf9-/-; Wnt4-/-
SOX9 AMH DNA
CDH1 3β-HSD DNA
SCP3 DNA
A
B
C
D
E
F
G
H
I
J
K
L
M
N
O

We also examined whether germ cells labeled by CDH1 (E-cadherin) were clustered into the testis cords and whether Leydig cells expressing the steroidogenic enzyme 3β-HSD were present outside of the testis cords (in the interstitium). The germ cells in the XX control were not clustered into testis cords and Leydig cells labeled with 3β-HSD were not present (Figure 21F). In contrast, XY controls and *Wnt4* mutants had germ cells clustered into testis cords and Leydig cells (Figure 21G-H). XY *Fgf9* mutants resembled ovaries in that the germ cells were not clustered into testis cords and Leydig cells were absent (Figure 21I), but deleting *Wnt4* in an *Fgf9* mutant rescued the presence of germ cells in cords and Leydig cells (Figure 21J). In 1 of 3 double mutant XY samples, there was reduced CDH1 staining (data not shown), but germ cells were still present in the testis cords based on nuclear staining. Thus, all aspects of somatic testis development that we examined were rescued in XY *Fgf9*$^{-/-}$ mice by deleting *Wnt4*.

FGF9 was reported to inhibit the entry of the germ cells into meiosis (Bowles et al. 2010; Barrios et al. 2010). However, *Fgf9* does not appear required to prevent the entry of the germ cells into meiosis. Nuclear SCP3 labels meiotic germ cells, which are present in XX controls and absent from both XY controls and XY *Wnt4* mutants (Figure 21K-M). Faint cytoplasmic staining with SCP3 could be observed in some XY germ cells, but it was not nuclear (data not shown). The germ cells in *Fgf9* mutants are in meiosis (Figure 21N) (Bowles et al. 2010). However, when both *Fgf9* and *Wnt4* are deleted, SCP3 is absent. Together, these results show that both the somatic and germ cell sex reversal phenotype of the XY *Fgf9* mutants is rescued by deleting *Wnt4*, supporting the *Wnt4* repression model of Fgf action

5.3.3 *Fgf9* represses *Wnt4* by E11.75 in XY gonads

It was previously shown that *Wnt4* was elevated in *Fgf9* mutants at E12.5, by the time gonads were sex reversed (Kim et al. 2006), but whether derepression of *Wnt4* occurred before or after *Sox9* expression declined was not determined. While it was possible that the elevated *Wnt4* levels observed at E12.5 were a consequence of SOX9 loss, our model proposed that elevated *Wnt4* expression was a result of *Fgf9* loss and therefore should be detectable prior to the loss of SOX9.

To determine if *Wnt4* up-regulation preceded *Sox9* down-regulation in XY *Fgf9* mutants, we measured mRNA levels of *Sox9* and *Wnt4* in XY and XX *Fgf9*$^{+/+}$ and XY *Fgf9*$^{-/-}$ gonads at E11.75 (Figure 22). SOX9 protein was previously shown to be expressed in XY *Fgf9* mutants through E12.0 (Kim et al. 2006). Similarly, we found that *Sox9* transcript levels were normal in XY *Fgf9*$^{-/-}$ gonads at E11.75, indicating that the initial male developmental program is intact. However, *Wnt4* was already derepressed in E11.75 XY *Fgf9*$^{-/-}$ gonads, demonstrating that elevation of *Wnt4* precedes the loss of *Sox9*. We also found elevated levels of *Rspo1*, which is also upstream of β-catenin signaling during female development (Chassot et al. 2008; Parma et al. 2006). Thus, the derepression of the Wnt signaling components of the female pathway preceded the loss of SOX9, as required by the *Wnt4* repression model.

Figure 22: Female pathway components were derepressed in XY *Fgf9* mutants prior to loss of *Sox9*.

qRT-PCR data from XY *Fgf9*$^{+/+}$, XY *Fgf9*$^{-/-}$ (blue), and XX *Fgf9*$^{+/+}$ (pink) gonads at E11.75. Expression is reported as a fold change relative to XY *Fgf9*$^{+/+}$ levels (1 on the log scale), and *Canx* was used as the normalizing gene (van den Bergen et al. 2009). *Sox9* levels showed no difference between XY *Fgf9*$^{+/+}$ and XY *Fgf9*$^{-/-}$ samples (ns), but there was a significant difference (p-value < .05) between XY *Fgf9*$^{-/-}$ levels and XX *Fgf9*$^{+/+}$ levels (*). "*" over the error bars indicates a significant difference from XY controls. "*" over the horizontal line indicates a significant difference between the XY *Fgf9*$^{-/-}$ and XX *Fgf9*$^{+/+}$ samples. XX *Fgf9*$^{+/+}$ levels of *Sox9* were different from XY *Fgf9*$^{+/+}$ levels, but only at a p-value < .1 (§). However, levels of *Wnt4* and *Rspo1* were significantly higher in the XY *Fgf9*$^{-/-}$ samples and XX *Fgf9*$^{+/+}$ samples compared to the XY *Fgf9*$^{+/+}$ samples. There was no significant difference between the XY *Fgf9*$^{-/-}$ samples and XX *Fgf9*$^{+/+}$ samples for *Wnt4* and *Rspo1*. Thus, XY *Fgf9* mutants express male levels of *Sox9*, and female levels of *Wnt4* and *Rspo1* at E11.75.

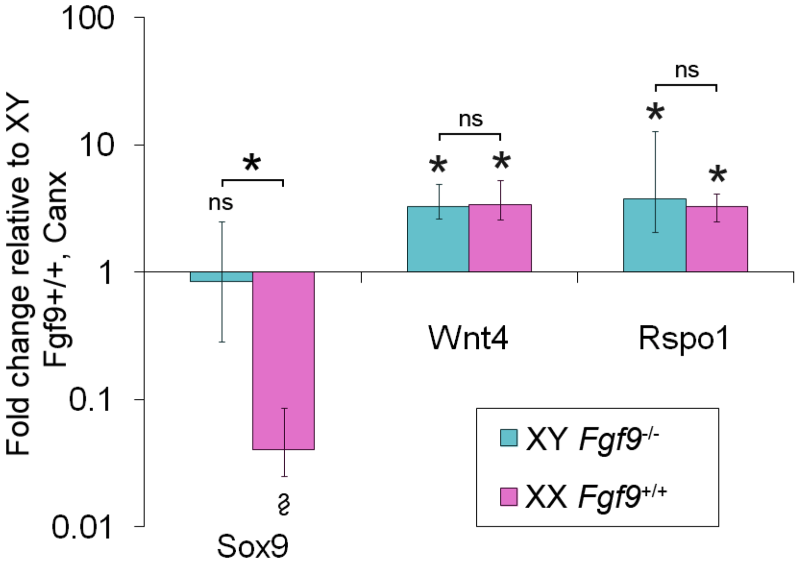
100
10
1
0.1
0.01
Fold change relative to XY Fgf9+/+, Canx
ns
*
§
Sox9
ns
*
*
Wnt4
ns
*
*
Rspo1
XY *Fgf9*-/-
XX *Fgf9*+/+

5.3.4 The partial sex reversal phenotype of XX *Wnt4* mutants is not rescued by deletion of *Fgf9*.

XX *Wnt4*$^{-/-}$ gonads develop features normally only seen in XY gonads: a coelomic vessel and steroidogenic cells unlike XX controls (Jeays-Ward et al. 2003; Vainio et al. 1999) (Figure 23A-D). Previous work exploring the antagonism between *Fgf9* and *Wnt4* signaling showed that FGF9 is elevated in XX *Wnt4* mutants (Kim et al. 2006). It has also previously been shown that FGF9 can induce migration of mesonephric endothelial cells into the XX gonad (Colvin et al. 2001). Thus, we hypothesized that elevation of FGF9 in XX *Wnt4*$^{-/-}$ gonads might be responsible for development of the testis-like characteristics in these mutants. To investigate this possibility, we examined XX *Fgf9*$^{-/-}$; *Wnt4*$^{-/-}$ gonads. In E16.5-E17.5 XX *Wnt4* mutants, we identified the coelomic vessel deep in the gonad as well as ectopic steroidogenic cells (Figure 23C-D). Neither the steroidogenic cells nor the ectopic vessel were apparent in the XX *Fgf9*$^{-/-}$ gonads (Figure 23E-F). However, the XX *Fgf9*$^{-/-}$; *Wnt4*$^{-/-}$ mice developed a coelomic vessel and steroidogenic cells similar to the *Wnt4* mutants (Figure 23G-H). The number of steroidogenic cells was variable in both XX *Wnt4*$^{-/-}$ and *Fgf9*$^{-/-}$; *Wnt4*$^{-/-}$ gonads (data not shown), but steroidogenic cells were present in three gonads of each genotype. The presence of an ectopic vessel and steroidogenic cells in the absence of *Fgf9*, indicates that Fgf signaling is not necessary for coelomic vessel formation or steroidogenesis *in vivo*. In further support of this conclusion, deleting *Fgfr2* in endothelial cells had no effect on coelomic vessel formation in XY gonads (Figure 24). These results show that development of the male-like characteristics in XX *Wnt4*$^{-/-}$ gonads depends on mechanisms that do not require *Fgf9*.

Figure 23: Deleting *Fgf9* did not rescue the phenotypes of XX *Wnt4* mutants.

(A, C, E, and G) PECAM1 (green) labels both the endothelial cells and the germ cells, but with varying intensity in the germ cells at E16.5-E17.5. (B, D, F, H) E16.5-E17.5 gonads labeled with the steroidogenic marker 3β-HSD (red). For XX *Wnt4* (C-D) and *Fgf9* (E-F) single mutants, the other locus could be homozygous wild type or heterozygous (designated "*Fgf9*$^{+}$" and "*Wnt4*$^{+}$"). Unlike XX control ovaries (A-B), XX *Wnt4* mutants developed an ectopic coelomic vessel (C, arrows) and steroidogenic cells (D). (E-F) In the presence of one or more functional copies of *Wnt4*, *Fgf9* mutants did not develop this ectopic vessel or steroidogenic cells. However, both the ectopic vessel (G, arrows) and steroidogenic cells (H) were present in the *Wnt4*/*Fgf9* double mutants. (A, C, E, and G) The images shown are maximum intensity projections of 10 images over approximately 10 μm taken using a 40X objective. (B, D, F, H) The images shown are maximum intensity projections of 10 images over approximately 30 μm taken using a 20X objective. Scale bars = 100 μm.

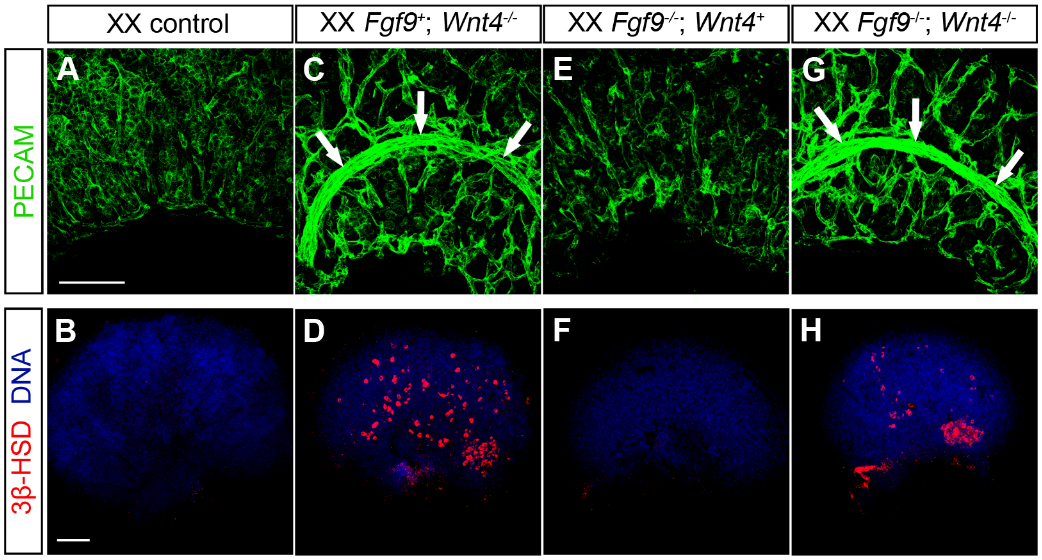
XX control
XX *Fgf9*⁺; *Wnt4*⁻/⁻
XX *Fgf9*⁻/⁻; *Wnt4*⁺
XX *Fgf9*⁻/⁻; *Wnt4*⁻/⁻
PECAM
3β-HSD DNA
A
B
C
D
E
F
G
H

Figure 24: Deleting *Fgfr2* in endothelial cells does not disrupt coelomic vessel formation.

Flk1-Cre (Motoike et al. 2003) was crossed onto the mixed *Fgfr2*$^{flox/flox}$ line. (A) Control XY mice developed a coelomic vessel positive for PECAM1 and NRP1 (arrows, blue and green), and SOX9-positive testis cords (red). (B) The same was observed in mice lacking *Fgfr2* in endothelial cells (XY *Flk1-Cre*$^{+}$; *Fgfr2*$^{flox/flox}$), showing that Fgf signaling through *Fgfr2* is not required for coelomic vessel formation. Scale bar = 100 μm.

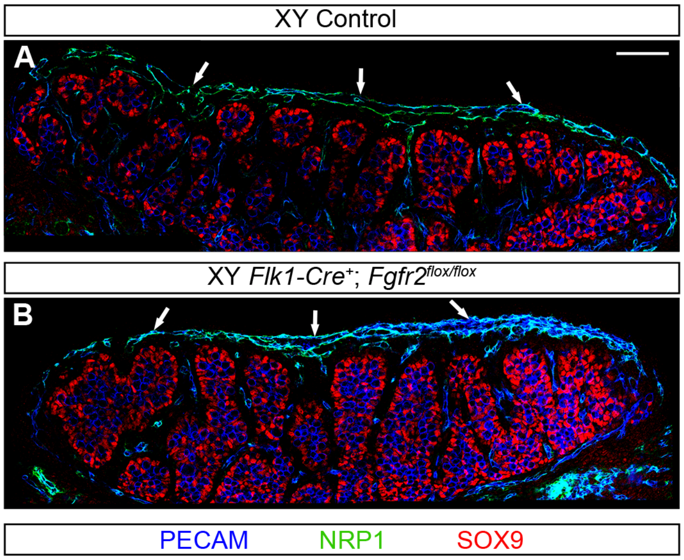
XY Control
A
XY Flk1-Cre+; Fgfr2flox/flox
B
PECAM
NRP1
SOX9

5.4 Discussion

Mammalian sex determination depends on the fate decision that occurs in the supporting cell lineage of the gonad. Work in this dissertation (chapter 4) and by others suggests that these cells are poised, albeit unequally, between male and female fates (Kim et al. 2006; Chassot et al. 2008; Swain et al. 1998; Munger et al. 2009; Vainio et al. 1999; Kent et al. 1996; Morais da Silva et al. 1996; Bradford et al. 2009). Many genes that will later be exclusively associated with either the male or female fate are simultaneously expressed in early XX and XY supporting cells. This pattern of bipotential "lineage priming" has been reported in progenitors in other developmental systems (Delorme et al. 2009; Hu et al. 1997; Ng et al. 2009; Zipori 2004; Miyamoto et al. 2002; Enver and Greaves 1998; Hipp et al. 2010; Golan-Mashiach et al. 2005; Guo et al. 2010). A central question in development is how transcriptional cascades and extracellular signals lead to the resolution of this pattern when cells commit to a single fate. Consistent with other network analyses (Davidson et al. 2002), we show that that the fate commitment of the supporting cells requires both the activation of one transcriptional program and the repression of the other.

In XY gonads, expression of the Y-linked gene *Sry* diverts the fate of the supporting cells toward Sertoli cell differentiation (Figure 25A). SRY acts directly to up-regulate *Sox9* transcription by binding to the TESCO element in the *Sox9* promoter. Once activated, SOX9 binds its own promoter to maintain expression (Sekido and Lovell-

Badge 2008). However, continued SOX9 expression is also critically dependent on the extracellular signaling molecule *Fgf9* and its receptor *Fgfr2.* In the absence of Fgf signaling in XY gonads, SOX9 expression is lost and the gonad switches to the female fate expressing genes such as *Wnt4* (Kim et al. 2007; Kim et al. 2006).

Figure 25: Model of sex determination.

(A) A model of the genetic interactions during early gonad development. SRY up-regulates SOX9 in XY gonads, and SOX9 becomes self-regulating (Sekido and Lovell-Badge 2008). SOX9 up-regulates *Fgf9* (Kim et al. 2006) to repress *Wnt4*. A failure to repress *Wnt4* (in *Fgf9* or *Fgfr2* mutants) results in repression of SOX9 by *Wnt4* signaling and loss of male development. Thus, male development requires (1) the additional activation of male pathway genes (i.e., *Sox9*) and (2) the repression of the female program (i.e., *Wnt4*) that would otherwise repress male genes. (B) A model of sex determination with graphs of the hypothetical gene expression associated with male and female development. Initially, the sexually undifferentiated XX and XY supporting cells express both genes characteristic of the male pathway (blue arrows) and genes characteristic of the female pathway (pink arrows), but the female factors are overrepresented (chapter 4). In XX gonads, the over-represented female program with *Wnt4* drives female development (♀), and male gene expression is lost. In XY gonads, *Sry* up-regulates *Sox9* to drive expression of the male program, including *Fgf9*. By E11.75, *Fgf9* represses *Wnt4* and female development. The expression of male genes and the repression of female genes results in male development (♂). In *Fgf9* mutants, both the male and female programs are active as the female program is not repressed. Once the female program crosses a critical threshold, likely of β-catenin signaling, it can repress the robust activation of the male program to result in female development.

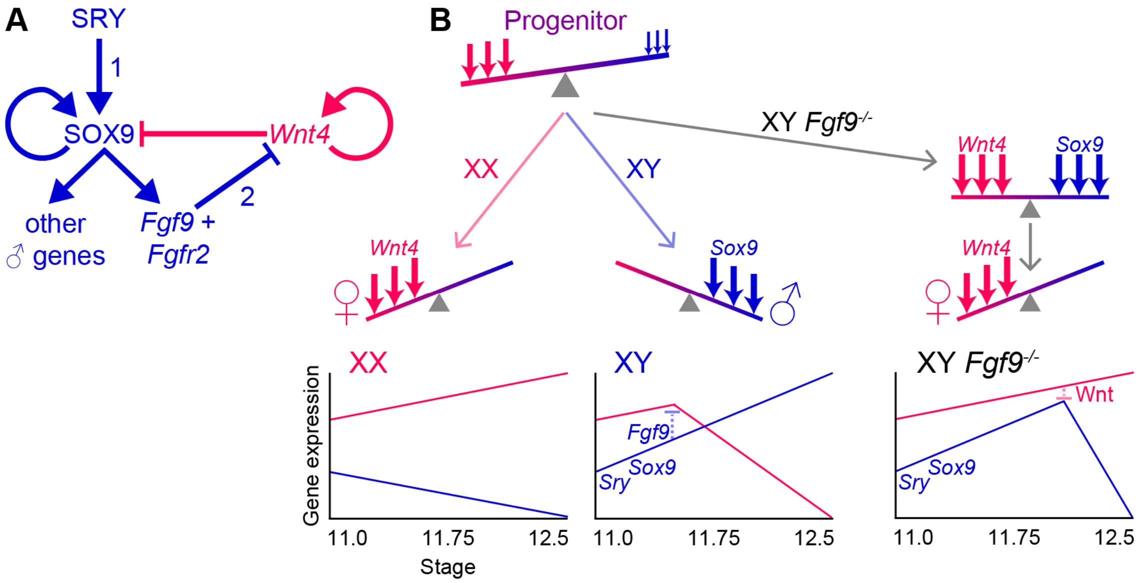
A
SRY
1
SOX9
Wnt4
2
other
♂ genes
Fgf9 +
Fgf2
B
Progenitor
XX
XY
XY Fgf9-/-
Wnt4
Sox9
Wnt4
Sox9
Wnt4
♀
♂
♀
XX
XY
XY Fgf9-/-
Gene expression
Fgf9
Sry
Sox9
Sry
Sox9
Wnt
11.0
11.75
12.5
11.0
11.75
12.5
11.0
11.75
12.5
Stage

These results led to the proposal that *Fgf9* and *Sox9* (which promote male development) are in a mutually antagonistic relationship with *Wnt4* and β-catenin (which promote female development) to control the fate of the gonad. We proposed that *Fgf9* and SOX9 create a positive feed-forward loop to stabilize SOX9 and repress *Wnt4* (Kim et al. 2006). However, our present results show that *Fgf9* is not required to positively activate SOX9, and lead to the surprising conclusion that the effect of *Fgf9* on SOX9 expression is indirect: the primary role of *Fgf9* is the repression of the antagonist of male development, *Wnt4* (Figure 25A).

Wnt4 is initially expressed in both XX and XY gonads and positively reinforces its own expression (Liu et al. 2009; Maatouk et al. 2008; Vainio et al. 1999; Nef et al. 2005) (Figure 25A). However, its expression declines by E11.5 in XY gonads, soon after *Sry*/*Sox9* activation and coincident with a pulse of *Fgf9* expression (Vainio et al. 1999; Nef et al. 2005) (Figure 25B). In XY *Fgf9*$^{-/-}$ gonads, *Wnt4* expression was derepressed by E11.75, preceding *Sox9* loss. This, coupled with the ability of *Wnt4* deletion to rescue both the *Fgfr2* and *Fgf9* male-to-female sex reversal phenotypes, demonstrates that the primary function of Fgf signaling is to repress *Wnt4*.

The corollary of this finding is that *Wnt4* is required for the sex reversal of XY gonads in the absence of *Fgf9*. A failure to repress *Wnt4* blocks testis development. The identification of XX patients that develop testes in the absence of the *SRY* gene led to the proposal that a female-promoting "Z" gene normally blocks male development in the bipotential gonad, and that "Z" is itself blocked by SRY (McElreavey et al. 1993). In some respects, *Wnt4* fits the "Z" paradigm: it can block male development and is itself blocked by *Fgf9* downstream of *Sry*. However, full male development does not occur in XX gonads if *Wnt4* pathway components (*Wnt4*, *Rspo1*, or β-catenin) are individually deleted (Liu et al. 2009; Chassot et al. 2008; Vainio et al. 1999; Jeays-Ward et al. 2003), suggesting that initiation of male development requires additional influences.

It is important to consider the antagonism between *Fgf9* and *Wnt4* in the context of the broader antagonistic subnetworks in the gonad of which they are a part (Tevosian and Manuylov 2008; Hiramatsu et al. 2009; Munger et al. 2009). We showed in chapter 4 that genes that later become specific to the XX or XY cells are initially co-expressed in the sexually undifferentiated supporting cells, but there is an overrepresentation of female-associated genes in these early cells (Figure 25B). This implies that the underlying transcriptional program and signaling environment is biased toward the female fate. Thus, the initially weak male program may require the up-regulation of *Sox9* by *Sry* to maintain itself, which explains why the XX Wnt pathway mutants fail to sex reverse (Liu et al. 2009; Chassot et al. 2008; Vainio et al. 1999; Jeays-Ward et al. 2003). In XX supporting cells, male gene expression is likely lost due to a failure of the male program to be self-reinforcing in the absence *Sry*, leading naturally to the adoption of the female fate.

However, it is also clear that while the up-regulation of *Sox9* by *Sry* is necessary for male development (Chaboissier et al. 2004), it is not sufficient (Hiramatsu et al. 2009; Kim et al. 2006; Maatouk et al. 2008; Chang et al. 2008). Our experiments demonstrate that loss of *Wnt4*, either through repression or deletion, is also necessary for male development. In XY *Fgf9* mutants, the male pathway is activated by *Sry*, but the female program is not repressed, resulting in the co-expression of the strong male and female programs (Figure 25B). Once the female program crosses a critical threshold (likely of β-catenin signaling), it can repress the male program activated by *Sry*. Therefore, we propose a two-part model of male fate commitment in mammals that requires (1) activation of the male pathway (i.e., *Sox9*) by *Sry* and (2) repression of the female program (i.e., *Wnt4*) that would otherwise repress male genes (Figure 25A). *Fgf9* couples the activation of the male program to the repression of the female program.

These findings are directly relevant to the priming model proposed in chapter 4. First, these data identify *Fgf9* as a factor mediating the repression of female-primed genes (*Wnt4* and *Rspo1*, Supplemental File 5A) initially expressed in both XX and XY supporting cell progenitors. Second, these data demonstrate that the repression of female-primed genes (i.e., *Wnt4*) in the XY gonad is required for male development because a failure to do so the *Fgf9* or *Fgfr2* mutants causes male-to-female sex reversal. Therefore, the adoption of the male supporting cell fate appears to be defined as much by gene repression as activation.

The ability of *Wnt4* to repress the male program in the *Fgf9* mutants is interesting since the over-expression of *Wnt4* or *Rspo1* alone was not sufficient to induce male to female sex reversal in mice (Buscara et al. 2009; Jeays-Ward et al. 2003; Jordan et al. 2003). Nevertheless, it is consistent with the ability of constitutive activation of β-catenin to sex reverse male gonads (Maatouk et al. 2008; Chang et al. 2008). In humans a duplication containing *Wnt4* and *Rspo1* can disrupt male development (Jordan et al. 2001; Tevosian and Manuylov 2008), and it may be that *Rspo1* and *Wnt4* are both required to achieve a level of β-catenin signaling that crosses the threshold to repress male development. This is consistent with our data because *Rspo1* and *Wnt4* are both de-repressed in XY *Fgf9* mutants, and deleting just one (*Wnt4*) is sufficient to prevent sex reversal.

There is an asymmetry in the relationship between *Fgf9* and *Wnt4* in the supporting cells. Since the *Fgf9* phenotypes were the result of *Wnt4* de-repression, we investigated whether the XX *Wnt4* mutant phenotypes were caused by derepression of *Fgf9*. We show that this is not the case: the XX *Wnt4* mutant phenotypes were not rescued by the deletion of *Fgf9*. Even though exogenous FGF9 can induce migration of mesonephric endothelial cells into the XX gonad (Colvin et al. 2001), endogenous FGF9 does not appear to have this function *in vivo*. This finding reinforces that the primary function of *Fgf9* is the repression of *Wnt4*.

Work to clarify the intracellular mechanisms through which *Fgf9* and *Wnt4* exert their repressive functions is ongoing. Downstream of Wnt signaling, β-catenin activation can transcriptionally repress *Sox9* by blocking *Sf1* (*Nr5a1*) association with and activation of the TESCO element of the *Sox9* enhancer (Bernard et al. 2011). There is also evidence in chondrocytes that β-catenin represses SOX9 at the protein level through a physical interaction, leading to mutual protein degradation (Akiyama et al. 2004). FGF9 likely represses *Wnt4* at the transcriptional level since the level of *Wnt4* transcript is affected early in *Fgf9* mutants. How this transcriptional repression is mediated remains to be determined. Nevertheless, this double negative repression mechanism is a common feature of many developmental systems (Davidson et al. 2002; Ferrell 2002; Bracken et al. 2008; Revilla-i-Domingo et al. 2007; Johnston et al. 2005).

The precise role of *Fgf9* in the development of other cell types in the gonad is also not clear. The fate of the supporting cells determines the fate of the germ cells (Adams and McLaren 2002). However, *Fgf9* has been reported to promote male germ cell development and repress the female program of meiotic entry (Barrios et al. 2010; Bowles et al. 2010). However, we show that *Fgf9* is not required to block meiosis in the context of male development. It is likely that rescuing male supporting cell development rescues CYP26B1 expression to degrade the meiosis inducing signal from the mesonephros (Bowles et al. 2006; Kumar et al. 2011; Koubova et al. 2006; Byskov 1974; O and Baker 1976). While *Fgf9* may subtly reinforce the male germ cell fate, it may not be required to block meiosis in the context of normal male development.

Spatial and temporal expression patterns are likely to be important in the adoption of the male or female fate by the supporting cells. Elegant experiments demonstrated that maintenance of SOX9 expression in the polar (anterior and posterior) domains of the testis requires diffusion of a signal (possibly FGF9) from the central domain (Hiramatsu et al. 2010). Because reducing *Wnt4* signals in the polar domains did not rescue the loss of *Sox9*, the authors suggested that *Fgf9* acts on *Sox9* to stabilize expression (Hiramatsu et al. 2010). However, our results indicate that there must be another explanation since SOX9 expression is stabilized in an XY *Fgf9*$^{-/-}$;*Wnt4*$^{-/-}$ mutant background. Nevertheless, using an inducible *Sry* transgene, Hiramatsu et al. showed that *Sry* can activate testis development when it is expressed in XX gonads prior to E11.25, but not after this time point (Hiramatsu et al. 2009). This may reflect the fact that the early pulse of *Fgf9* downstream of *Sry* must occur prior to the time that *Wnt4* signaling exceeds the critical β-catenin threshold required to repress male gene expression. Consistent with this interpretation, reduction of *Wnt4* levels expanded the window when the male pathway could be initiated (Hiramatsu et al., 2009). The relative timing and levels of these two signals--*Wnt4*, which is initially expressed in XX and XY gonads, and *Fgf9*, which is activated downstream of *Sry* in XY gonads—may determine the close of the bipotential window during normal development.

While *Wnt4* and *Fgf9* are clearly important for sex determination, the sex determination system is completely operational in the absence of both factors. This supports the idea that there is a complex and robust network underlying sex determination (Munger et al. 2009). Single gene mutations are informative in understanding cell fate decisions, but they can also be misleading by placing too much emphasis on too few genes. It is increasingly important to use a combination of approaches including both the deletion of individual genes and analysis of whole systems to obtain a complete picture of development.

In conclusion, Fgf9 is required for male sex determination. However, it is not required to promote SOX9 expression as previously proposed. Instead, it is critical to a repression program in the XY gonad that is required to block female development. Using *Fgfr2/Wnt4* and *Fgf9/Wnt4* double mutant mice, we show that Fgf signaling promotes male sex determination by repressing the female-promoting gene *Wnt4*. If the male program is unable to repress *Wnt4* due to loss of either *Fgf9* or *Fgfr2*, male development is aborted. Thus, the decision to adopt the male fate is based not only on whether male genes, such as SOX9, are expressed, but also on the repression of female genes, such as *Wnt4*.

A manuscript containing the work in Chapter 5 is under review with Developmental Biology.

6. Future Directions

6.1 Alternative transcript processing during gonad development

We carefully characterized gene expression at the transcript level in our microarray analysis (chapters 3-4). However, the Affymetrix Genechip Mouse Gene 1.0 ST Arrays have probe sets along the entire transcript, which allows analysis of alternative transcript processing (including the use of alternative internal, 5′, and 3′ exons). Thus, we would also like to characterize alternative transcript processing during gonad development.

To this end, I worked with Matthew Marengo and Tim Robinson in Mariano Garcia-Blanco's lab to adapt an updated version of their program SplicerEX (Robinson et al. 2010) to annotate the mouse microarray data, and Matthew kindly generated lists of alternative processing candidate genes in male and female supporting cells and germ cells at E11.5, E12.5, and E13.5 (Supplemental File 6). For this analysis, we re-normalized just the germ and supporting cell microarrays using RMAExpress with log base 2 transformation, background correction, quantile normalization, and median polish summarization. The background for SplicerEX was set to 8. Supplemental File 6 contains the output of the SplicerEX program, which included the type of alternative processing event identified and which probe sets were considered.

We examined these lists to select candidates for further examination. For example, we would like to investigate the splicing of *Kdm4c* (lysine (K)-specific demethylase 4C), which is a histone H3-K9 demethylase (Figure 26A). Some exons were more often included in XY supporting cells, and others were more often included in XX supporting cells. H3-K9 methylation is associated with gene repression (Lachner et al. 2003). Thus, changes in splicing of *Kdm4c* could affect the activation of silenced genes. Similarly, *Epc1* (enhancer of polycomb homolog 1) also had male- and female-specific exons in supporting cells (Figure 26A). *Epc1* was reported to both activate and repress gene expression (Shimono et al. 2000; Kee et al. 2007), be involved in the regulation of cell cycle genes (Attwooll et al. 2005), and be involved in histone acetylation (Galarneau et al. 2000). *Epc1* is an interesting candidate since deletion of a polycomb component (*M33*) results in gonad developmental defects with male-to-female sex reversal (Katoh-Fukui et al. 1998). We are eager to follow up on these candidates because these genes could affect the expression of many other genes at the level of chromatin. Our immediate plans are to validate the alternative processing of these and other genes by qRT-PCR in the sorted supporting cells.

Figure 26: Alternative processing candidate genes.

Probe set expression for some genes identified by SplicerEX as candidates for alternative transcript processing. The graphs display the expression level (Y axis, log-transformed, normalized intensity values) of each probe set for a gene in numerical order (X axis). There is not necessarily a 1:1 correlation between probe sets and exons. The error bars are standard error. Pink arrows indicate a subset of probe sets that where more highly expressed in XX cells, and the blue arrows indicate a subset of probe sets expressed more highly in XY cells. Supporting cell data at E12.5 is shown in blue (A-B), and germ cell data at E13.5 is shown in green (C-D). Male expression is indicated with solid lines, female expression is indicated with dashed lines. *Kdm4c* (A) and *Epc1* (B) appeared to be alternatively spliced in supporting cells with both male- and female-specific probe sets. Similar patterns were identified in the germ cells, such as those shown for *Utrn* (C) and *Llgl2* (D), although only female-specific probe sets were identified for *Llgl2*.

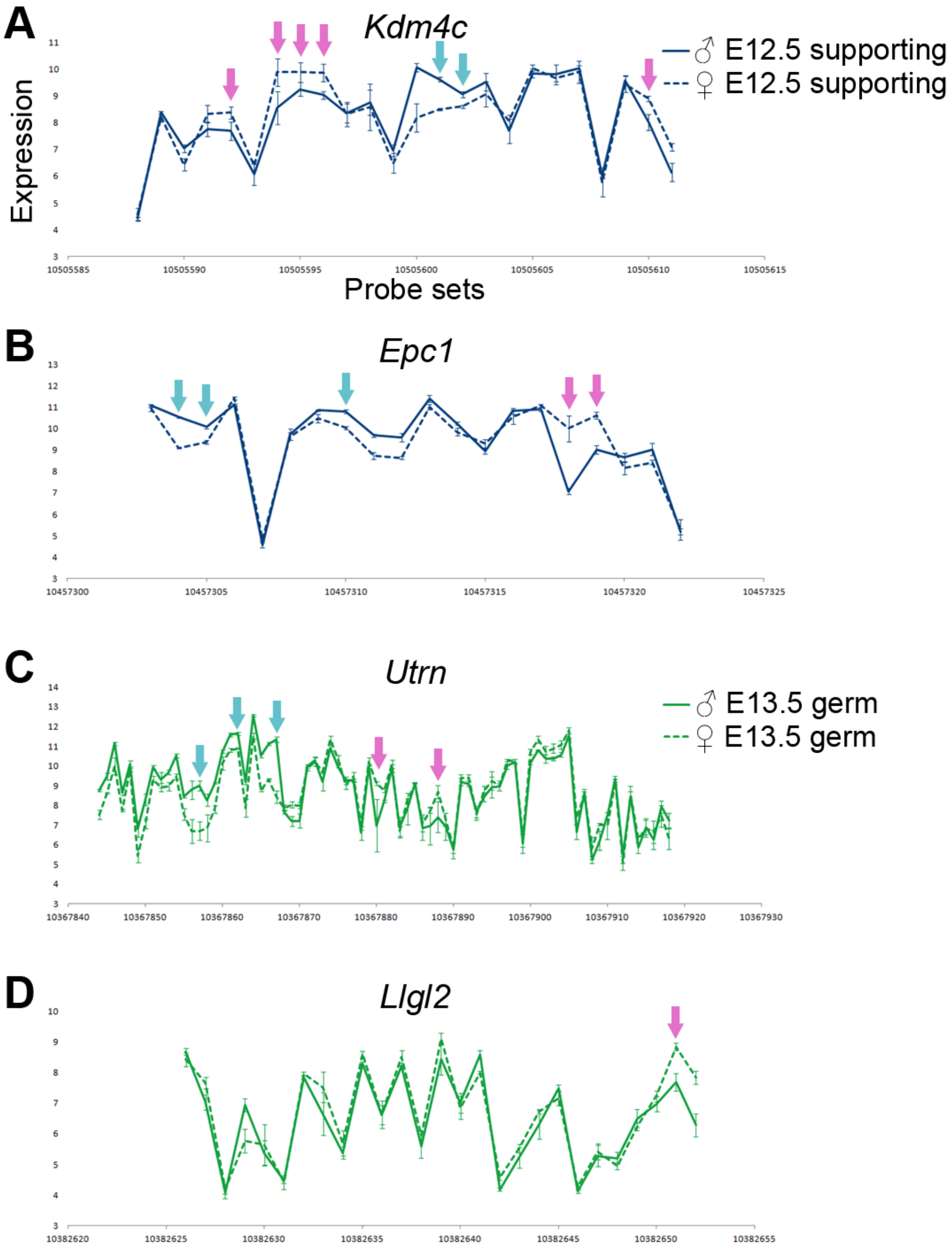
A
Kdm4c
♂ E12.5 supporting
♀ E12.5 supporting
Expression
Probe sets
11
10
9
8
7
6
5
4
3
10505585
10505590
10505595
10505600
10505605
10505610
10505615
B
Epc1
13
12
11
10
9
8
7
6
5
4
3
10457300
10457305
10457310
10457315
10457320
10457325
C
Utrn
♂ E13.5 germ
♀ E13.5 germ
14
13
12
11
10
9
8
7
6
5
4
3
10367840
10367850
10367860
10367870
10367880
10367890
10367900
10367910
10367920
10367930
D
Llgl2
10
9
8
7
6
5
4
3
10382620
10382625
10382630
10382635
10382640
10382645
10382650
10382655

The alternative processing of candidate genes identified in germ cells was more enigmatic. The strongest candidate in germ cells, *Utrn* (Utrophin), is associated with neuromuscular junctions (Rafael et al. 1998) (Figure 26C). *Llgl2* (lethal giant larvae homolog 2) is involved in asymmetric cell division and cell polarity (Ohshiro et al. 2000; Peng et al. 2000) (Figure 26D). We are also planning to validate some of these candidate genes by qRT-PCR in the sorted germ cell population.

6.2 The mechanisms of repression of female genes in the XY supporting cells

The work of a previous graduate student, Steve Munger, showed that the XY gonad had both male and female subnetworks of coexpressed genes using a subset of genes known to be involved in sex determination (Munger et al. 2009). The work in this dissertation extended this finding using the whole transcriptome to show that there was both a male and female subnetwork in the XX and XY supporting cells of the gonad (Chapter 4). However, much of the analysis in the previous work was focused on the activation of male-associated genes, rather than the repression of female-associated genes since the significant repression program was not previously appreciated. Therefore, we would like to further explore the mechanisms of this repressive program during XY supporting cell development.

First, it will be informative to determine how broad the effect of *Fgf9* deletion is on the primed network by performing microarrays on *Fgf9* mutants at one or more early time points. If *Fgf9* affects the expression of only a few female-primed genes, there could be many different male genes involved in the repression of the female program in the XY supporting cells. Alternatively, if *Fgf9* affects the expression of a large proportion of the female primed-program, we would predict that there are likely to be a small number of master repressor genes involved in the repression of the female program in the XY supporting cells.

If there are multiple genes in XY cells involved in the repression of female primed genes, we would like to determine their identity. An interesting way to do so may be to exploit known differences between the C57BL/6J strain and the 129S1/SvImJ strain. The C57BL/6J strain is more susceptible to sex reversal than other strains (Eicher et al. 1982; Meeks et al. 2003; Brennan and Capel 2004). In particular, the *Fgf9* mutation produces a more severe sex reversal on the C57BL/6J strain than on a mixed 129; C57BL/6 strain (Colvin et al. 2001; Schmahl et al. 2004). It was previously shown that XY gonads from the C57BL/6J strain express higher levels of female-associated genes (Munger et al. 2009). However, data in this dissertation demonstrated that as much as 30% of the female program becomes sexually dimorphic (ie. over-expressed in the XX supporting cells) at least in part due to repression in the XY supporting cells (Figure 14), and it will be informative to determine whether the C57BL/6J strain has a defect in the repression of the female program. Expression differences between C57BL/6J and 129S1/SvImJ may help identify candidates for other factors involved in this repression. Anirudh Natarajan and Steve Munger are analyzing another microarray time course to address this and other questions related to the relationship of these two strains.

Also, while previous work identified a coexpression network (Munger et al. 2009), we have yet to determine the majority of the functional connections that actually regulate the expression of genes during gonad development. We would like to build an interaction network as has been done in the sea urchin (Davidson et al. 2002). Examining the expression profile of *Fgf9* mutants over time by microarray will be a step in this direction since we can begin to determine the direct effects of Fgf signaling on the gonad expression network.

While we know that Fgf signaling is required early in the supporting cells for proper testis development, the precise widow of time Fgf signaling is required is still unclear. In particular, we are interested to determine whether Fgf signaling is required during only a brief window of time around E11.5, or whether it is continuously required throughout early gonad development to maintain the repression of *Wnt4*. This is relevant because there may be continuous repression of the alternative fate in the supporting cell lineage in neonatal life: *Dmrt1* is required in the postnatal testis to maintain the repression of the female fate (Matson et al. 2011), and *Foxl2* is required in the postnatal ovary to maintain the repression of the male fate (Uhlenhaut et al. 2009).

However, multiple lines of evidence suggest that Fgf signaling may be required only for the initial adoption of the male fate. The expression level of *Fgf9* in XY supporting cells declines between E11.5 and E13.5, and *Fgfr2* is repressed over the same time period (A). The partial sex reversal in the *Fgfr2* mutants is also consistent with a narrow window of Fgf activity. In these mutants, the center of the gonad was testicular, and the poles of the gonad (anterior and posterior) were ovarian (Figure 19D). The cells in the center of the gonad are committed to the male fate before those at the poles because *Sry* has a pulse of expression that begins in the center of the gonad and moves toward the poles (Bullejos and Koopman 2001). Therefore, it may be that *Fgfr2* is required only for a short period of time that ends earlier in the center of the gonad (since these cells become committed to the male fate first) and later in the poles of the gonad. Because *Sf1-Cre* acts after E11.5, it could delete *Fgfr2* when the cells in the center of the gonad no longer require Fgf signaling, but those at the poles still do require Fgf signaling. This would result in the center of the gonad remaining male and the poles becoming sex-reversed to female upon the deletion of *Fgfr2*, which is what we observe (Figure 19D).

Figure 27: Gene expression during gonad development.

Expression was determined based the microarray data analyzed in chapters 3-4. Expression in XX cells is indicated by dashed lines, while expression in XY cells is indicated by solid lines. The cell types are shown in the same colors used previously (Figure 1). The error bars are standard error. (A) Expression patterns of *Fgf9* and *Fgfr2* that show the expression of both decline in the XY supporting cells after E11.5. (B) Possible candidates mediating the repression of *Wnt4* downstream of Fgf signaling (*Dkk1*, *Dmrt1*, and *Dusp6*) all become significantly dimorphic after E11.5, when *Wnt4* is already dimorphic. *Sf1-EGFP* data (Nef et al. 2005) was used when our sorted cell data did not provide information for a transcript. (C) *Mapk13* is over-expressed in XY supporting cells by E11.5, making it a reasonable candidate for transducing the Fgf signal to repress *Wnt4.*

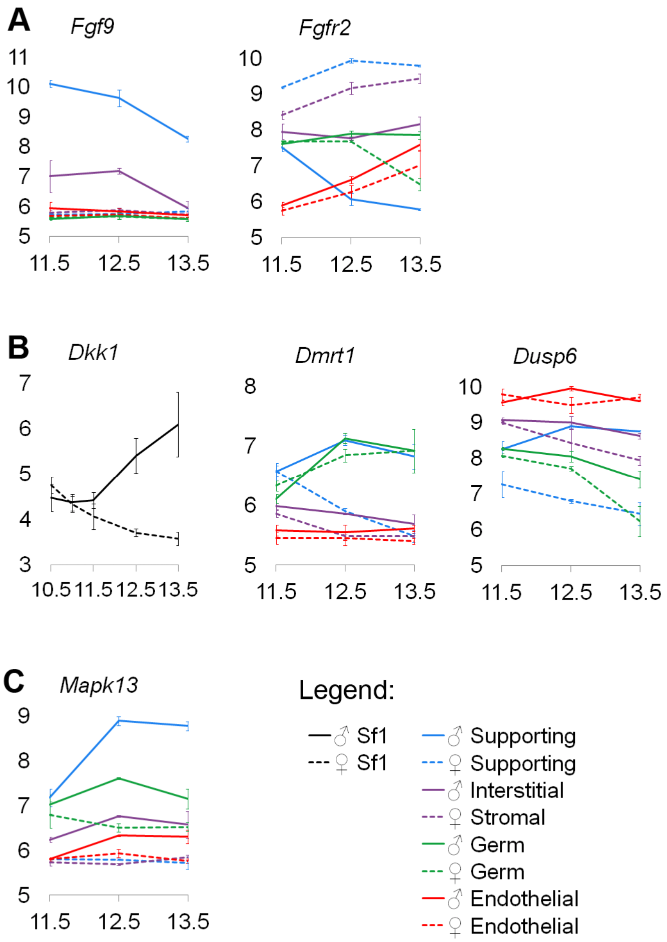
A
Fgf9
11
10
9
8
7
6
5
11.5
12.5
13.5
Fgfr2
10
9
8
7
6
5
11.5
12.5
13.5
B
Dkk1
7
6
5
4
3
10.5
11.5
12.5
13.5
Dmrt1
8
7
6
5
11.5
12.5
13.5
Dusp6
10
9
8
7
6
5
11.5
12.5
13.5
C
Mapk13
9
8
7
6
5
11.5
12.5
13.5
Legend:
♂ Sf1
♀ Sf1
♂ Supporting
♀ Supporting
♂ Interstitial
♀ Stromal
♂ Germ
♀ Germ
♂ Endothelial
♀ Endothelial

We first attempted to test when *Fgfr2* was required in the supporting cells by deleting it with a Tamoxifen-inducible Cre (Hayashi and McMahon 2002). We injected pregnant females with Tamoxifen both before and after E11.5 to induce the Cre in the embryos. However, Tamoxifen treatments before E11.5 of *Fgfr2*$^{flox/flox}$ embryos carrying this Cre did not produce a gonad phenotype (data not shown). This suggests that we did not get adequate Cre induction following Tamoxifen treatment because other Cre lines do produce a phenotype on this *Fgfr2* line (Kim et al. 2007; Bagheri-Fam et al. 2008) (Figure 19D). Thus, we are going to determine when *Fgfr2* is required using an *in vitro* system. An Fgf signaling inhibitor SU5402 (EMD) is reported to affect SOX9 expression when added to gonad cultures before E11.5 (Hiramatsu et al. 2010). We will treat gonads both before and after E11.5 *in vitro* to determine when Fgf signaling is required in the supporting cells.

We are also interested in understanding the intracellular mechanisms downstream of Fgf signaling that mediate the transcriptional repression of *Wnt4*. *Fgf9* could indirectly repress *Wnt4* expression by up-regulating an intermediary gene. Previous studies suggested possible mediators of this repression. Over-expression of the Wnt inhibitor *Dkk1* caused ovarian developmental defects in the *Gata4*/*Fog2* mutants, although it did not affect *Wnt4* transcript levels (Manuylov et al. 2008). Loss of *Dmrt1* in testes resulted in the loss of SOX9 and the adoption of the female fate after birth, but not before (Matson et al. 2011). *Dusp6* is reported to be a transcriptional target of *Fgf9* in the testis (Hiramatsu et al. 2010). However, it appears that none of these genes are sexually dimorphic early enough to cause the repression of *Wnt4* by E11.75, thus they may serve a maintenance role (Figure 27B).

The rapid response of *Wnt4* to *Fgf9* activation, suggests a direct repression of *Wnt4* by an intracellular signaling cascade initiated by FGF9. We initially suspected that Erk signaling could be involved because preliminary data with an inhibitor reported to block both RasGAP and ERK1 called SC1 (Chen et al. 2006) recapitulated aspects of the Fgf knockout phenotype, including rescue of the phenotype by *Wnt4* deletion (data not shown). However, a more specific Erk inhibitor (U0126) did not affect male gonad development (Bogani et al. 2009), suggesting that the Fgf signal does not proceed through Erk. Thus, SC1 may have other off-target effects that block Fgf signaling.

Nevertheless, other MapK pathways could play a critical role downstream of Fgf signaling. The JNK pathway has been implicated in Fgf-mediated repression in the liver (Holt et al. 2003), and p38 has been shown to repress myogenic genes (Suelves et al. 2004). A p38 inhibitor also reduced *Sox9* expression in cultured gonads (Bogani et al. 2009), which is similar to the effects of *Fgf9* loss. *Map3k4* is upstream of p38 and *Map3k4* mutants have defective testis development, but FGF9 is unlikely to signal through *Map3k4* (Bogani et al. 2009). However, *Map3k4* is only one of multiple kinases upstream of p38 activation (Zarubin and Han 2005), and *Mapk13* (p38 δ), is over-expresed in XY compared to XX supporting cells by E11.5 (Figure 27C).

Because there are multiple redundant p38 genes, we are planning to test whether p38 is involved in the repression of *Wnt4* in the gonad also using the *in vitro* gonad culture system. Since much work has already been done with the p38 inhibitor SB202190 (Sigma-Aldrich) (Bogani et al. 2009), we are going to determine the effects of a p38 agonist. Arsenite is believed to specifically activate the p38 signaling pathway (Ludwig et al. 1998). Thus, we will first apply arsenite to cultured wild type gonads to determine if activation of the p38 pathway leads to repression of *Wnt4* and produces the associated *Wnt4* mutant phenotypes in XX samples. Second, we will apply arsenite to cultured XY *Fgf9* mutant gonads to determine if activation of p38 can rescue the *Fgf9* mutant phenotype, demonstrating that p38 is downstream of Fgf signaling during gonad development.

An intriguing possibility is that Fgf signaling could result in widespread chromatin remodeling to repress *Wnt4* and other female genes. One characteristic of lineage priming could be bivalent chromatin, although, in other systems, bivalent loci are typically expressed at low levels (Bernstein et al. 2006), unlike our primed genes. Although p38 has been reported to recruit the SWI-SNF nucleosome remodeling complex (Simone et al. 2004; Serra et al. 2007) and histone methyltransferases (Rampalli et al. 2007), these chromatin modifiers are typically associated with gene activation rather than gene repression. To determine if there are differences in histone modifications or DNA methylation in the *Fgf9* mutants, we are presently crossing our

Sry-EGFP reporter onto the *Fgf9* mutant line so that we can sort the mutant supporting cells for carrier ChIP (O'Neill et al. 2006) and bisulfite sequencing (Clark et al. 1994).

6.3 Exploring the divergence of the supporting cells, interstitial/stromal cells, and the coelomic domain

An interesting cell population that we could not collect for our sorted cell microarray analysis was the coelomic epithelium. The coelomic epithelium gives rise to both the supporting cells and the interstitial/stromal cells (Karl and Capel 1998). In fact, the same cell in the coelomic epithelium can give rise to cells of both lineages (Karl and Capel 1998). However, the basis of the divergence between supporting and interstitial cells is not known.

An interesting possibility is that the coelomic epithelium changes over time to give rise to different cell populations. Other work from the lab suggests that the coelomic epithelium in the female gives rise to different populations of supporting cells at different times (Mork et al. 2011). This idea is also consistent with observations in the early male gonad. It is believed that all of the cells that express *Sry* differentiate into Sertoli cells (Sekido et al. 2004). When determining that SRY was present in the *αSma-EYFP* population (Figure 5), it appeared that the majority of the somatic cells in the gonad were SRY positive based on antibody staining, although this requires further confirmation (data not shown). Thus, the first cells arising from the XY coelomic domain may be a population of supporting cell precursors, and the next cells specified may be the population of interstitial/stromal cells.

This idea is also consistent with earlier proliferation data from the lab, which also indicated that the coelomic domain changes expression over time. In XY gonads, there is an initial burst of proliferation at 16-18 tail somites (around E11.5) that can give rise to supporting cells, and a second phase of this proliferation from 19-25 tail somites (E11.5 to just before E12.5) that can no longer give rise to supporting cells (Schmahl et al. 2000). The first proliferative phase is in the SF1-positive cells of the coelomic domain, and during the second proliferative phase the coelomic domain becomes SF1-negative (Schmahl et al. 2000). In contrast, the coelomic domain of the XX gonads continued to give rise to supporting cell precursors through E12.5 (Mork et al. 2011), and the coelomic domain in the XX gonad remained SF1-positive (Schmahl et al. 2000). Thus, in addition to temporal changes in the coelomic domain, there may also be sex-specific differences.

Given these findings, we would like to determine the transcriptional profile of the coelomic epithelium over time, how it relates to the supporting and interstitial/stromal cells, how it changes over time, and how it differs in XX and XY gonads. It would be ideal to perform microarrays on sorted coelomic epithelial cells. There are several options for isolating these cells. While there is an *Lhx9-EGFP* transgenic line (http://www.gensat.org/index.html) and *Lhx9* is expressed in the coelomic epithelium, the expression of *Lhx9* is unlikely to be restricted to this domain

(Birk et al. 2000; Mazaud et al. 2002). Rather than attempting to identify a specific fluorescent reporter, it may be possible to fluorescently label the cells on the surface of the gonad and use FACS to isolate them based on this fluorescent label. For example, MitoTracker dye (Invitrogen) can be used to label the cells on the surface of the gonad (Mork et al. 2011).

The expression profiling of the coelomic epithelium could provide a number of interesting insights into the development of the gonad. For example, we would like to determine whether there is lineage priming of a progenitor for the supporting cell and interstitial cell fates, or if there is low level priming that may be involved in maintenance of a more undifferentiated state (Laslo et al. 2006). Similarly, by comparing the transcriptional profile of the coelomic epithelium to the supporting cells, we can begin to study the factors involved in the adoption of a lineage-specific fate from the multipotent progenitors. For example, recent work suggests that notch signaling maintains the undifferentiated state of the coelomic epithelium (Linsey Mork, unpublished), and it would be interesting to determine the targets of Notch in this population.

Another informative line of experiments could be following the individual cells of the coelomic domain in three dimensions over time. We could label nuclei by using either a mouse line with fluorescently labeled histones (Hadjantonakis and Papaioannou 2004; Meilhac et al. 2009) or a vital DNA dye (Smith et al. 2000). One of these DNA markers can then be used in combination with a fluorescent marker of a cell type, such as *Sox9-ECFP* (Kim et al. 2007), to determine when the different cell populations arise from the coelomic epithelium.

Appendix A: Localization of FGFR2

The role of FGFR2 in testis development is unquestioned because *Fgfr2* deletion causes XY mice to develop an ovary rather than a testis (Kim et al. 2007). *Fgfr2* deletion affected male Sertoli cell differentiation (Kim et al. 2007), and immunostaining with a commercial antibody to FGFR2 showed localization in the nucleus of Sertoli cells (Santa Cruz sc-122 C17) (Schmahl et al. 2004). Although it was reassuring to see that the FGFR2 antibody detected nuclear localization in a cell type that was affected by the loss of the *Fgfr2* gene, nuclear localiztion of FGFR2 was surprising, raising questions about the fidelity of the antibody.

In fact, there was increasing data suggesting that the commercial antibody was not faithfully reporting FGFR2 localization. Unpublished work from multiple other laboratories in the field suggested that this commercial FGFR2 antibody cross-reacted with SOX9, and that it detected SOX9 in the nucleus of the XY supporting cells. We also found that the nuclear staining with the FGFR2 antibody was not consistent between different lots.

However, there was also data (using antibody lots that showed nuclear localization) suggesting that the antibody did not recognize SOX9. If the FGFR2 antibody recognized SOX9, we expected that in every case where SOX9 was present, FGFR2 would also be nuclear. Instead, there were instances in which SOX9 was present without nuclear enrichment of FGFR2. In contrast to wild type E12.0 gonads, XY *Fgf9*$^{-/-}$

gonads expressed nuclear SOX9, but did not show nuclear FGFR2 staining (Figure 28A). Because FGF9 could regulate the localization of its receptor FGFR2, loss of nuclear FGFR2 was expected in *Fgf9*$^{-/-}$ gonads.

Figure 28: Data inconsistent with the FGFR2 antibody recognizing SOX9.

(A) Immunofluorescence of E12.0 XY *Fgf9*$^{+/-}$ and *Fgf9*$^{-/-}$ whole gonads. Germ cells and vasculature were labeled (red), along with either SOX9 (gift of F. Poulat) or FGFR2 (green). Both the SOX9 and FGFR2 antibodies were raised in rabbit and so could not be used for co-localization. While the *Fgf9*$^{+/-}$ gonads exhibited nuclear staining for both SOX9 and FGFR2, the *Fgf9*$^{-/-}$ gonads lacked nuclear FGFR2 staining, despite having nuclear SOX9. Scale bar = 50 μm. Image courtesy of Yuna Kim. (B) Western blot of E13.5 XY and XX gonad protein extracts, probed with the FGFR2 antibody. A male-specific band is marked with an asterisk at approximately 70 kDa based on protein standards (Bio-rad, 161-0375). (C) Western blot of E13.5 and E14.5 XY gonad protein extracts, probed with the FGFR2 antibody. The male-specific band is marked with an asterisk. All large bands were absent at E14.5 even though SOX9 is still present at this stage. The Western blot conditions were not identical across the blots in B-C. (D) Immunofluorescence of FGFR2 with *Sox9-ECFP* (blue) or DNA (red) in XY gonads from E11.5 to E14.5. While FGFR2 is nuclear at E11.5 and E12.5, the specific nuclear stain is lost by E14.5, although *Sox9* is still present. Arrowheads indicate Sertoli cell nuclei in cells expressing the *Sox9-ECFP* transgene.

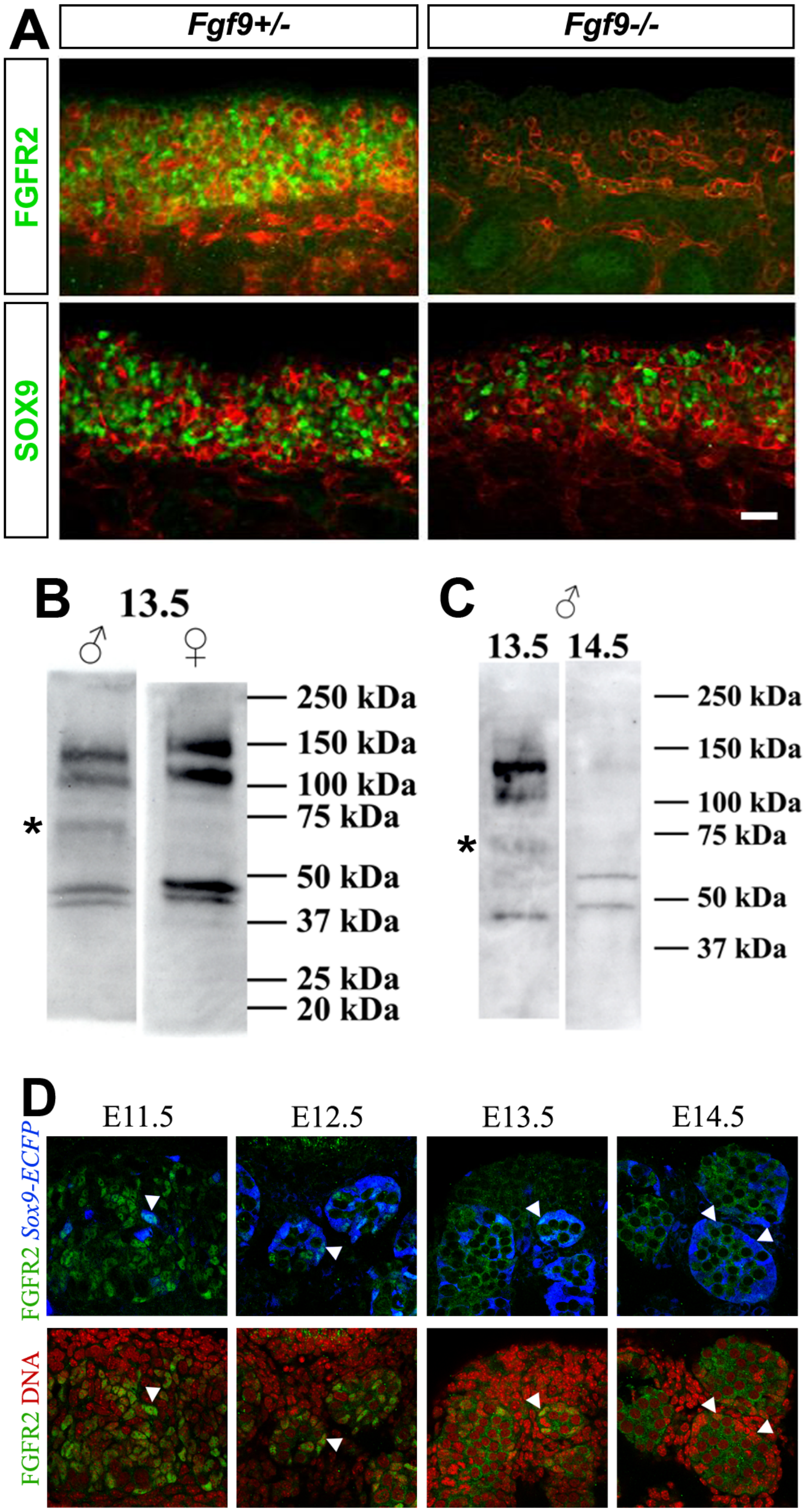
A
Fgf9+/-
Fgf9-/-
FGFR2
SOX9
B
13.5
♂
♀
*
250 kDa
150 kDa
100 kDa
75 kDa
50 kDa
37 kDa
25 kDa
20 kDa
C
♂
13.5
14.5
*
250 kDa
150 kDa
100 kDa
75 kDa
50 kDa
37 kDa
D
E11.5
E12.5
E13.5
E14.5
FGFR2 Sox9-ECFP
FGFR2 DNA

The antibody also stained specific bands on a Western blot, although it did so inconsistently. In successful blots, one of the bands was present in male, but not female, gonad extracts (Figure 28B). This has also been observed by other laboratories. While this is close to the expected 56 kDa size of SOX9, it is not the same. However, the size of a protein as determined by comparison to protein standards is merely an estimate. Nevertheless, the larger bands on the Western blot, including the male-specific band, appeared to be lost at E14.5 (Figure 28C), even though SOX9 is still present at E14.5, although these results were not sufficiently repeated. We also observed less specific nuclear staining by immunofluorescence over developmental time even though *Sox9* (as indicated by the expression of the *Sox9-ECFP* transgene) was still present (Figure 28D). However, this loss over developmental time could be due either to increased staining outside the nucleus, or the loss of nuclear staining.

Rather than detecting SOX9, we proposed that the male-specific band detected on the Western blot was an alternatively spliced form of FGFR2 since there are a diversity of known splice forms (Powers et al. 2000). We proposed that the FGFR2 protein was processed to produce this smaller product similar to FGFR1, which can be cleaved extracellularly by a metalloprotease (Levi et al. 1996). Another tyrosine kinase receptor, ERBB-4, can be cleaved both in the extracellular region by a metalloprotease and in the transmembrane region to release an intracellular fragment that localizes to the nucleus (Ni et al. 2001). However, we were not able to determine if this smaller band was a nuclear localizing form of FGFR2.

Based on results with the antibody alone, there was conflicting data as to whether FGFR2 localized to the nucleus. To directly address whether FGFR2 localized to the nucleus without relying on the antibody, I continued work started by Yuna Kim to make and test the localization of *Fgfr2-EGFP* tagged constructs. I started by creating a construct with *Fgfr2-EGFP* driven by a *Sox9* enhancer element that results in Sertoli cell specific expression (Sekido and Lovell-Badge 2008) (Figure 29A). Since we were examining localization in mixed populations, we wanted to ensure that we only examined the localization in Sertoli cells (or similar cells also expressing SOX9), which showed nuclear localization of FGFR2 by antibody stain (Schmahl et al. 2004). We used Lipofectamine 2000 (Invitrogen) to transfect primary dissociated gonadal cells and NTERA-2cl.D1 cells (Figure 29D-E), which are a human testicular embryonal carcinoma cell line expressing many Sertoli cell genes including *SOX9* (Knower et al. 2007). After transfection of both cell types, we could observe nuclear localization of FGFR2-EGFP in some cells (Figure 29B). The nuclear localization seemed quite specific because in a rare case individual nuclei appeared to be in the same GFP positive cytoplasm, with only one nucleus showing nuclear FGFR2 localization (Figure 29C).

Figure 29: Localization of FGFR2-EGFP.

(A) The series of *Fgfr2-EGFP* constructs that we created to test the localization of FGFR2. The gray bars indicate the *Sox9* enhancer element with a minimal promoter, the green bars indicate the *Fgfr2-EGFP*, and the internal text indicates the possible translational start sites (ATG). (B) Examples of FGFR2-EGFP localization (green) that was and was not nuclear in dissociated E12.5 gonadal cells and NTERA-2cl.D1 cells with the "original" construct. Scale bar = 10 μm. The nuclear envelop was labeled with Lamin B (Santa Cruz Biotechnology, red). (C) A cell that appeared to have two nuclei (Lamin B, red). One nucleus had FGFR2-EGFP (green, arrow), but the other did not (arrowhead). The percentage of transfected E12.5 dissociated gonadal cells (D) and NTERA-2cl.D1 cells (E) that had nuclear localization with the various constructs. A new preparation of the original plasmid did not have the same localization as the original preparation, and no other construct showed substantial nuclear localization. (E) To determine whether full length FGFR2-EGFP was expressed, we transfected HEK 293 cells with a CMV driven *Fgfr2-EGFP* or empty vector with *EGFP* alone. We collected the cells 24 and 72 hours after transfection. The blot was probed with an anti-GFP antibody. With the empty vector, a small protein the size of GFP was detected. With the *Fgfr2-EGFP* construct, a large band around the expected size of FGFR2-EGFP was detectable 72 hours after transfection. Curiously, another band just below 75 kDa ("?") was also detected at 72 hours in the *Fgfr2-EGFP* transfected cells.

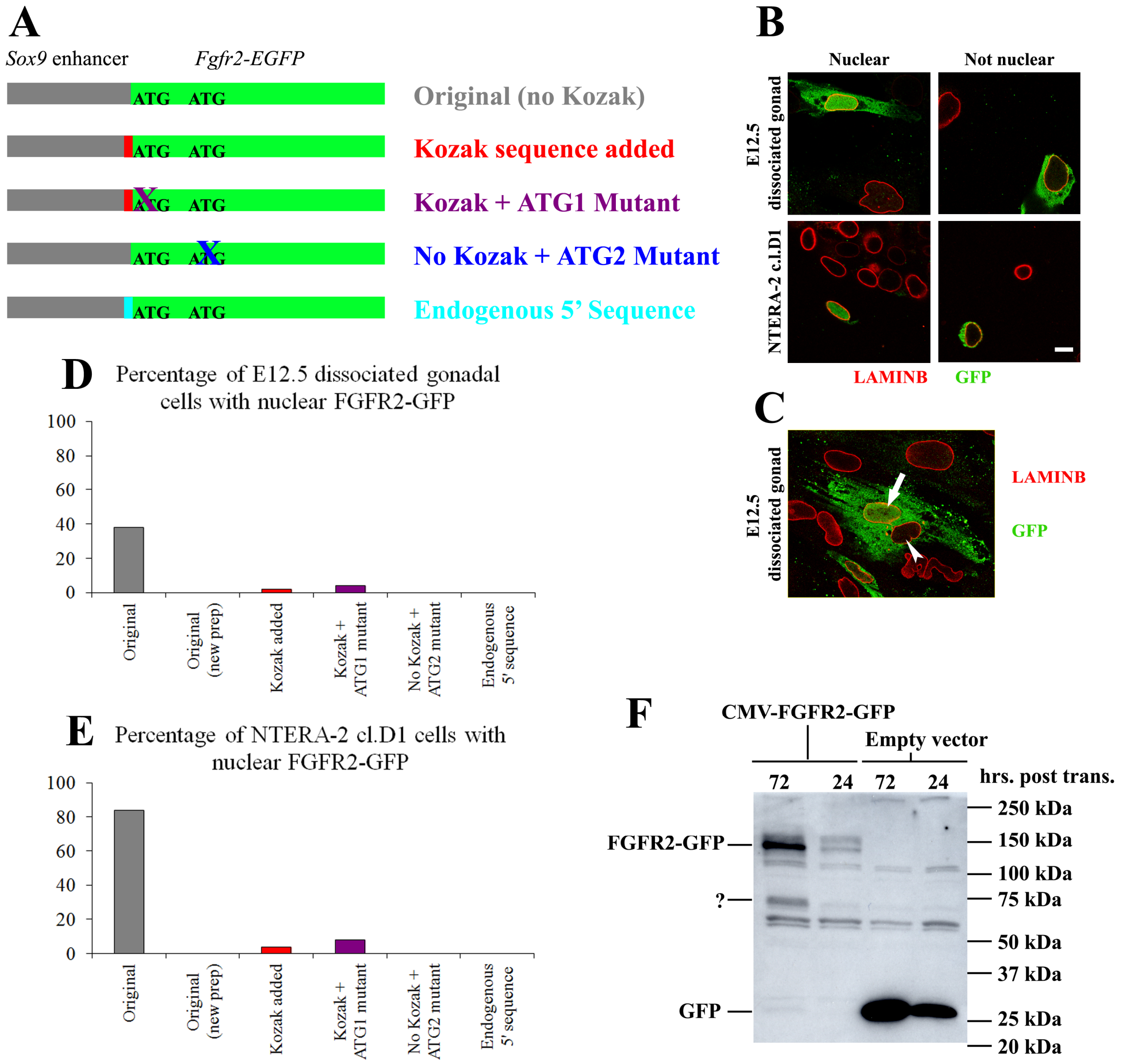
A
Sox9 enhancer
Fgfr2-EGFP
ATG ATG
Original (no Kozak)
Kozak sequence added
Kozak + ATG1 Mutant
No Kozak + ATG2 Mutant
Endogenous 5' Sequence
B
Nuclear
Not nuclear
E12.5 dissociated gonad
NTERA-2 c.l.D1
LAMINB
GFP
C
E12.5 dissociated gonad
LAMINB
GFP
D
Percentage of E12.5 dissociated gonadal cells with nuclear FGFR2-GFP
100
80
60
40
20
0
Original
Original (new prep)
Kozak added
Kozak + ATG1 mutant
No Kozak + ATG2 mutant
Endogenous 5' sequence
E
Percentage of NTERA-2 cl.D1 cells with nuclear FGFR2-GFP
100
80
60
40
20
0
Original
Original (new prep)
Kozak added
Kozak + ATG1 mutant
No Kozak + ATG2 mutant
Endogenous 5' sequence
F
CMV-FGFR2-GFP
Empty vector
72
24
72
24
hrs. post trans.
FGFR2-GFP
?
GFP
250 kDa
150 kDa
100 kDa
75 kDa
50 kDa
37 kDa
25 kDa
20 kDa

This “original” construct showed nuclear localization in almost 40% of transfected E12.5 dissociated gonadal cells and almost 85% of NTERA-2cl.D1 cells (Figure 29D-E). There was variability in expression level and the amount of nuclear localization between different trials. We altered multiple variables in an attempt to optimize the conditions (including varying the dissociation methods, the timing between the transfection and the collection, the scoring methods, etc.), and the data shown here is a subset of the more consistent experimental conditions.

To try to improve expression of the *Fgfr2-EGFP* construct, I added a consensus translation initiation sequence to promote translation (Kozak 1987) (“Kozak added” or “Kozak sequence added”), but this appeared to reduce nuclear localization (Figure 29D-E). We proposed this was due to alternative translation initiation since there were multiple in frame ATGs with good consensus translation initiation sites. Alternative translation initiation sites were demonstrated for one of the Fgf ligands (Bugler et al. 1991). We hypothesized that using the first ATG prevented nuclear localization, but the second promoted nuclear localization. To test this, we mutated these ATG codons (Figure 29A). We expected that mutation of the second ATG to GTG (coding for valine since it is also nonpolar and neutral) would prevent nuclear localization, which was the case (Figure 29D-E) (“No Kozak + ATG2 mutant”). However, we predicted that mutating the first ATG site should rescue nuclear localization as translation would begin at the second ATG (“Kozak + ATG1 mutant”). This was not the case, and nuclear localization was still infrequent with this construct (Figure 29D-E). We predicted that adding the first 34 bases of the 5′ UTR (“endogenous 5′ sequence”) would place the first ATG in the proper context to result in nuclear localization if there was alternative translation that resulted in the skipping of this first ATG, but this construct also failed to produce nuclear localization (Figure 29D-E). Experiments with these constructs (Figure 29A, D-E) were not sufficiently repeated.

Given these findings, we suspected that technical issues were affecting our results. This was most apparent when multiple subsequent preparations (“new prep”) of the “original” construct did not localize to the nucleus (Figure 29D-E is data for a single new preparation, data not shown for others). The original construct and one subsequent preparation of it (as well as the other constructs shown) were fully sequenced from the enhancer through the GFP stop codon, and no mutations were detected.

Because we generally had low expression of these constructs and low transfection efficiencies, it was difficult to determine whether some of the inconsistencies in the data arose from low expression levels. We tried growing a new preparation of the original plasmid in methylation deficient bacteria, which increased nuclear localization slightly (data not shown), suggesting this might have been the case.

To ensure that the expression problems were not caused by a failure to translate the *Fgfr2-EGFP* construct, we validated that our *Fgfr2-EGFP* sequence was capable of producing full length FGFR2-EGFP. Since we generally had low transfection efficiency in the dissociated gonadal cells and NTERA-2cl.D1 cells, we transfected HEK 293 cells to collect protein. We did not expect these cells to express *SOX9*, and so we used CMV driven constructs with either *EGFP* alone (empty vector) or *Fgfr2-EGFP*. We collected protein 24 and 72 hours after transfection. Using an antibody against GFP, we detected the small EGFP protein in cells transfected with the empty vector, and a larger protein consistent with full length FGFR2-EGFP in cells transfected with that construct (Figure 29F). Curiously, we also detected a smaller band in the *Fgfr2-EGFP* transfected cells just below 75 kDa, which was similar to what was observed in gonad protein extracts with the FGFR2 antibody (Figure 28B-C). However, if it was the same protein fragment, we expected this fragment would be larger since it was GFP tagged.

To determine if some of our problems were an artifact of the cell culture system, we also attempted to electroporate whole gonads (Nakamura et al. 2002) with the *Fgfr2-EGFP* construct driven by the *Sox9* enhancer or CMV based on the protocol used in the Joan Jorgensen laboratory. We initially had several problems with lethality in the cultures due to the electroporation, but the gonads were able to survive when we electroporated in a 7 μl droplet of PBS and DNA on a glass slide on ice using wire electrodes with five 50 ms pulses of 25V at 100 ms intervals (Figure 30A). The Fan Wang lab graciously allowed us to use their equipment for electroporations. As a control, we electroporated the empty vector with the CMV promoter driving GFP (Figure 30B). We could detect EGFP in some cells indicating that our electroporation was successful, although the efficiency was low. When we electroporated an *Fgfr2-EGFP* construct, few cells were positive for GFP, and they frequently had no or weak SOX9 expression. Even when we detected weak SOX9, the cell did not have nuclear FGFR2-EGFP. However, this result was not sufficiently repeated.

Figure 30: Gonads electroporated with *Fgfr2-EGFP*.

(A) For electroporation, the gonads were dissected and placed in a droplet of PBS containing the plasmid of interest, wire electrodes were placed on either side of the gonad, and a current was applied. The gonad was then transferred to a droplet of media for culture. (B) Electroporation of an E12.5 gonad with the empty vector (the CMV promoter driving GFP) (green) and an E11.5 gonad with the *Fgfr2-EGFP* driven by the Sox9 enhancer (green). We immunostained for Lamin B to label the nuclear envelope (red) and SOX9 (blue). While our efficiency was generally low, we could identify cells expressing the EGFP alone. However, the rare cell transfected with *Fgfr2-EGFP* that had detectable SOX9 did not show nuclear localization of the FGFR2-EGFP. Scale bar = 10 μm.

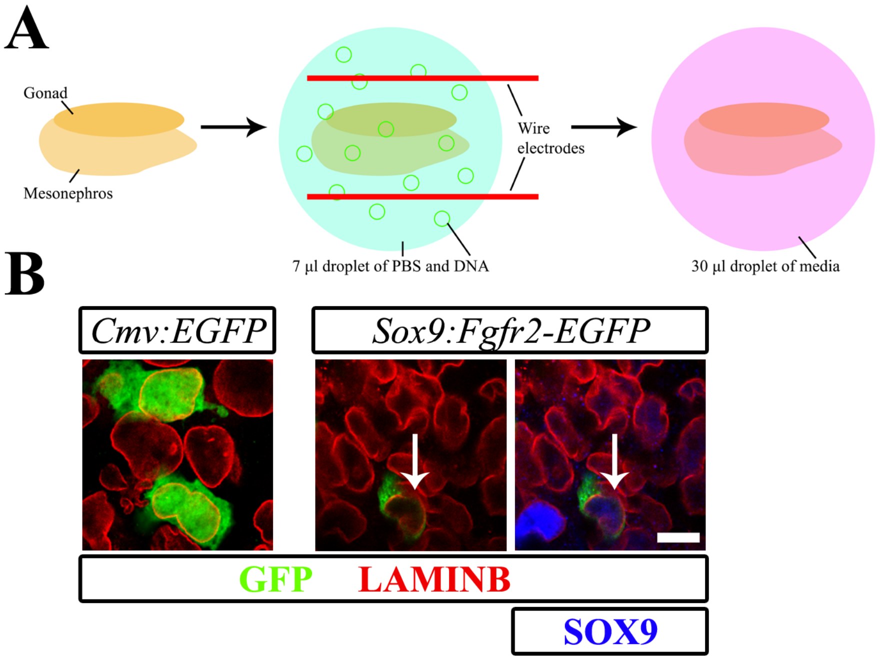
A
Gonad
Mesonephros
Wire electrodes
7 µl droplet of PBS and DNA
30 µl droplet of media
B
Cmv:EGFP
Sox9:Fgfr2-EGFP
GFP
LAMINB
SOX9

In general, these experiments were inconclusive. We were not able to overcome the technical challenges and inconsistencies we encountered while performing them. Also, the increasing weight of contrary data from other laboratories suggested it was best to focus our efforts on other avenues of investigation. Thus, most of these experiments were not completed in a final form.

Appendix B: Analysis of *Fgfrl1* mutants

Given the role of Fgf signaling during gonad development (Kim et al. 2007; Kim et al. 2006; Bagheri-Fam et al. 2008), we were interested in determining whether *Fgfrl1* also played a role in gonad development. The extracellular domain of *Fgfrl1* is similar to other Fgf receptors, but it lacks the tyrosine kinase domains, thus cannot transduce an Fgf signal (Wiedemann and Trueb 2001). *Fgfrl1* is reported to act by either binding Fgf ligand to dampen an Fgf signal (Wiedemann and Trueb 2000; Steinberg et al. 2010) or promoting cell adhesion (Rieckmann et al. 2008). While gonad development was reported to occur normally in *Fgfrl1* mutants, the published images suggested there could be subtle reproductive system defects (Gerber et al. 2009). Thus, we established a collaboration with the Beat Trueb laboratory in Switzerland to examine the reproductive system of the *Fgfrl1* mutants. The Trueb laboratory was kind enough to ship all of the samples analyzed in this portion of the dissertation because we could not import the mice.

While male development of the reproductive system appeared normal in *Fgfrl1* mutants, female development was abnormal (Figure 31A-B). In XX controls (*Fgfrl1*$^{+/+}$ and *Fgfrl1*$^{+/-}$ (designated "*Fgfrl1*$^{+}$")), the ovary adopted a kidney shape and was wrapped in the oviduct at E18.5. A thick uterus was also apparent in wild type animals. In XX *Fgfrl1*$^{-/-}$ samples, the gonad was elongated, we did not observe the coiling of the oviduct, and there was variable loss of the uterus. There was variability even between the two horns of the uterus in the same mouse (Figure 31B).

Figure 31: Reproductive system phenotypes in XX *Fgfrl1* mutants.

(A-B) Brightfield images of E18.5 XX and XY control (*Fgfrl1*$^{+}$) and *Fgfrl1* mutant gonads and upper reproductive tracts. (A) XX and XY gonads with the XX gonads outlined in red. The XX control gonad had a kidney shape, while the XX *Fgfrl1* mutants remained elongated. XY *Fgfrl1*$^{-/-}$ samples appeared normal. (B) In XX controls, the oviduct wrapped around the ovary (arrowhead), and a thick uterus was apparent (arrow). In XX *Fgfrl1*$^{-/-}$ samples, the oviduct did not coil around the ovary (arrowhead), and the uterus was lost in some samples (arrow). The two portions of the reproductive tract in a single image were from the same mouse. (C) We examined the expression of AMH (green) and 3β-HSD (red) in E18.5 XX and XY control and *Fgfrl1*$^{-/-}$ gonads. DNA is blue. Both proteins were present in XY samples as expected, and absent from XX control and *Fgfrl1*$^{-/-}$ samples. While control and *Fgfrl1*$^{-/-}$ images for each experiment are to scale, images in different panels are not.

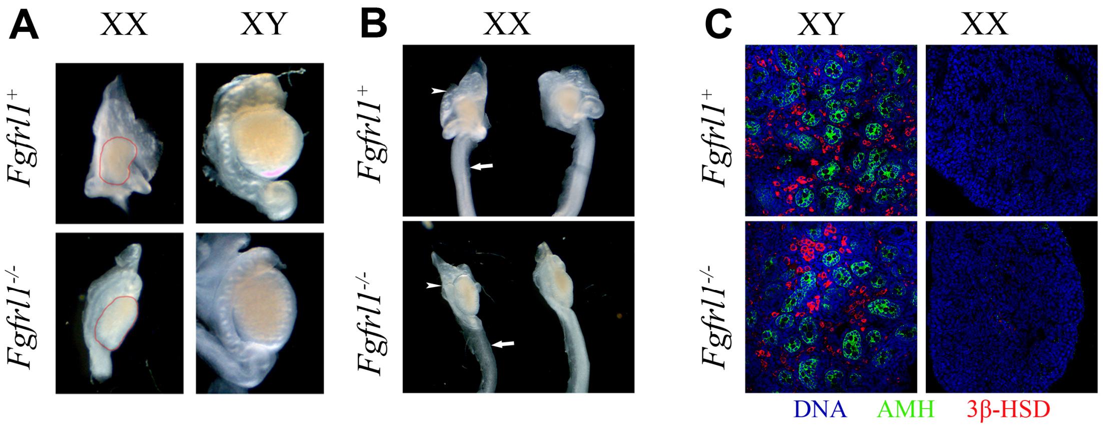
A
XX
XY
Fgfrl1+
Fgfrl1-/-
B
XX
Fgfrl1+
Fgfrl1-/-
C
XY
XX
Fgfrl1+
Fgfrl1-/-
DNA
AMH
3β-HSD

The sex-specific development of the reproductive ducts is determined by AMH and testosterone. Testosterone from the XY gonad (produced by Leydig cells expressing 3β-HSD) maintains the Wolffian duct that develops into the male epididymis and vas deferens. AMH (also produced by the XY gonad) induces the regression of the Müllerian duct, which otherwise develops into the oviduct and uterus (Maatouk and Capel 2008). To determine if aberrant expression of either factor could be responsible for the defects in the *Fgfrl1*$^{-/-}$ oviduct and uterus, we immunostained an XX *Fgfrl1*$^{-/-}$ gonad with AMH and 3β-HSD. However, neither factor was expressed (Figure 31C).

Given that we did not observe any differences in gonadal genes affecting reproductive duct development, we examined Müllerian duct formation at E12.5. Regardless of the sex of the embryo, the Müllerian duct invaginates from the surface of the mesonephros and elongates along the Wolffian duct (Orvis and Behringer 2007; Guioli et al. 2007). The two ducts are in contact at the growing tip of the Müllerian duct, but subsequently are separated by mesenchymal cells (Orvis and Behringer 2007). This is what we observed in the control sample, but not in the *Fgfrl1* mutant (Figure 32). In the *Fgfrl1* mutant, the Müllerian duct was never separated from the Wolffian duct by mesenchymal cells. This suggested a mesenchymal defect in the development of the Müllerian duct. This can be contrasted to the *Wnt4* mutant that also has Müllerian duct defects, but in the *Wnt4* mutant the Müllerian duct does not form (Vainio et al. 1999).

Figure 32: Müllerian duct development in an *Fgfrl1* mutant.

In the control sample (*Fgfrl1*$^{+}$) at E12.5, the Müllerian duct (arrow) extends a portion of the way down the Wolffian duct (arrow head). These images are cross-sections of the ducts. The Wolffian duct is labeled by E-cadherin (green). The Müllerian duct is the E-cadherin negative ring of nuclei (DNA is blue). In the control, the ducts are separated by mesenchymal cells. In an *Fgfrl1* mutant, mesenchymal cells never separated the Wolffian and Müllerian ducts. Scale bar = 50 μm.

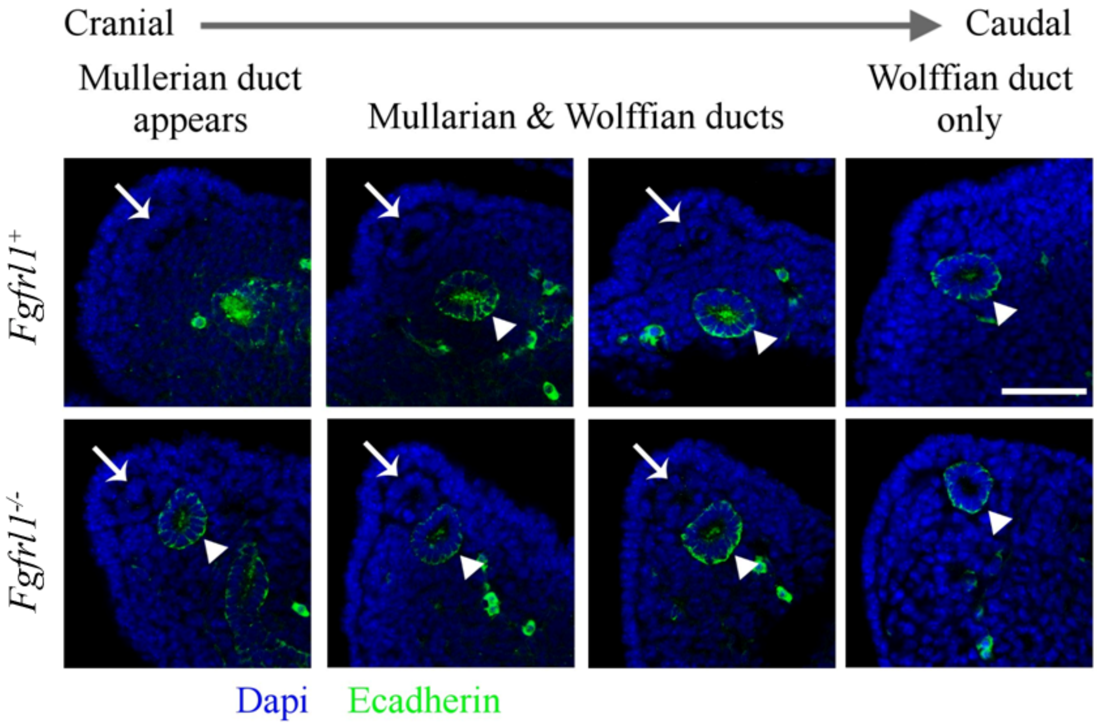
Cranial
Caudal
Mullerian duct appears
Mullarian & Wolffian ducts
Wolffian duct only
Fgfrl1+
Fgfrl1-/-
Dapi
Ecadherin

The Trueb laboratory kindly performed an *in situ* for *Fgfrl1* at E12.5 to determine if it was expressed in the Müllerian duct or the mesonephric mesenchyme (Figure 33). However, they found that *Fgfrl1* was expressed in the portion of the mesonephros with no apparent phenotype: the Wolffian duct. Thus, the effect of deleting *Fgfrl1* on the mesenchyme and Müllerian duct derivatives may be indirect.

Figure 33: *In situ* of *Fgfrl1* in an E12.5 XX gonad and mesonephros.

Fgfrl1 was expressed in the gonad (arrowhead), and also in the Wolffian duct (arrow), but not the Müllerian duct or mesonephric mesenchyme. Image courtesy of the Trueb laboratory.

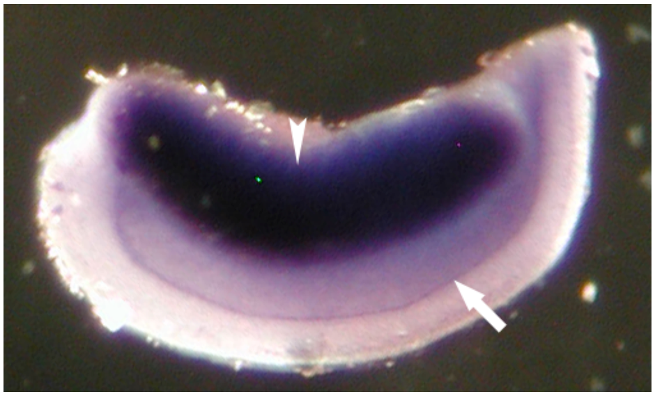

We also attempted to further characterize the XX gonadal phenotype of the *Fgfrl1* mutants. While we detected some differences between XX control and mutant samples at the transcriptional level (Figure 34A, data not shown), most genes examined appeared normally expressed (data not shown). Also, protein expression of important developmental factors appeared normal (Figure 34B-C). For example, even though *Fgf9* promotes the expression of the male germ cell marker *Nanos2* (Bowles et al. 2010; Barrios et al. 2010; Tsuda et al. 2003), XX *Fgfrl1* mutants had reduced *Fgf9* levels and elevated *Nanos2* levels at E18.5 (Figure 34A). Despite having elevated *Nanos2* levels, the germ cells were meiotic (as indicated by SCP3) by E16.5, indicating that they adopted the female fate (Figure 34C). Other markers of the female fate (FOXL2 and p27) were also normal in the XX *Fgfrl1* mutants at E12.5 (Figure 34B) and E16.5 (data not shown). Thus, any molecular gonad developmental phenotype may be subtle, may arise late in development, or may not be detectable with the markers presently available.

Figure 34: Gene expression in XX *Fgfrl1* mutant gonads.

(A) qRT-PCR fold change between an E18.5 XY control (normalized to 1) and individual XX control (*Fgfrl1*$^{+}$, red) and XX *Fgfrl1*$^{-/-}$ (purple) gonad samples. XX *Fgfrl1* mutants appear to have lower levels of *Fgf9*, but higher levels of the male germ cell gene *Nanos2*. One XX *Fgfrl1* mutant had male levels of *Nanos2*. (B) However, looking at earlier protein expression, the E12.5 XX *Fgfrl1* mutant, like the control, expressed the female gene FOXL2 (green) and p27 (red) in the somatic cells. PECAM1 (white) labels germ cells and vasculature. (C) Similarly, an E16.5 *Fgfrl1* control and mutant sample had meiotic germ cells labeled with SCP3 (red) surrounded by GATA4-positive (green) somatic cells.

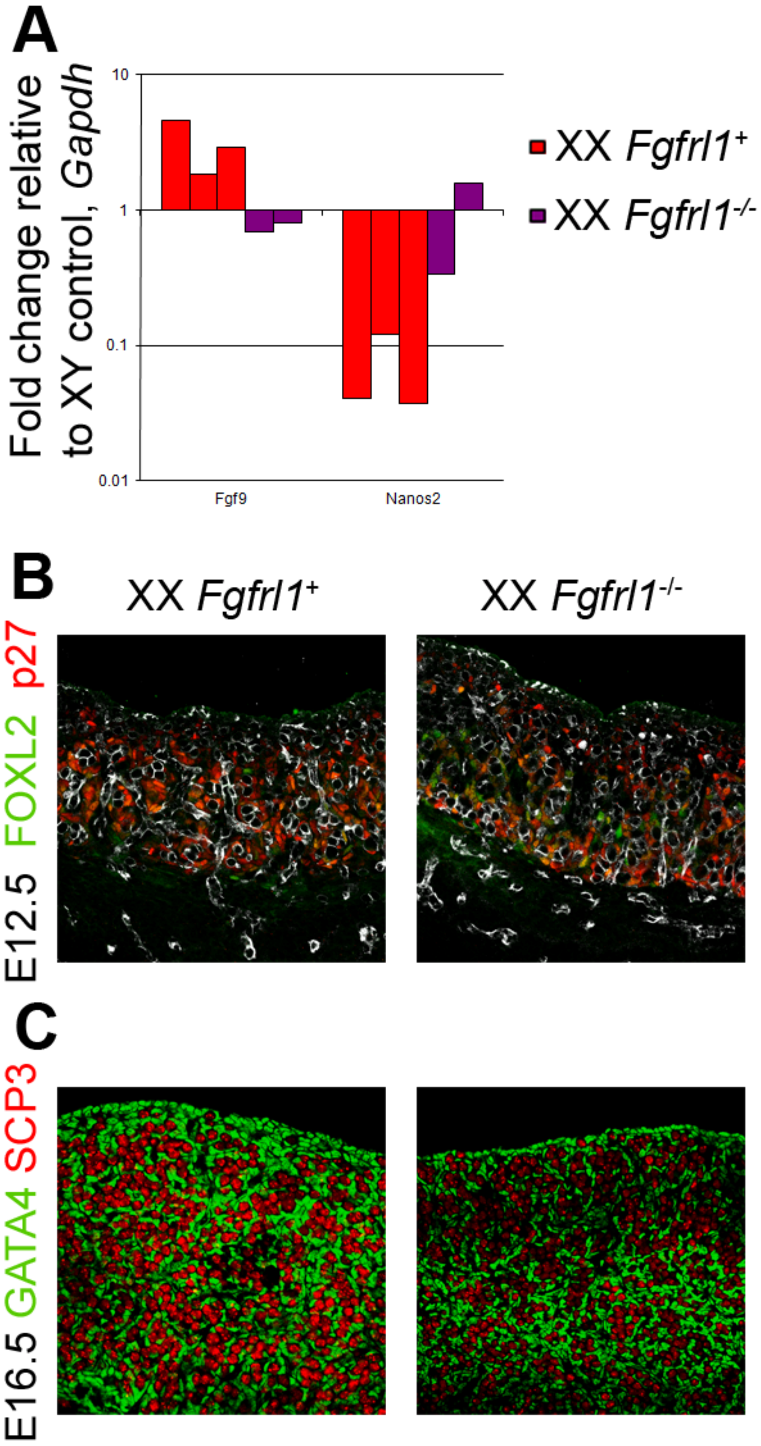
A
Fold change relative to XY control, Gapdh
10
1
0.1
0.01
Fgf9
Nanos2
🟥 XX Fgfrl1+
🟪 XX Fgfrl1-/-
B
XX Fgfrl1+
XX Fgfrl1-/-
E12.5 FOXL2 p27
C
E16.5 GATA4 SCP3

The XX *Fgfrl1* mutants had a clear morphological defect in gonad development (Figure 31), but we were not able to identify a molecular basis of that defect within the gonad (Figure 34). Thus, we hypothesized that the mesonephric defect contributed to the defect in ovarian morphology. Before addressing this in the mutants, we were first interested in determining whether cells of the mesonephros contributed directly to the development of the ovary during normal development. It had previously been shown that endothelial cells migrate specifically into the XY gonad during testis cord formation (Coveney et al. 2008a; Martineau et al. 1997). To determine whether there was migration into or out of the ovary, we recombined a GFP labeled mesonephros with an unlabeled gonad, or vice versa. We were surprised to find that there was a notable migration of endothelial cells out of the gonad, but less migration from the mesonephros into the gonad at all stages we examined (E12.5-E16.5, Figure 35 and data not shown). Because the mesonephros contributed few cells to the XX gonad, a failure in this process cannot be the basis of the gonad developmental defects in the XX *Fgfrl1* mutant. Nevertheless, it is possible that there are indirect effects of the mesonephric defect on the *Fgfrl1* mutant gonads.

Figure 35: Vascular migration out of the ovary.

48 hour co-cultures of a gonad and mesonephros from different mice. In each case, the gonad and mesonephros were the same sex (XX or XY), but one was from a mouse constitutively expressing GFP, and the other was not expressing GFP. This allowed us to track the movement of GFP positive cells (green) from the mesonephros into the gonad (top) or the gonad into the mesonephros (bottom). The images shown are from E15.5-E16.5 samples. Endothelial cells were labeled with PECAM1 (red). DNA is blue. There was little migration into or out of the XY gonads. However, migration of endothelial cells out of the ovary was observed (arrows). Scale bar = 100 μm.

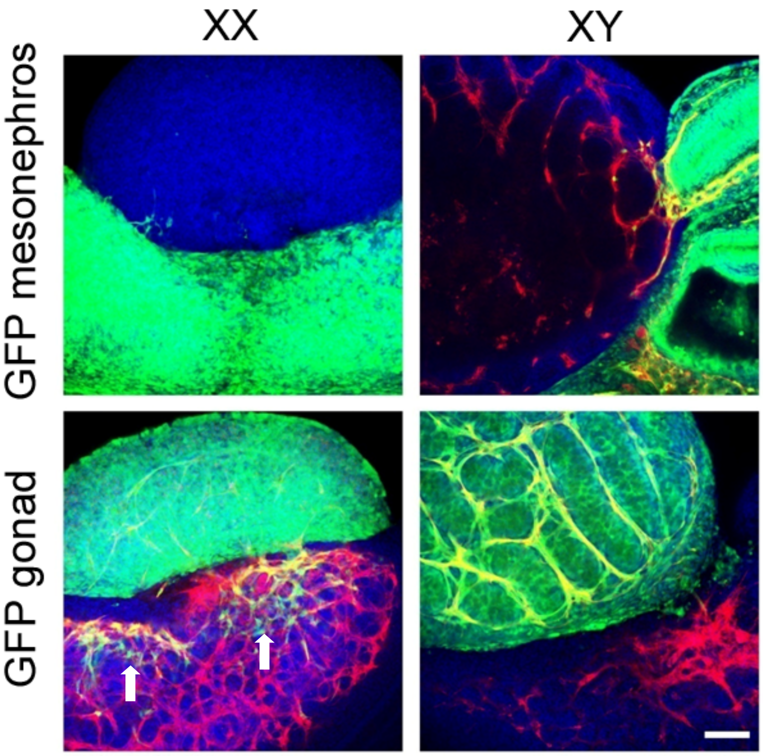
XX
XY
GFP mesonephros
GFP gonad

In conclusion, while the XX *Fgfrl1* mutants do have defects in reproductive system development, we have been unable to draw conclusions about their molecular basis. Our inability to import the mice, as well as the variability of the phenotypes, also complicated the analysis. Thus, we have not pursued these mutants further.

References

Adams, I. R., and A. McLaren. 2002. Sexually dimorphic development of mouse primordial germ cells: switching from oogenesis to spermatogenesis. *Development* 129 (5):1155-64.

Akiyama, H., J. P. Lyons, Y. Mori-Akiyama, X. Yang, R. Zhang, Z. Zhang, J. M. Deng, M. M. Taketo, T. Nakamura, R. R. Behringer, P. D. McCrea, and B. de Crombrugghe. 2004. Interactions between Sox9 and beta-catenin control chondrocyte differentiation. *Genes Dev* 18 (9):1072-87.

Albrecht, K. H., and E. M. Eicher. 2001. Evidence that *Sry* is expressed in pre-Sertoli cells and Sertoli and granulosa cells have a common precursor. *Dev Biol* 240 (1):92-107.

Attwooll, C., S. Oddi, P. Cartwright, E. Prosperini, K. Agger, P. Steensgaard, C. Wagener, C. Sardet, M. C. Moroni, and K. Helin. 2005. A novel repressive E2F6 complex containing the polycomb group protein, EPC1, that interacts with EZH2 in a proliferation-specific manner. *J Biol Chem* 280 (2):1199-208.

Badie, C., J. E. Itzhaki, M. J. Sullivan, A. J. Carpenter, and A. C. Porter. 2000. Repression of CDK1 and other genes with CDE and CHR promoter elements during DNA damage-induced G(2)/M arrest in human cells. *Mol Cell Biol* 20 (7):2358-66.

Bagheri-Fam, S., H. Sim, P. Bernard, I. Jayakody, M. M. Taketo, G. Scherer, and V. R. Harley. 2008. Loss of Fgfr2 leads to partial XY sex reversal. *Dev Biol* 314 (1):71-83.

Barrios, F., D. Filipponi, M. Pellegrini, M. P. Paronetto, S. Di Siena, R. Geremia, P. Rossi, M. De Felici, E. A. Jannini, and S. Dolci. 2010. Opposing effects of retinoic acid and FGF9 on *Nanos2* expression and meiotic entry of mouse germ cells. *J Cell Sci* 123 (Pt 6):871-80.

Barske, L. A., and B. Capel. 2010. Estrogen represses SOX9 during sex determination in the red-eared slider turtle Trachemys scripta. *Dev Biol* 341 (1):305-14.

Beckervordersandforth, R., P. Tripathi, J. Ninkovic, E. Bayam, A. Lepier, B. Stempfhuber, F. Kirchhoff, J. Hirrlinger, A. Haslinger, D. C. Lie, J. Beckers, B. Yoder, M. Irmler, and M. Gotz. 2010. In vivo fate mapping and expression analysis reveals molecular hallmarks of prospectively isolated adult neural stem cells. *Cell Stem Cell* 7 (6):744-58.

Bernard, P., J. Ryan, H. Sim, D. P. Czech, A. H. Sinclair, P. Koopman, and V. R. Harley. 2011. Wnt Signaling in Ovarian Development Inhibits Sf1 Activation of Sox9 via the Tesco Enhancer. *Endocrinology*.

Bernstein, B. E., T. S. Mikkelsen, X. Xie, M. Kamal, D. J. Huebert, J. Cuff, B. Fry, A. Meissner, M. Wernig, K. Plath, R. Jaenisch, A. Wagschal, R. Feil, S. L. Schreiber, and E. S. Lander. 2006. A bivalent chromatin structure marks key developmental genes in embryonic stem cells. *Cell* 125 (2):315-26.

Best, D., D. A. Sahlender, N. Walther, A. A. Peden, and I. R. Adams. 2008. *Sdmg1* is a conserved transmembrane protein associated with germ cell sex determination and germline-soma interactions in mice. *Development* 135 (8):1415-25.

Beverdam, A., and P. Koopman. 2006. Expression profiling of purified mouse gonadal somatic cells during the critical time window of sex determination reveals novel candidate genes for human sexual dysgenesis syndromes. *Hum Mol Genet* 15 (3):417-31.

Bingham, N. C., S. Verma-Kurvari, L. F. Parada, and K. L. Parker. 2006. Development of a steroidogenic factor 1/Cre transgenic mouse line. *Genesis* 44 (9):419-24.

Birk, O. S., D. E. Casiano, C. A. Wassif, T. Cogliati, L. Zhao, Y. Zhao, A. Grinberg, S. Huang, J. A. Kreidberg, K. L. Parker, F. D. Porter, and H. Westphal. 2000. The LIM homeobox gene Lhx9 is essential for mouse gonad formation. *Nature* 403 (6772):909-13.

Bishop, C. E., D. J. Whitworth, Y. Qin, A. I. Agoulnik, I. U. Agoulnik, W. R. Harrison, R. R. Behringer, and P. A. Overbeek. 2000. A transgenic insertion upstream of sox9 is associated with dominant XX sex reversal in the mouse. *Nat Genet* 26 (4):490-4.

Bogani, D., P. Siggers, R. Brixey, N. Warr, S. Beddow, J. Edwards, D. Williams, D. Wilhelm, P. Koopman, R. A. Flavell, H. Chi, H. Ostrer, S. Wells, M. Cheeseman, and A. Greenfield. 2009. Loss of mitogen-activated protein kinase kinase kinase 4 (MAP3K4) reveals a requirement for MAPK signalling in mouse sex determination. *PLoS Biol* 7 (9):e1000196.

Bouma, G. J., J. P. Affourtit, C. J. Bult, and E. M. Eicher. 2007. Transcriptional profile of mouse pre-granulosa and Sertoli cells isolated from early-differentiated fetal gonads. *Gene Expr Patterns* 7 (1-2):113-23.

Bouma, G. J., Q. J. Hudson, L. L. Washburn, and E. M. Eicher. 2010. New candidate genes identified for controlling mouse gonadal sex determination and the early stages of granulosa and Sertoli cell differentiation. *Biol Reprod* 82 (2):380-9.

Bowles, J., C. W. Feng, C. Spiller, T. L. Davidson, A. Jackson, and P. Koopman. 2010. FGF9 suppresses meiosis and promotes male germ cell fate in mice. *Dev Cell* 19 (3):440-9.

Bowles, J., D. Knight, C. Smith, D. Wilhelm, J. Richman, S. Mamiya, K. Yashiro, K. Chawengsaksophak, M. J. Wilson, J. Rossant, H. Hamada, and P. Koopman. 2006. Retinoid signaling determines germ cell fate in mice. *Science* 312 (5773):596-600.

Bracken, C. P., P. A. Gregory, N. Kolesnikoff, A. G. Bert, J. Wang, M. F. Shannon, and G. J. Goodall. 2008. A double-negative feedback loop between ZEB1-SIP1 and the microRNA-200 family regulates epithelial-mesenchymal transition. *Cancer Res* 68 (19):7846-54.

Bradford, S. T., R. Hiramatsu, M. P. Maddugoda, P. Bernard, M. C. Chaboissier, A. Sinclair, A. Schedl, V. Harley, Y. Kanai, P. Koopman, and D. Wilhelm. 2009. The cerebellin 4 precursor gene is a direct target of SRY and SOX9 in mice. *Biol Reprod* 80 (6):1178-88.

Brady, S. M., D. A. Orlando, J. Y. Lee, J. Y. Wang, J. Koch, J. R. Dinneny, D. Mace, U. Ohler, and P. N. Benfey. 2007. A high-resolution root spatiotemporal map reveals dominant expression patterns. *Science* 318 (5851):801-6.

Brady, S. M., L. Zhang, M. Megraw, N. J. Martinez, E. Jiang, C. S. Yi, W. Liu, A. Zeng, M. Taylor-Teeples, D. Kim, S. Ahnert, U. Ohler, D. Ware, A. J. Walhout, and P. N. Benfey. 2011. A stele-enriched gene regulatory network in the Arabidopsis root. *Mol Syst Biol* 7:459.

Brennan, J., and B. Capel. 2004. One tissue, two fates: molecular genetic events that underlie testis versus ovary development. *Nat Rev Genet* 5 (7):509-21.

Brunskill, E. W., B. J. Aronow, K. Georgas, B. Rumballe, M. T. Valerius, J. Aronow, V. Kaimal, A. G. Jegga, J. Yu, S. Grimmond, A. P. McMahon, L. T. Patterson, M. H. Little, and S. S. Potter. 2008. Atlas of gene expression in the developing kidney at microanatomic resolution. *Dev Cell* 15 (5):781-91.

Bugler, B., F. Amalric, and H. Prats. 1991. Alternative initiation of translation determines cytoplasmic or nuclear localization of basic fibroblast growth factor. *Mol Cell Biol* 11 (1):573-7.

Bullejos, M., and P. Koopman. 2001. Spatially dynamic expression of Sry in mouse genital ridges. *Dev Dyn* 221 (2):201-5.

Burgoyne, P. S., M. Buehr, P. Koopman, J. Rossant, and A. McLaren. 1988. Cell-autonomous action of the testis-determining gene: Sertoli cells are exclusively XY in XX----XY chimaeric mouse testes. *Development* 102 (2):443-50.

Buscara, L., F. Montazer-Torbati, S. Chadi, A. Auguste, J. Laubier, A. A. Chassot, L. Renault, B. Passet, J. Costa, M. Pannetier, M. Vilotte, M. C. Chaboissier, J. L. Vilotte, E. Pailhoux, and F. Le Provost. 2009. Goat RSPO1 over-expression rescues sex-reversal in Rspo1-knockout XX mice but does not perturb testis differentiation in XY or sex-reversed XX mice. *Transgenic Res* 18 (4):649-54.

Byskov, A. G. 1974. Does the rete ovarii act as a trigger for the onset of meiosis? *Nature* 252 (5482):396-7.

Capel, B. 1998. Sex in the 90s: SRY and the switch to the male pathway. *Annu Rev Physiol* 60:497-523.

Chaboissier, M. C., A. Kobayashi, V. I. Vidal, S. Lutzkendorf, H. J. van de Kant, M. Wegner, D. G. de Rooij, R. R. Behringer, and A. Schedl. 2004. Functional analysis of Sox8 and Sox9 during sex determination in the mouse. *Development* 131 (9):1891-901.

Chang, H., F. Gao, F. Guillou, M. M. Taketo, V. Huff, and R. R. Behringer. 2008. Wt1 negatively regulates beta-catenin signaling during testis development. *Development* 135 (10):1875-85.

Chassot, A. A., F. Ranc, E. P. Gregoire, H. L. Roepers-Gajadien, M. M. Taketo, G. Camerino, D. G. de Rooij, A. Schedl, and M. C. Chaboissier. 2008. Activation of beta-catenin signaling by *Rspo1* controls differentiation of the mammalian ovary. *Hum Mol Genet* 17 (9):1264-77.

Chen, S., J. T. Do, Q. Zhang, S. Yao, F. Yan, E. C. Peters, H. R. Scholer, P. G. Schultz, and S. Ding. 2006. Self-renewal of embryonic stem cells by a small molecule. *Proc Natl Acad Sci U S A* 103 (46):17266-71.

Chuma, S., and N. Nakatsuji. 2001. Autonomous transition into meiosis of mouse fetal germ cells in vitro and its inhibition by gp130-mediated signaling. *Dev Biol* 229 (2):468-79.

Clark, S. J., J. Harrison, C. L. Paul, and M. Frommer. 1994. High sensitivity mapping of methylated cytosines. *Nucleic Acids Res* 22 (15):2990-7.

Colvin, J. S., R. P. Green, J. Schmahl, B. Capel, and D. M. Ornitz. 2001. Male-to-female sex reversal in mice lacking fibroblast growth factor 9. *Cell* 104 (6):875-89.

Cook, M. S., D. Coveney, I. Batchvarov, J. H. Nadeau, and B. Capel. 2009. BAX-mediated cell death affects early germ cell loss and incidence of testicular teratomas in *Dnd1(Ter/Ter)* mice. *Dev Biol* 328 (2):377-83.

Cook, M. S., S. C. Munger, J. H. Nadeau, and B. Capel. 2011. Regulation of male germ cell cycle arrest and differentiation by DND1 is modulated by genetic background. *Development* 138 (1):23-32.

Cool, J., F. D. Carmona, J. C. Szucsik, and B. Capel. 2008. Peritubular myoid cells are not the migrating population required for testis cord formation in the XY gonad. *Sex Dev* 2 (3):128-33.

Coveney, D., J. Cool, T. Oliver, and B. Capel. 2008a. Four-dimensional analysis of vascularization during primary development of an organ, the gonad. *Proc Natl Acad Sci U S A* 105 (20):7212-7.

Coveney, D., A. J. Ross, J. D. Slone, and B. Capel. 2008b. A microarray analysis of the XX *Wnt4* mutant gonad targeted at the identification of genes involved in testis vascular differentiation. *Gene Expr Patterns* 8 (7-8):529-37.

Davidson, E. H., J. P. Rast, P. Oliveri, A. Ransick, C. Calestani, C. H. Yuh, T. Minokawa, G. Amore, V. Hinman, C. Arenas-Mena, O. Otim, C. T. Brown, C. B. Livi, P. Y. Lee, R. Revilla, A. G. Rust, Z. Pan, M. J. Schilstra, P. J. Clarke, M. I. Arnone, L. Rowen, R. A. Cameron, D. R. McClay, L. Hood, and H. Bolouri. 2002. A genomic regulatory network for development. *Science* 295 (5560):1669-78.

DeFalco, T., S. Takahashi, and B. Capel. 2011. Two distinct origins for Leydig cell progenitors in the fetal testis. *Dev Biol* 352 (1):14-26.

Delorme, B., J. Ringe, C. Pontikoglou, J. Gaillard, A. Langonne, L. Sensebe, D. Noel, C. Jorgensen, T. Haupl, and P. Charbord. 2009. Specific lineage-priming of bone marrow mesenchymal stem cells provides the molecular framework for their plasticity. *Stem Cells* 27 (5):1142-51.

Dietrich, J. E., and T. Hiiragi. 2007. Stochastic patterning in the mouse pre-implantation embryo. *Development* 134 (23):4219-31.

Dietrich, P., I. Dragatsis, S. Xuan, S. Zeitlin, and A. Efstratiadis. 2000. Conditional mutagenesis in mice with heat shock promoter-driven cre transgenes. *Mamm Genome* 11 (3):196-205.

DiNapoli, L., J. Batchvarov, and B. Capel. 2006. FGF9 promotes survival of germ cells in the fetal testis. *Development* 133 (8):1519-27.

Eicher, E. M., and L. L. Washburn. 1986. Genetic control of primary sex determination in mice. *Annu Rev Genet* 20:327-60.

Eicher, E. M., L. L. Washburn, J. B. Whitney, 3rd, and K. E. Morrow. 1982. Mus poschiavinus Y chromosome in the C57BL/6J murine genome causes sex reversal. *Science* 217 (4559):535-7.

Enver, T., and M. Greaves. 1998. Loops, lineage, and leukemia. *Cell* 94 (1):9-12.

Ewen, K. A., and P. Koopman. 2010. Mouse germ cell development: from specification to sex determination. *Mol Cell Endocrinol* 323 (1):76-93.

Farini, D., M. L. Scaldaferri, S. Iona, G. La Sala, and M. De Felici. 2005. Growth factors sustain primordial germ cell survival, proliferation and entering into meiosis in the absence of somatic cells. *Dev Biol* 285 (1):49-56.

Ferrell, J. E., Jr. 2002. Self-perpetuating states in signal transduction: positive feedback, double-negative feedback and bistability. *Curr Opin Cell Biol* 14 (2):140-8.

Fong, G. H., J. Rossant, M. Gertsenstein, and M. L. Breitman. 1995. Role of the Flt-1 receptor tyrosine kinase in regulating the assembly of vascular endothelium. *Nature* 376 (6535):66-70.

Francavilla, S., and L. Zamboni. 1985. Differentiation of mouse ectopic germinal cells in intra- and perigonadal locations. *J Exp Zool* 233 (1):101-9.

Fujikura, J., E. Yamato, S. Yonemura, K. Hosoda, S. Masui, K. Nakao, J. Miyazaki Ji, and H. Niwa. 2002. Differentiation of embryonic stem cells is induced by GATA factors. *Genes Dev* 16 (7):784-9.

Galarneau, L., A. Nourani, A. A. Boudreault, Y. Zhang, L. Heliot, S. Allard, J. Savard, W. S. Lane, D. J. Stillman, and J. Cote. 2000. Multiple links between the NuA4 histone acetyltransferase complex and epigenetic control of transcription. *Mol Cell* 5 (6):927-37.

Gerber, S. D., F. Steinberg, M. Beyeler, P. M. Villiger, and B. Trueb. 2009. The murine Fgfrl1 receptor is essential for the development of the metanephric kidney. *Dev Biol* 335 (1):106-19.

Golan-Mashiach, M., J. E. Dazard, S. Gerecht-Nir, N. Amariglio, T. Fisher, J. Jacob-Hirsch, B. Bielorai, S. Osenberg, O. Barad, G. Getz, A. Toren, G. Rechavi, J. Itskovitz-Eldor, E. Domany, and D. Givol. 2005. Design principle of gene expression used by human stem cells: implication for pluripotency. *FASEB J* 19 (1):147-9.

Gubbay, J., J. Collignon, P. Koopman, B. Capel, A. Economou, A. Munsterberg, N. Vivian, P. Goodfellow, and R. Lovell-Badge. 1990. A gene mapping to the sex-determining region of the mouse Y chromosome is a member of a novel family of embryonically expressed genes. *Nature* 346 (6281):245-50.

Guioli, S., R. Sekido, and R. Lovell-Badge. 2007. The origin of the Mullerian duct in chick and mouse. *Dev Biol* 302 (2):389-98.

Guo, G., M. Huss, G. Q. Tong, C. Wang, L. Li Sun, N. D. Clarke, and P. Robson. 2010. Resolution of cell fate decisions revealed by single-cell gene expression analysis from zygote to blastocyst. *Dev Cell* 18 (4):675-85.

Hacker, A., B. Capel, P. Goodfellow, and R. Lovell-Badge. 1995. Expression of Sry, the mouse sex determining gene. *Development* 121 (6):1603-14.

Hadjantonakis, A. K., and V. E. Papaioannou. 2004. Dynamic in vivo imaging and cell tracking using a histone fluorescent protein fusion in mice. *BMC Biotechnol* 4:33.

Hayashi, S., and A. P. McMahon. 2002. Efficient recombination in diverse tissues by a tamoxifen-inducible form of Cre: a tool for temporally regulated gene activation/inactivation in the mouse. *Dev Biol* 244 (2):305-18.

Hipp, J. A., J. D. Hipp, A. Atala, and S. Soker. 2010. Functional genomics: new insights into the 'function' of low levels of gene expression in stem cells. *Curr Genomics* 11 (5):354-8.

Hiramatsu, R., K. Harikae, N. Tsunekawa, M. Kurohmaru, I. Matsuo, and Y. Kanai. 2010. FGF signaling directs a center-to-pole expansion of tubulogenesis in mouse testis differentiation. *Development* 137 (2):303-12.

Hiramatsu, R., S. Matoba, M. Kanai-Azuma, N. Tsunekawa, Y. Katoh-Fukui, M. Kurohmaru, K. Morohashi, D. Wilhelm, P. Koopman, and Y. Kanai. 2009. A critical time window of Sry action in gonadal sex determination in mice. *Development* 136 (1):129-38.

Holt, J. A., G. Luo, A. N. Billin, J. Bisi, Y. Y. McNeill, K. F. Kozarsky, M. Donahee, D. Y. Wang, T. A. Mansfield, S. A. Kliewer, B. Goodwin, and S. A. Jones. 2003. Definition of a novel growth factor-dependent signal cascade for the suppression of bile acid biosynthesis. *Genes Dev* 17 (13):1581-91.

Hu, M., D. Krause, M. Greaves, S. Sharkis, M. Dexter, C. Heyworth, and T. Enver. 1997. Multilineage gene expression precedes commitment in the hemopoietic system. *Genes Dev* 11 (6):774-85.

Huang, B., S. Wang, Y. Ning, A. N. Lamb, and J. Bartley. 1999. Autosomal XX sex reversal caused by duplication of SOX9. *Am J Med Genet* 87 (4):349-53.

Huang da, W., B. T. Sherman, and R. A. Lempicki. 2009a. Bioinformatics enrichment tools: paths toward the comprehensive functional analysis of large gene lists. *Nucleic Acids Res* 37 (1):1-13.

———. 2009b. Systematic and integrative analysis of large gene lists using DAVID bioinformatics resources. *Nat Protoc* 4 (1):44-57.

Huber, O., R. Korn, J. McLaughlin, M. Ohsugi, B. G. Herrmann, and R. Kemler. 1996. Nuclear localization of beta-catenin by interaction with transcription factor LEF-1. *Mech Dev* 59 (1):3-10.

Ideker, T., T. Galitski, and L. Hood. 2001. A new approach to decoding life: systems biology. *Annu Rev Genomics Hum Genet* 2:343-72.

Ikeda, Y., W. H. Shen, H. A. Ingraham, and K. L. Parker. 1994. Developmental expression of mouse steroidogenic factor-1, an essential regulator of the steroid hydroxylases. *Mol Endocrinol* 8 (5):654-62.

Jeanes, A., D. Wilhelm, M. J. Wilson, J. Bowles, P. J. McClive, A. H. Sinclair, and P. Koopman. 2005. Evaluation of candidate markers for the peritubular myoid cell lineage in the developing mouse testis. *Reproduction* 130 (4):509-16.

Jeays-Ward, K., M. Dandonneau, and A. Swain. 2004. Wnt4 is required for proper male as well as female sexual development. *Dev Biol* 276 (2):431-40.

Jeays-Ward, K., C. Hoyle, J. Brennan, M. Dandonneau, G. Alldus, B. Capel, and A. Swain. 2003. Endothelial and steroidogenic cell migration are regulated by WNT4 in the developing mammalian gonad. *Development* 130 (16):3663-70.

Jho, E. H., T. Zhang, C. Domon, C. K. Joo, J. N. Freund, and F. Costantini. 2002. Wnt/beta-catenin/Tcf signaling induces the transcription of *Axin2*, a negative regulator of the signaling pathway. *Mol Cell Biol* 22 (4):1172-83.

Johnston, R. J., Jr., S. Chang, J. F. Etchberger, C. O. Ortiz, and O. Hobert. 2005. MicroRNAs acting in a double-negative feedback loop to control a neuronal cell fate decision. *Proc Natl Acad Sci U S A* 102 (35):12449-54.

Jordan, B. K., M. Mohammed, S. T. Ching, E. Delot, X. N. Chen, P. Dewing, A. Swain, P. N. Rao, B. R. Elejalde, and E. Vilain. 2001. Up-regulation of WNT-4 signaling and dosage-sensitive sex reversal in humans. *Am J Hum Genet* 68 (5):1102-9.

Jordan, B. K., J. H. Shen, R. Olaso, H. A. Ingraham, and E. Vilain. 2003. Wnt4 overexpression disrupts normal testicular vasculature and inhibits testosterone synthesis by repressing steroidogenic factor 1/beta-catenin synergy. *Proc Natl Acad Sci U S A* 100 (19):10866-71.

Jorgensen, J. S., and L. Gao. 2005. *Irx3* is differentially up-regulated in female gonads during sex determination. *Gene Expr Patterns* 5 (6):756-62.

Jost, A. 1947. Recherches sur la diff'erenciation sexuelle de l'embryon de lapin. *Arch Anat Microsc Morph Exp* (36):271–315.

Karl, J., and B. Capel. 1998. Sertoli cells of the mouse testis originate from the coelomic epithelium. *Dev Biol* 203 (2):323-33.

Katoh-Fukui, Y., R. Tsuchiya, T. Shiroishi, Y. Nakahara, N. Hashimoto, K. Noguchi, and T. Higashinakagawa. 1998. Male-to-female sex reversal in M33 mutant mice. *Nature* 393 (6686):688-92.

Kee, H. J., J. R. Kim, K. I. Nam, H. Y. Park, S. Shin, J. C. Kim, Y. Shimono, M. Takahashi, M. H. Jeong, N. Kim, K. K. Kim, and H. Kook. 2007. Enhancer of polycomb1, a novel homeodomain only protein-binding partner, induces skeletal muscle differentiation. *J Biol Chem* 282 (10):7700-9.

Kent, J., S. C. Wheatley, J. E. Andrews, A. H. Sinclair, and P. Koopman. 1996. A male-specific role for SOX9 in vertebrate sex determination. *Development* 122 (9):2813-22.

Kim, Y., N. Bingham, R. Sekido, K. L. Parker, R. Lovell-Badge, and B. Capel. 2007. Fibroblast growth factor receptor 2 regulates proliferation and Sertoli differentiation during male sex determination. *Proc Natl Acad Sci U S A* 104 (42):16558-63.

Kim, Y., A. Kobayashi, R. Sekido, L. DiNapoli, J. Brennan, M. C. Chaboissier, F. Poulat, R. R. Behringer, R. Lovell-Badge, and B. Capel. 2006. *Fgf9* and *Wnt4* act as antagonistic signals to regulate mammalian sex determination. *PLoS Biol* 4 (6):e187.

Knower, K. C., H. Sim, P. J. McClive, J. Bowles, P. Koopman, A. H. Sinclair, and V. R. Harley. 2007. Characterisation of urogenital ridge gene expression in the human embryonal carcinoma cell line NT2/D1. *Sex Dev* 1 (2):114-26.

Koopman, P., J. Gubbay, N. Vivian, P. Goodfellow, and R. Lovell-Badge. 1991. Male development of chromosomally female mice transgenic for *Sry*. *Nature* 351 (6322):117-21.

Koubova, J., D. B. Menke, Q. Zhou, B. Capel, M. D. Griswold, and D. C. Page. 2006. Retinoic acid regulates sex-specific timing of meiotic initiation in mice. *Proc Natl Acad Sci U S A* 103 (8):2474-9.

Kozak, M. 1987. An analysis of 5'-noncoding sequences from 699 vertebrate messenger RNAs. *Nucleic Acids Res* 15 (20):8125-48.

Kumar, S., C. Chatzi, T. Brade, T. J. Cunningham, X. Zhao, and G. Duester. 2011. Sex-specific timing of meiotic initiation is regulated by Cyp26b1 independent of retinoic acid signalling. *Nat Commun* 2:151.

Lachner, M., R. J. O'Sullivan, and T. Jenuwein. 2003. An epigenetic road map for histone lysine methylation. *J Cell Sci* 116 (Pt 11):2117-24.

Larina, I. V., W. Shen, O. G. Kelly, A. K. Hadjantonakis, M. H. Baron, and M. E. Dickinson. 2009. A membrane associated mCherry fluorescent reporter line for studying vascular remodeling and cardiac function during murine embryonic development. *Anat Rec (Hoboken)* 292 (3):333-41.

Larsson, O., C. Scheele, Z. Liang, J. Moll, C. Karlsson, and C. Wahlestedt. 2004. Kinetics of senescence-associated changes of gene expression in an epithelial, temperature-sensitive SV40 large T antigen model. *Cancer Res* 64 (2):482-9.

Laslo, P., C. J. Spooner, A. Warmflash, D. W. Lancki, H. J. Lee, R. Sciammas, B. N. Gantner, A. R. Dinner, and H. Singh. 2006. Multilineage transcriptional priming and determination of alternate hematopoietic cell fates. *Cell* 126 (4):755-66.

Levi, E., R. Fridman, H. Q. Miao, Y. S. Ma, A. Yayon, and I. Vlodavsky. 1996. Matrix metalloproteinase 2 releases active soluble ectodomain of fibroblast growth factor receptor 1. *Proc Natl Acad Sci U S A* 93 (14):7069-74.

Liu, C. F., N. Bingham, K. Parker, and H. H. Yao. 2009. Sex-specific roles of beta-catenin in mouse gonadal development. *Hum Mol Genet* 18 (3):405-17.

Liu, G., A. E. Loraine, R. Shigeta, M. Cline, J. Cheng, V. Valmeekam, S. Sun, D. Kulp, and M. A. Siani-Rose. 2003. NetAffx: Affymetrix probesets and annotations. *Nucleic Acids Res* 31 (1):82-6.

Ludwig, S., A. Hoffmeyer, M. Goebeler, K. Kilian, H. Hafner, B. Neufeld, J. Han, and U. R. Rapp. 1998. The stress inducer arsenite activates mitogen-activated protein kinases extracellular signal-regulated kinases 1 and 2 via a MAPK kinase 6/p38-dependent pathway. *J Biol Chem* 273 (4):1917-22.

Maatouk, D. M., and B. Capel. 2008. Sexual development of the soma in the mouse. *Curr Top Dev Biol* 83:151-83.

Maatouk, D. M., L. DiNapoli, A. Alvers, K. L. Parker, M. M. Taketo, and B. Capel. 2008. Stabilization of beta-catenin in XY gonads causes male-to-female sex-reversal. *Hum Mol Genet* 17 (19):2949-55.

Mansson, R., A. Hultquist, S. Luc, L. Yang, K. Anderson, S. Kharazi, S. Al-Hashmi, K. Liuba, L. Thoren, J. Adolfsson, N. Buza-Vidas, H. Qian, S. Soneji, T. Enver, M. Sigvardsson, and S. E. Jacobsen. 2007. Molecular evidence for hierarchical transcriptional lineage priming in fetal and adult stem cells and multipotent progenitors. *Immunity* 26 (4):407-19.

Manuylov, N. L., F. O. Smagulova, L. Leach, and S. G. Tevosian. 2008. Ovarian development in mice requires the GATA4-FOG2 transcription complex. *Development* 135 (22):3731-43.

Martineau, J., K. Nordqvist, C. Tilmann, R. Lovell-Badge, and B. Capel. 1997. Male-specific cell migration into the developing gonad. *Curr Biol* 7 (12):958-68.

Matson, C. K., M. W. Murphy, A. L. Sarver, M. D. Griswold, V. J. Bardwell, and D. Zarkower. 2011. DMRT1 prevents female reprogramming in the postnatal mammalian testis. *Nature*.

Mazaud, S., E. Oreal, C. J. Guigon, D. Carre-Eusebe, and S. Magre. 2002. Lhx9 expression during gonadal morphogenesis as related to the state of cell differentiation. *Gene Expr Patterns* 2 (3-4):373-7.

McElreavey, K., E. Vilain, N. Abbas, I. Herskowitz, and M. Fellous. 1993. A regulatory cascade hypothesis for mammalian sex determination: SRY represses a negative regulator of male development. *Proc Natl Acad Sci U S A* 90 (8):3368-72.

McLaren, A. 1991. Development of the mammalian gonad: the fate of the supporting cell lineage. *Bioessays* 13 (4):151-6.

McLaren, A., and D. Southee. 1997. Entry of mouse embryonic germ cells into meiosis. *Dev Biol* 187 (1):107-13.

Meeks, J. J., J. Weiss, and J. L. Jameson. 2003. Dax1 is required for testis determination. *Nat Genet* 34 (1):32-3.

Meilhac, S. M., R. J. Adams, S. A. Morris, A. Danckaert, J. F. Le Garrec, and M. Zernicka-Goetz. 2009. Active cell movements coupled to positional induction are involved in lineage segregation in the mouse blastocyst. *Dev Biol* 331 (2):210-21.

Menke, D. B., J. Koubova, and D. C. Page. 2003. Sexual differentiation of germ cells in XX mouse gonads occurs in an anterior-to-posterior wave. *Dev Biol* 262 (2):303-12.

Mise, N., T. Fuchikami, M. Sugimoto, S. Kobayakawa, F. Ike, T. Ogawa, T. Tada, S. Kanaya, T. Noce, and K. Abe. 2008. Differences and similarities in the developmental status of embryo-derived stem cells and primordial germ cells revealed by global expression profiling. *Genes Cells* 13 (8):863-77.

Miyamoto, T., H. Iwasaki, B. Reizis, M. Ye, T. Graf, I. L. Weissman, and K. Akashi. 2002. Myeloid or lymphoid promiscuity as a critical step in hematopoietic lineage commitment. *Dev Cell* 3 (1):137-47.

Morais da Silva, S., A. Hacker, V. Harley, P. Goodfellow, A. Swain, and R. Lovell-Badge. 1996. *Sox9* expression during gonadal development implies a conserved role for the gene in testis differentiation in mammals and birds. *Nat Genet* 14 (1):62-8.

Moriguchi, T., M. Hamada, N. Morito, T. Terunuma, K. Hasegawa, C. Zhang, T. Yokomizo, R. Esaki, E. Kuroda, K. Yoh, T. Kudo, M. Nagata, D. R. Greaves, J. D. Engel, M. Yamamoto, and S. Takahashi. 2006. *MafB* is essential for renal development and F4/80 expression in macrophages. *Mol Cell Biol* 26 (15):5715-27.

Mork, L., D. M. Maatouk, J. A. McMahon, J. J. Guo, P. Zhang, A. P. McMahon, and B. Capel. 2011. Temporal Differences in Granulosa Cell Specification in the Ovary Reflect Distinct Follicle Fates in Mice. *Biol Reprod*.

Motoike, T., D. W. Markham, J. Rossant, and T. N. Sato. 2003. Evidence for novel fate of Flk1+ progenitor: contribution to muscle lineage. *Genesis* 35 (3):153-9.

Mroz, K., L. Carrel, and P. A. Hunt. 1999. Germ cell development in the XXY mouse: evidence that X chromosome reactivation is independent of sexual differentiation. *Dev Biol* 207 (1):229-38.

Munger, S. C., D. L. Aylor, H. A. Syed, P. M. Magwene, D. W. Threadgill, and B. Capel. 2009. Elucidation of the transcription network governing mammalian sex determination by exploiting strain-specific susceptibility to sex reversal. *Genes Dev* 23 (21):2521-36.

Nakamura, Y., M. Yamamoto, and Y. Matsui. 2002. Introduction and expression of foreign genes in cultured mouse embryonic gonads by electroporation. *Reprod Fertil Dev* 14 (5-6):259-65.

Nef, S., O. Schaad, N. R. Stallings, C. R. Cederroth, J. L. Pitetti, G. Schaer, S. Malki, M. Dubois-Dauphin, B. Boizet-Bonhoure, P. Descombes, K. L. Parker, and J. D. Vassalli. 2005. Gene expression during sex determination reveals a robust female genetic program at the onset of ovarian development. *Dev Biol* 287 (2):361-77.

Ng, S. Y., T. Yoshida, J. Zhang, and K. Georgopoulos. 2009. Genome-wide lineage-specific transcriptional networks underscore *Ikaros*-dependent lymphoid priming in hematopoietic stem cells. *Immunity* 30 (4):493-507.

Ni, C. Y., M. P. Murphy, T. E. Golde, and G. Carpenter. 2001. gamma -Secretase cleavage and nuclear localization of ErbB-4 receptor tyrosine kinase. *Science* 294 (5549):2179-81.

O'Neill, L. P., M. D. VerMilyea, and B. M. Turner. 2006. Epigenetic characterization of the early embryo with a chromatin immunoprecipitation protocol applicable to small cell populations. *Nat Genet* 38 (7):835-41.

O, W., and T. G. Baker. 1976. Initiation and control of meiosis in hamster gonads in vitro. *J Reprod Fertil* 48 (2):399-401.

Ohshiro, T., T. Yagami, C. Zhang, and F. Matsuzaki. 2000. Role of cortical tumour-suppressor proteins in asymmetric division of Drosophila neuroblast. *Nature* 408 (6812):593-6.

Orvis, G. D., and R. R. Behringer. 2007. Cellular mechanisms of Mullerian duct formation in the mouse. *Dev Biol* 306 (2):493-504.

Parma, P., O. Radi, V. Vidal, M. C. Chaboissier, E. Dellambra, S. Valentini, L. Guerra, A. Schedl, and G. Camerino. 2006. R-spondin1 is essential in sex determination, skin differentiation and malignancy. *Nat Genet* 38 (11):1304-9.

Peng, C. Y., L. Manning, R. Albertson, and C. Q. Doe. 2000. The tumour-suppressor genes lgl and dlg regulate basal protein targeting in Drosophila neuroblasts. *Nature* 408 (6812):596-600.

Pfaffl, M. W. 2001. A new mathematical model for relative quantification in real-time RT-PCR. *Nucleic Acids Res* 29 (9):e45.

Phillips, B. T., K. Gassei, and K. E. Orwig. 2010. Spermatogonial stem cell regulation and spermatogenesis. *Philos Trans R Soc Lond B Biol Sci* 365 (1546):1663-78.

Plusa, B., A. Piliszek, S. Frankenberg, J. Artus, and A. K. Hadjantonakis. 2008. Distinct sequential cell behaviours direct primitive endoderm formation in the mouse blastocyst. *Development* 135 (18):3081-91.

Poche, R. A., I. V. Larina, M. L. Scott, J. E. Saik, J. L. West, and M. E. Dickinson. 2009. The *Flk1-myr::mCherry* mouse as a useful reporter to characterize multiple aspects of ocular blood vessel development and disease. *Dev Dyn* 238 (9):2318-26.

Powers, C. J., S. W. McLeskey, and A. Wellstein. 2000. Fibroblast growth factors, their receptors and signaling. *Endocr Relat Cancer* 7 (3):165-97.

Rafael, J. A., T. L. Hutchinson, C. N. Lumeng, S. M. Marfatia, A. H. Chishti, and J. S. Chamberlain. 1998. Localization of Dlg at the mammalian neuromuscular junction. *Neuroreport* 9 (9):2121-5.

Rampalli, S., L. Li, E. Mak, K. Ge, M. Brand, S. J. Tapscott, and F. J. Dilworth. 2007. p38 MAPK signaling regulates recruitment of Ash2L-containing methyltransferase complexes to specific genes during differentiation. *Nat Struct Mol Biol* 14 (12):1150-6.

Raymond, C. S., M. W. Murphy, M. G. O'Sullivan, V. J. Bardwell, and D. Zarkower. 2000. *Dmrt1*, a gene related to worm and fly sexual regulators, is required for mammalian testis differentiation. *Genes Dev* 14 (20):2587-95.

Raz, E. 2000. The function and regulation of vasa-like genes in germ-cell development. *Genome Biol* 1 (3):REVIEWS1017.

Revilla-i-Domingo, R., P. Oliveri, and E. H. Davidson. 2007. A missing link in the sea urchin embryo gene regulatory network: hesC and the double-negative specification of micromeres. *Proc Natl Acad Sci U S A* 104 (30):12383-8.

Rieckmann, T., I. Kotevic, and B. Trueb. 2008. The cell surface receptor FGFRL1 forms constitutive dimers that promote cell adhesion. *Exp Cell Res* 314 (5):1071-81.

Robinson, T. J., M. A. Dinan, M. Dewhirst, M. A. Garcia-Blanco, and J. L. Pearson. 2010. SplicerAV: a tool for mining microarray expression data for changes in RNA processing. *BMC Bioinformatics* 11:108.

Rolland, A. D., K. P. Lehmann, K. J. Johnson, K. W. Gaido, and P. Koopman. 2011. Uncovering gene regulatory networks during mouse fetal germ cell development. *Biol Reprod* 84 (4):790-800.

Saitou, M., S. C. Barton, and M. A. Surani. 2002. A molecular programme for the specification of germ cell fate in mice. *Nature* 418 (6895):293-300.

Schmahl, J., E. M. Eicher, L. L. Washburn, and B. Capel. 2000. Sry induces cell proliferation in the mouse gonad. *Development* 127 (1):65-73.

Schmahl, J., Y. Kim, J. S. Colvin, D. M. Ornitz, and B. Capel. 2004. Fgf9 induces proliferation and nuclear localization of FGFR2 in Sertoli precursors during male sex determination. *Development* 131 (15):3627-36.

Sekido, R., I. Bar, V. Narvaez, G. Penny, and R. Lovell-Badge. 2004. SOX9 is up-regulated by the transient expression of SRY specifically in Sertoli cell precursors. *Dev Biol* 274 (2):271-9.

Sekido, R., and R. Lovell-Badge. 2008. Sex determination involves synergistic action of SRY and SF1 on a specific *Sox9* enhancer. *Nature* 453 (7197):930-4.

Serra, C., D. Palacios, C. Mozzetta, S. V. Forcales, I. Morantte, M. Ripani, D. R. Jones, K. Du, U. S. Jhala, C. Simone, and P. L. Puri. 2007. Functional interdependence at the chromatin level between the MKK6/p38 and IGF1/PI3K/AKT pathways during muscle differentiation. *Mol Cell* 28 (2):200-13.

Shimono, Y., H. Murakami, Y. Hasegawa, and M. Takahashi. 2000. RET finger protein is a transcriptional repressor and interacts with enhancer of polycomb that has dual transcriptional functions. *J Biol Chem* 275 (50):39411-9.

Simone, C., S. V. Forcales, D. A. Hill, A. N. Imbalzano, L. Latella, and P. L. Puri. 2004. p38 pathway targets SWI-SNF chromatin-remodeling complex to muscle-specific loci. *Nat Genet* 36 (7):738-43.

Smith, P. J., N. Blunt, M. Wiltshire, T. Hoy, P. Teesdale-Spittle, M. R. Craven, J. V. Watson, W. B. Amos, R. J. Errington, and L. H. Patterson. 2000. Characteristics of a novel deep red/infrared fluorescent cell-permeant DNA probe, DRAQ5, in intact human cells analyzed by flow cytometry, confocal and multiphoton microscopy. *Cytometry* 40 (4):280-91.

Stark, K., S. Vainio, G. Vassileva, and A. P. McMahon. 1994. Epithelial transformation of metanephric mesenchyme in the developing kidney regulated by Wnt-4. *Nature* 372 (6507):679-83.

Steinberg, F., L. Zhuang, M. Beyeler, R. E. Kalin, P. E. Mullis, A. W. Brandli, and B. Trueb. 2010. The FGFRL1 receptor is shed from cell membranes, binds fibroblast growth factors (FGFs), and antagonizes FGF signaling in Xenopus embryos. *J Biol Chem* 285 (3):2193-202.

Suelves, M., F. Lluis, V. Ruiz, A. R. Nebreda, and P. Munoz-Canoves. 2004. Phosphorylation of MRF4 transactivation domain by p38 mediates repression of specific myogenic genes. *EMBO J* 23 (2):365-75.

Swain, A., and R. Lovell-Badge. 1999. Mammalian sex determination: a molecular drama. *Genes Dev* 13 (7):755-67.

Swain, A., V. Narvaez, P. Burgoyne, G. Camerino, and R. Lovell-Badge. 1998. *Dax1* antagonizes *Sry* action in mammalian sex determination. *Nature* 391 (6669):761-7.

Szabo, P. E., K. Hubner, H. Scholer, and J. R. Mann. 2002. Allele-specific expression of imprinted genes in mouse migratory primordial germ cells. *Mech Dev* 115 (1-2):157-60.

Tevosian, S. G., and N. L. Manuylov. 2008. To beta or not to beta: canonical beta-catenin signaling pathway and ovarian development. *Dev Dyn* 237 (12):3672-80.

Tsuda, M., Y. Sasaoka, M. Kiso, K. Abe, S. Haraguchi, S. Kobayashi, and Y. Saga. 2003. Conserved role of nanos proteins in germ cell development. *Science* 301 (5637):1239-41.

Uhlenhaut, N. H., S. Jakob, K. Anlag, T. Eisenberger, R. Sekido, J. Kress, A. C. Treier, C. Klugmann, C. Klasen, N. I. Holter, D. Riethmacher, G. Schutz, A. J. Cooney, R. Lovell-Badge, and M. Treier. 2009. Somatic sex reprogramming of adult ovaries to testes by FOXL2 ablation. *Cell* 139 (6):1130-42.

Upadhyay, S., and L. Zamboni. 1982. Ectopic germ cells: natural model for the study of germ cell sexual differentiation. *Proc Natl Acad Sci U S A* 79 (21):6584-8.

Vainio, S., M. Heikkila, A. Kispert, N. Chin, and A. P. McMahon. 1999. Female development in mammals is regulated by *Wnt-4* signalling. *Nature* 397 (6718):405-9.

van den Bergen, J. A., D. C. Miles, A. H. Sinclair, and P. S. Western. 2009. Normalizing gene expression levels in mouse fetal germ cells. *Biol Reprod* 81 (2):362-70.

Vidal, V. P., M. C. Chaboissier, D. G. de Rooij, and A. Schedl. 2001. Sox9 induces testis development in XX transgenic mice. *Nat Genet* 28 (3):216-7.

Wagner, T., J. Wirth, J. Meyer, B. Zabel, M. Held, J. Zimmer, J. Pasantes, F. D. Bricarelli, J. Keutel, E. Hustert, and et al. 1994. Autosomal sex reversal and campomelic dysplasia are caused by mutations in and around the SRY-related gene SOX9. *Cell* 79 (6):1111-20.

Wiedemann, M., and B. Trueb. 2000. Characterization of a novel protein (FGFRL1) from human cartilage related to FGF receptors. *Genomics* 69 (2):275-9.

———. 2001. The mouse Fgfrl1 gene coding for a novel FGF receptor-like protein. *Biochim Biophys Acta* 1520 (3):247-50.

Wylie, C. 1999. Germ cells. *Cell* 96 (2):165-74.

Yao, H. H., J. Aardema, and K. Holthusen. 2006. Sexually dimorphic regulation of inhibin beta B in establishing gonadal vasculature in mice. *Biol Reprod* 74 (5):978-83.

Yao, H. H., M. M. Matzuk, C. J. Jorgez, D. B. Menke, D. C. Page, A. Swain, and B. Capel. 2004. Follistatin operates downstream of Wnt4 in mammalian ovary organogenesis. *Dev Dyn* 230 (2):210-5.

Yu, K., J. Xu, Z. Liu, D. Sosic, J. Shao, E. N. Olson, D. A. Towler, and D. M. Ornitz. 2003. Conditional inactivation of FGF receptor 2 reveals an essential role for FGF signaling in the regulation of osteoblast function and bone growth. *Development* 130 (13):3063-74.

Zarubin, T., and J. Han. 2005. Activation and signaling of the p38 MAP kinase pathway. *Cell Res* 15 (1):11-8.

Zipori, D. 2004. The nature of stem cells: state rather than entity. *Nat Rev Genet* 5 (11):873-8.

Biography

Samantha Ann Jameson was born Samantha Ann James on March 3, 1981 in Milwaukee, Wisconsin to Andrea and Christopher James. Her childhood was spent predominately in Milwuakee, Wisconsin and Plano, Texas; with summers in West Palm Beach, Florida and Columbia, South Carolina. Samantha graduated from Skyline High School in Issaquah, Washington and then attended the University of Washington in Seattle. She graduated from the University of Washington in 2004, the same year she married Martin Alan Watson (now Martin Alan Jameson). They then moved to Durham, North Carolina, where Samantha began her studies at Duke University pursuing her J.D. and Ph.D. She matriculated into the Cell and Molecular Biology program and received a James B. Duke Fellowship as well as a scholarship from the Law School. She became a registered patent agent with the United States Patent and Trademark Office in 2005. In 2007, Samantha obtained her J.D. and M.A. in Cell Biology, and passed the North Carolina Bar Examination to become a registered attorney. She received her J.D. *magna cum laude*, Order of the Coif, and received the 2007 Intellectual Property and Technology Award from the Duke University School of Law. Also in 2007, she joined Blanche Capel's laboratory. On March 8, 2009, Samantha and Martin celebrated the arrival of their daughter, Keena Taite Jameson.

Manuscript provisionally accepted, pending revisions, by PLoS Genetics:

Jameson SA, Natarajan A, Cool J, DeFalco T, Maatouk DM, Mork L, Munger SC, and

Capel B. *Temporal Transcriptional Profiling of Somatic and Germ Cells Reveals Biased Lineage Priming of Sexual Fate in the Fetal Mouse Gonad.*

Manuscript under review with Developmental Biology:

Jameson SA and Capel B. *Testis Development Requires the Repression of Wnt4 by Fgf Signaling.*

Previous Scientific Publications:

Ryan T. Nitta, Samantha A. Jameson, Brian A. Kudlow, Lindus A. Conlan & Brian K. Kennedy, *Stabilization of the Retinoblastoma Protein by A-Type Nuclear Lamins Is Required for INK4A-Mediated Cell Cycle Arrest*, 26 MOLECULAR & CELLULAR BIOLOGY 5360 (2006).

Richard L. Frock, Brian A. Kudlow, Angela M. Evans, Samantha A. Jameson, Stephen D. Hauschka & Brian K. Kennedy, *Lamin A/C and Emerin Are Critical for Skeletal Muscle Satellite Cell Differentiation*, 20 GENES & DEV. 486 (2006).

Brian A. Kudlow, Samantha A. Jameson & Brian K. Kennedy, *HIV Protease Inhibitors Block Adipocyte Differentiation Independently of Lamin A/C*, 19 AIDS 1565 (2005).

Previous Legal Publications:

Samantha A. Jameson, *A Comparison of the Patentability and Patent Scope of Biotechnological Inventions in the United States and the European Union*, 35 AIPLA Q.J. 193 (2007).

Samantha A. Jameson, *The Problems of the Utility Analysis in* Fisher *and Its Associated Policy Implications and Flaws*, 56 DUKE L.J. 311 (2006).